



# Opportunistic Experiments to Constrain Aerosol Effective Radiative Forcing

Matthew Christensen<sup>1,2</sup>, Andrew Gettelman<sup>3</sup>, Jan Cermak<sup>4,5</sup>, Guy Dagan<sup>1</sup>, Michael Diamond<sup>6,7,8</sup>, Alyson Douglas<sup>1</sup>, Graham Feingold<sup>7</sup>, Franziska Glassmeier<sup>9</sup>, Tom Goren<sup>10</sup>, Daniel P. Grosvenor<sup>11</sup>, Edward Gryspeerdt<sup>12</sup>, Ralph Kahn<sup>13</sup>, Zhanqing Li<sup>14</sup>, Po-Lun Ma<sup>2</sup>, Florent Malavelle<sup>15</sup>, Isabel McCoy<sup>16,17</sup>, Daniel McCoy<sup>18</sup>, Greg McFarquhar<sup>19,20</sup>, Johannes Mülmenstädt<sup>2</sup>, Sandip Pal<sup>21</sup>, Anna Possner<sup>22</sup>, Adam Povey<sup>1,23</sup>, Johannes Quaas<sup>10</sup>, Daniel Rosenfeld<sup>24</sup>, Anja Schmidt<sup>25,26</sup>, Roland Schrödner<sup>27</sup>, Armin Sorooshian<sup>28,29</sup>, Philip Stier<sup>1</sup>, Velle Toll<sup>30</sup>, Duncan Watson-Parris<sup>1</sup>, Robert Wood<sup>6</sup>, Mingxi Yang<sup>31</sup>, and Tianle Yuan<sup>32,33</sup>

<sup>1</sup>Atmospheric, Oceanic and Planetary Physics, Department of Physics, University of Oxford, Oxford OX1 3PU, United Kingdom

<sup>2</sup>Atmospheric Science & Global Change Division, Pacific Northwest National Laboratory, Richland, WA 99352, Washington, USA

<sup>3</sup>National Center for Atmospheric Research, Boulder, CO, USA

<sup>4</sup>Karlsruhe Institute of Technology (KIT), Institute of Meteorology and Climate Research, Karlsruhe, Germany

<sup>5</sup>Karlsruhe Institute of Technology (KIT), Institute of Photogrammetry and Remote Sensing, Karlsruhe, Germany

<sup>6</sup>Department of Atmospheric Sciences, University of Washington, Seattle, USA

<sup>7</sup>NOAA Chemical Sciences Laboratory (CSL), Boulder, Colorado, USA

<sup>8</sup>Cooperative Institute for Research in Environmental Sciences (CIRES), University of Colorado, Boulder, Colorado, USA

<sup>9</sup>Department Geoscience and Remote Sensing, Delft University of Technology, PO Box 5048, 2600GA Delft, Netherlands

<sup>10</sup>Universität Leipzig, Institute for Meteorology, Leipzig, Germany

<sup>11</sup>National Centre for Atmospheric Sciences, School of Earth and Environment, University of Leeds, Leeds, LS2 9JT, UK

<sup>12</sup>Space and Atmospheric Physics Group, Imperial College London, UK

<sup>13</sup>Earth Science Division, NASA Goddard Space Flight Center, Greenbelt MD USA

<sup>14</sup>Dept of Atmospheric and Oceanic Science, University of Maryland, USA

<sup>15</sup>Met Office, Atmospheric Dispersion and Air Quality, Fitzroy Rd, Exeter EX1 3PB, UK

<sup>16</sup>Rosenstiel School of Marine and Atmospheric Science, University of Miami, Miami, FL, USA

<sup>17</sup>University Corporation for Atmospheric Research, Boulder, CO, USA

<sup>18</sup>Department of Atmospheric Sciences, University of Wyoming, Laramie, USA

<sup>19</sup>Cooperative Institute for Mesoscale Meteorological Studies (CIMMS) and School of Meteorology

<sup>20</sup>University of Oklahoma, Norman, OK

<sup>21</sup>Department of Geosciences, Texas Tech University

<sup>22</sup>Institute for Atmospheric and Environmental Sciences, Goethe University Frankfurt, Frankfurt/Main, Germany

<sup>23</sup>National Centre for Earth Observation, University of Oxford, Oxford, OX1 3PU, United Kingdom

<sup>24</sup>The Hebrew University of Jerusalem, Israel

<sup>25</sup>Department of Geography, University of Cambridge, Cambridge, UK

<sup>26</sup>Department of Chemistry, University of Cambridge, Cambridge, UK

<sup>27</sup>Leibniz Institute for Tropospheric Research, Leipzig, Germany

<sup>28</sup>Department of Chemical and Environmental Engineering, University of Arizona, Tucson, AZ, USA

<sup>29</sup>Department of Hydrology and Atmospheric Sciences, University of Arizona, Tucson, AZ, USA

<sup>30</sup>University of Tartu, Institute of Physics, Tartu, Estonia

<sup>31</sup>Plymouth Marine Laboratory, Prospect Place, Plymouth, PL1 3DH, United Kingdom

<sup>32</sup>Joint Center for Earth Systems Technologies, University of Maryland, Baltimore County



<sup>33</sup>Earth Science Division, NASA Goddard Space Flight Center, Greenbelt, MD

**Correspondence:** Matthew Christensen (matt.christensen@pnnl.gov)

**Abstract.** Aerosol-cloud interactions (ACI) are considered to be the most uncertain driver of present-day radiative forcing due to human activities. The non-linearity of cloud-state changes to aerosol perturbations make it challenging to attribute causality in observed relationships of aerosol radiative forcing. Using correlations to infer causality can also be challenging when meteorological variability also drives both aerosol and cloud changes independently. Natural and anthropogenic aerosol perturbations from well defined sources provide ‘opportunistic experiments’ (also known as natural experiments) to investigate ACI in cases where causality may be more confidently inferred. These perturbations cover a wide range of locations and spatio-temporal scales, including point sources such as volcanic eruptions or industrial sources, plumes from biomass burning or forest fires, and tracks from individual ships or shipping corridors. We review the different experimental conditions and conduct a synthesis of the available satellite data sets and field campaigns to place these opportunistic experiments on a common footing, facilitating new insights and a clearer understanding of key uncertainties in aerosol radiative forcing. Strong liquid water path increases due to aerosol perturbations are largely ruled out by averaging across experiments. Cloud albedo perturbations are strongly sensitive to background meteorological conditions. Opportunistic experiments have significantly improved process level understanding of ACI, but it remains unclear how reliably the relationships found can be scaled to the global level, thus, demonstrating a need for deeper investigation in order to improve assessments of aerosol radiative forcing and climate change.

15

## 1 Introduction

Numerous studies have attempted to quantify the different aerosol effects on warm liquid clouds. As reviewed in the IPCC (2013) and Bellouin et al. (2020), multiple lines of evidence indicate that increases in aerosol loading increase cloud drop number and decrease drop size (the so-called Twomey effect; Twomey, 1974). Further microphysically-driven adjustments in cloud macrophysical properties like areal coverage and cloud water path are still uncertain.

A reduction in precipitation due to smaller cloud droplets can enhance cloudiness (the so-called lifetime effect; Albrecht, 1989), while at the same time a larger number of smaller cloud droplets can enhance the cloud-top evaporation and dry air entrainment (Wang et al., 2003) as well as reduced sedimentation of cloud droplets (Bretherton et al., 2007) thereby leading to feedbacks that reduce cloudiness. Cloud adjustments may therefore either compound or counteract the cloud albedo (i.e., reflectance) change due to the “Twomey effect” of higher cloud droplet number and smaller droplet size. There is ample evidence of aerosol-driven precipitation suppression in stratocumulus (Wood et al., 2011), but the effects of this process on liquid water path and cloud cover fraction remain uncertain. A complication is that while it is easy to control experiments in model simulations (where aerosol populations are perturbed in a controlled manner in the same environment), this is not possible in the real world. Comparison of two different clouds with different aerosol populations requires understanding how



30 the co-variability in aerosols and ‘meteorology’ (defined as the temperature, specific humidity, turbulence, vertical motion, etc) affects cloud microphysical properties (liquid water path, drop number/size) and ultimately cloud radiative effects.

When emissions perturb aerosols in ‘controlled’ (fixed or defined) conditions with minimal changes to meteorology, it is possible to use observations to understand ACI processes and to quantify the magnitude of anthropogenic aerosol radiative effects. These opportunistic experiments are defined as injections of aerosols into an environmental regime (‘laboratory’) where the unperturbed state is to some extent known. While these are sometimes called ‘natural laboratories’, some are natural (volcanoes) while some are human-caused (industrial plumes, ship tracks). So we will use the term ‘opportunistic’ to apply to both. A ‘laboratory’ refers to a regime and type of emission, while ‘experiment’ refers to a particular case.

For convenience, we will use the terms natural and opportunistic interchangeably, recognizing that ‘natural’ perturbations may be anthropogenic. These opportunistic experiments or ‘laboratories’ may also provide analogs for the effects of widespread, climatologically relevant anthropogenic emissions on clouds. The effect of such a perturbation on cloud properties can be reasonably expected to stand out compared to background variability of unrelated processes and phenomena (e.g. volcanic eruptions, large-scale biomass burning, hemispheric emissions). While mixed and ice phase clouds are critical to Earth’s radiation budget, and occur in many natural experiments and laboratories, we choose to focus on warm liquid clouds due to the wealth of existing knowledge and relative simplicity of this system.

45 The first type of experiment dates back to the 1960s when ship tracks, curvilinear cloud features that can be traced back to the movements of individual ships, were identified in Television Infrared Observation Satellite (TIROS) (Conover, 1966) imagery of marine stratus decks. Since then several similar laboratories have been explored, such as aerosols emitted from industrial sources, volcanoes, and biomass burning plumes (both natural and human). Opportunistic experiments include anthropogenic aerosol changes due to particular events, such as emission changes due to the 2008 Beijing Olympics, the ‘Great Recession’ of 2007-2009 or even the COVID-19 pandemic. Finally, weekly cycles or long term decadal trends have been used as laboratories to understand aerosol radiative forcing and cloud modification on local-to-regional scales (Quaas, 2015).

This review will analyze different types of aerosol perturbations (‘laboratories’ or ‘experiments’) and how they can be used to test hypotheses about ACI and to quantify their effects to better constrain total anthropogenic aerosol forcing for warm boundary layer clouds. Some examples of mixed-phase, ice cloud, and convective cloud opportunistic experiments are discussed but due to their episodic nature, heterogeneity of convection, and difficulty of detection, we primarily focus on warm cloud physics. Other examples such as aircraft contrails, dust events (e.g. Saharan air outbreaks), and cloud seeding to intentionally affect precipitation are also beyond the scope of this work.

The review is organized as follows. First we review the different types of opportunistic experiments (Section 2). Then we provide a linked summary database of different experiments that have been used in previous studies (Section 3). We describe different approaches to quantifying the effects of aerosols in opportunistic experiments in Section 4. Section 5 brings together the different experiment types and previous results to synthesize qualitative and quantitative aerosol effects across methods and experiment types. Section 6 provides a synthesis of these findings and their conclusions.



## 2 Overview of Opportunistic Experiments

Figure 1 highlights several key laboratories of significant interest and influence on clouds and potentially climate. A wealth of papers describing cloud microphysical properties and their changes associated with each laboratory is described in Table S1 and datasets generated for many of these papers are listed in Table S2. The following subsections provide a brief description of some of the primary characteristics of each laboratory and their strengths and limitations for teasing out process-level understanding of aerosol-cloud interactions.

Figure 2 shows an example of ship tracks off the coast of Portugal from the MODerate Resolution Imaging Spectroradiometer (MODIS) on the Aqua satellite. Although modeling studies are undoubtedly useful tools in the study of opportunistic experiments like ship tracks, they are arguably unnecessary for strong causal inferences to be made in many cases, unlike for other natural laboratories where the emissions are spread out over larger spatial scales (like a shipping corridor). Generally, as the spatial domain of the aerosol perturbation increases (e.g. from individual ship tracks to shipping corridors to the entire globe) different methodologies are required to compute a counterfactual ‘background’ (or unperturbed) cloud-state. For example, in some experiments like ship, fire, and volcano tracks the counterfactual can easily be established by selecting unpolluted clouds in nearby locations in the same cloud regime. Establishing the observed counterfactual for large smoke plumes, volcanic eruptions, and shipping corridors is not as evident. The difficulty of attribution changes how effectively each opportunistic experiment can be studied and what kinds of conclusions can be drawn. Some prominent examples (Figure 3) of opportunistic experiments and their relevance are described below.

### 2.1 Ship emissions (tracks and corridors)

For decades, ships burning high sulfur content fuels have crossed the world’s oceans, emitting aerosol and aerosol-precursor gases in regions with relatively low levels of natural aerosol (Capaldo et al., 1999; Eyring et al., 2010). The world’s major shipping routes have elevated concentrations of SO<sub>2</sub> emissions as evident in the Emissions Database for Global Atmospheric Research (EDGAR), version 5.0 (Crippa et al., 2018, 2020), shown in Figure S1. Ship tracks themselves have been studied since the mid-1960s, as soon as they were first identified in TIROS-VII imagery (Conover, 1966). The TIROS series was NASA’s first experiment with systematic satellite remote sensing of the Earth system. Multiple hypotheses, such as that the tracks were aircraft contrails or even secret missile tests, were considered before they were correctly identified as resulting from ships traveling through conditions of shallow, cloudy marine boundary layers (MBLs) with low background aerosol levels (Conover, 1966; Bowley, 1967; Twomey et al., 1968). In the late 1980s, satellite (Coakley et al., 1987) and aircraft (Radke et al., 1989) measurements confirmed the qualitative effects of ships on cloud properties hypothesized earlier. The apparent increase in liquid water content and decrease in drizzle-sized droplets in the ship tracks sampled by Radke et al. (1989) as well as cloud reductions around ship tracks from circulations (Scorer, 1987) served as a partial inspiration for the modeling work generally credited with establishing the cloud adjustment (‘drizzle suppression’) hypothesis (Albrecht, 1989).

More systematic measurements of ship tracks were taken during the Monterey Area Ship Track experiment (MAST) campaign in the mid-1990s (Ackerman et al., 2000; Durkee et al., 2000b, a; Hobbs et al., 2000; Ferek et al., 2000). An analysis of



131 ship tracks studied in MAST showed that the tracks tended to form in shallow boundary layers (300-750 m) and last for 7 hours on average, with many lasting longer than 12 hours (Durkee et al., 2000a). Cloud condensation nuclei (CCN) emitted from the ships directly and potentially coated by sulfate (from the SO<sub>2</sub> co-emitted with carbonaceous particles in fuel burning) were found to be responsible for influencing cloud properties, rather than any effects from sea salt produced in ships' wakes or from the temperature or moisture perturbations associated with fuel burning (Durkee et al., 2000b; Hobbs et al., 2000).

Some MAST observations did appear to support the lifetime effect hypothesis of Albrecht (1989), such as the finding that drizzle was generally reduced in ship tracks (Ferek et al., 2000). However, a weak anti-correlation was observed between liquid water content and cloud droplet number concentration ( $N_d$ ) within a sample of 69 ship tracks (Ackerman et al., 2000). Later satellite analyses of ship tracks also cast doubt on a unidirectional lifetime effect by demonstrating that decreased liquid water path (LWP) within ship tracks was a frequent occurrence (Coakley and Walsh, 2002). In approximately 30% of cases, this decrease in LWP is enough to offset the brightening from the Twomey effect entirely and actually darken the ship tracks (Chen et al., 2012). While darkened ship tracks can occur in satellite imagery (Supporting Information Figure S2), ship tracks (particularly those forming in typical closed cell stratocumulus) sometimes lack sufficient signal-to-noise in the near infrared reflectance between the polluted and surrounding unpolluted clouds, which can be a significant issue for estimating radiative forcing when the signal is relatively small (in contrast to the background clouds being highly noisy). Systematic studies of ship tracks from across many ocean basins suggest that ship emissions have a varied influence on LWP with large increases occurring under clean conditions and decreases under more polluted conditions (Gryspeerd et al., 2019b). However, the overall effect of LWP changes from all ship tracks has been estimated to be small compared to the relative changes in droplet number concentration on average (Toll et al., 2019). In particular, LWP tends to increase when clouds are drizzling (as inferred from CloudSat observations) and are topped by a relatively moist free troposphere, but decrease in non-precipitating and drier cases (Toll et al., 2017).

Other studies have investigated potential increases in cloud top height from in situ aircraft measurements (Taylor and Ackerman, 1999) and lidar retrievals from satellite data (Christensen and Stephens, 2011) as well as differences in responses between closed-cell and open-cell mesoscale convective organization (Christensen and Stephens, 2012). Ship emissions can increase cloud fraction ( $C_F$ ) even without changing cell structure (Feingold et al., 2015). Furthermore, transitions from open-cellular to closed-cellular convection induced by ship emissions provide evidence of a cloud fraction enhancement occurring over several days following the evolution several dozen ship tracks (Goren and Rosenfeld, 2012). These older, more diffuse ship tracks do not typically retain their original track-like characteristics, thereby making them difficult to detect without geostationary satellite observations and are thus underrepresented in nearly all ship track studies.

Ship emissions may also be important for mixed-phase cloud properties, although studies have suggested that the effect on cloud brightness is more muted than in warm clouds (Christensen et al., 2014; Possner et al., 2017). Shipping may even affect deep convective clouds: lightning appears to be enhanced over major shipping corridors in the northeastern Indian Ocean and the South China Sea, which has been hypothesized to be due to convective invigoration from shipping-related aerosol perturbations in a well-defined shipping lane flanked by lower background aerosol concentrations (Thornton et al., 2017; Blosssey et al., 2018; Grabowski and Morrison, 2020).



Ship track studies, thus, have been very helpful in formulating and testing many hypotheses about aerosol-cloud interaction mechanisms. However, observational studies aiming to quantify the effects from shipping at climatically-relevant temporal and spatial scales have tended to find negligible or undetectable effects (Schreier et al., 2007; Peters et al., 2011, 2014), at least until recently. Schreier et al. (2007) analyzed one year of manually-detected ship tracks within low-cloud-dominated satellite  
135 scenes and calculated a negligible global radiative forcing of  $-0.0004$  to  $-0.0006 \text{ Wm}^{-2}$ . However, a very large percentage of ship tracks likely go undetected, as there are on the order of 100,000 ships in the global fleet (Eyring et al., 2010) and yet studies of ship tracks tend to identify only hundreds to thousands of tracks per year (Campmany et al., 2009; Christensen et al., 2014; Toll et al., 2017, 2019; Gryspeerdt et al., 2019a). The under-identification of ship tracks is likely to be especially pronounced in more complex cloud scenes (Possner et al., 2018). New automated methods for identifying ship tracks using  
140 machine learning (Yuan et al., 2019) or by following air mass trajectories to interpolate between observed ship track segments (Gryspeerdt et al., 2019b) hold promise for identifying a substantially larger number of ship tracks than has previously been possible. An outstanding question is whether these weak tracks are frequent enough to have a noticeable effect on shortwave reflection to space, but because the tracks are weak numerous cases would be needed to contribute significantly to the radiation budget. Finally, Peters et al. (2013) showed significant radiative ( $0.3 \text{ Wm}^{-2}$ ) effects due to shipping in a modeling study,  
145 therefore the effects can be undetectable but with results that add up to be non-negligible.

In order to evaluate shipping effects more holistically, several studies have attempted to circumvent this identification issue by analyzing entire shipping corridors instead of focusing on individual tracks. Peters et al. (2011) evaluated satellite-derived cloud properties upstream and downstream of three tropical and subtropical shipping corridors in which low-level winds typically blow perpendicular to the corridors, under the hypothesis that observations upstream of the corridor would represent  
150 unpolluted clouds and those downstream would show the effect of shipping pollution. No statistically significant impacts from shipping could be detected. However, Peters et al. (2011) lacked the control conditions against which to contrast the changes due to shipping. A follow-up analysis applying this same methodology to climate model output confirmed that natural sources of meteorological variability and natural gradients in cloud properties obscure the effects of shipping (Peters et al., 2014). Diamond et al. (2020) found substantial increases in climatological  $N_d$  and cloud reflectance within a shipping corridor in the  
155 southeast Atlantic Ocean, the primary difference from the earlier work being that low-level winds, parallel with the shipping corridor, keep the ship emissions relatively concentrated. They employed a method in which the cloud and aerosol properties within the corridor that would be expected to exist in the absence of shipping emissions (the “counterfactual” situation) were estimated via a universal kriging algorithm trained on nearby, presumably non-shiping-affected values. The difference between the counterfactual so-calculated, and the observed or reanalysis cloud and aerosol properties (“factual”), was taken as  
160 the effect of shipping emissions.

Figure 4 shows a comparison of the results from Diamond et al. (2020) for  $N_d$  with output from the Community Earth System Model version 2 (CESM2) analyzed in a similar manner (see Supporting Information Text S1 for full details). In contrast to the MODIS/Aqua observations (Figure 4g), CESM2 does not show a clear, statistically significant enhancement in  $N_d$  coincident with the major southeast Atlantic shipping corridor (Figure 4h). A similar analysis performed for surface sulfate  
165 mass concentration (Supporting Information Figure S3) shows that there is a perturbation coincident with the shipping corridor



as expected, albeit weaker and more diffuse than that inferred from the Modern-Era Retrospective analysis for Research and Applications, Version 2 (MERRA-2; Randles et al., 2017). However, we must recognize the uncertainty in sulfate evolution from SO<sub>2</sub>, including primary sulfate fractions and size distributions that could contribute to these differences. Comparing the control run of CESM2 (with normal shipping emissions included, Figure 4c) with an experimental run with shipping emissions set to zero (Figure 4f) shows that shipping emissions cause a broad increase in  $N_d$  over the southeast Atlantic with some hint of a particular enhancement within the heavily-trafficked corridor (Figure 4i). Similarly, Figure S3 shows the greatest enhancement in sulfate from shipping emissions occurs within the corridor, but there is a sizable effect throughout the entire region as well (as also found by Peters et al., 2014). Thus, comparisons of the observational and reanalysis-based results of Diamond et al. (2020) with climate model data may not be straightforward. In part, this may be due to the much larger heterogeneity in the model mean cloud properties as compared to the observations, both in terms of the overall spread in values and their smoothness in space. Another potential caveat to consider is that the presence of black carbon may lead to cloud burn off and affect cloud properties in this shipping corridor off the coast of South Africa (Hu et al., 2021), although attempts to quantify this effect suggest its magnitude may be insignificant (Diamond et al., 2020). The effects of black carbon are unclear. It can strengthen the effective radiative forcing by aerosol-cloud interactions through reducing entrainment when it resides above the cloud, but burn off the cloud when it resides in the cloud layer (Johnson et al., 2004).

### 2.1.1 Ship emission regulations

Another example of a natural laboratory recently manifested itself temporally through a policy change. On January 1, 2020, the International Maritime Organisation (IMO) of the United Nations mandated that for all ships of decent size, the maximum allowed sulfur content relative to mass of fuel needs to be reduced from 3.5 to 0.5 %, hence reducing the amount of sulfur compounds emitted into the atmosphere. This regulation differs from most previous mandates in that it applies to the open ocean, and not just to Sulfur Emission Control Areas (SECA) near the US/European coasts (where only 0.1% of sulfur in the fuel is allowed). The primary goal of the Atmospheric Composition and Radiative forcing changes due to UN International Ship Emissions regulations (ACRUISE) project is to determine how this international regulation affects aerosols, clouds, and climate (discussed in more detail below). The change in regulations will be an interesting experiment, but it will take several years for a clear signal to emerge from the radical emissions changes in 2020 due to the COVID pandemic (see section 2.8.2)

## 2.2 Industrial sources

Industrial aerosol sources are responsible for a large part of the global anthropogenic aerosol forcing (Stevens et al., 2016). This means that cloud responses to emissions originating from a subset of strong industrial sources (e.g. smelters) may serve as an analogue for global anthropogenic impacts (Toll et al., 2019). Industrial perturbations cover a variety of spatial scales (Figure 3): from isolated factories with a single chimney inducing a narrow ship-track-like perturbation (Rosenfeld, 1999) to continental-scale industrial perturbations (Goren and Rosenfeld, 2015; McCoy et al., 2018). While cloud responses to emissions originating from localized isolated sources provide highest signal-to-noise ratio and are highly informative for process-level understanding (Toll et al., 2019), analysis of continental-scale perturbations is probably more suited for global forcing estimates



(McCoy et al., 2018). Industrial sources emit constantly, although emissions can change over time. As an example, copper and  
200 nickel production facilities in Norilsk, Russia emit more than 1 Mt of SO<sub>2</sub> each year, i.e. more than 1% of global anthropogenic  
SO<sub>2</sub> emissions (Fioletov et al., 2016). Such strong localized emissions induce a high contrast between clouds affected by the  
emissions of the Norilsk smelters and nearby less polluted clouds (Trofimov et al., 2020). The opening and closing of large  
factories and implementation of desulfurization devices can lead to rapid changes in emissions (Fioletov et al., 2016), providing  
additional insight into aerosol impacts on clouds. On the downside, since industrial sources are most often clustered into larger  
205 industrial regions, and therefore create a polluted background, means it can be difficult to observe the impact of individual  
sources.

One of the first discussions of the potential for aerosol-cloud-climate interactions in the literature involves the effect of  
pollution from an industrialized port in southeastern Australia (Twomey, 1974). An early confirmation of the Twomey effect  
of increasing  $N_d$  from pollution came from flights through plumes emitted by the Centralia coal plant in Washington State  
210 (Hobbs et al., 1980). Figure S1 shows sulfur dioxide emissions from the power industry and combustion for manufacturing  
sectors from EDGAR for 2015. The large concentration of pollution sources in rapidly industrializing regions like southern  
and eastern Asia is apparent. Given the number of sources in these regions, it may be hard to use individual power plants or  
industrial sites as natural experiments. In other more remote locations like Australia and Canada, however, there appear to be  
more frequently isolated but large sources. Toll et al. (2019) studied continental natural experiments influenced by industrial  
215 pollution in Russia, Kazakhstan, Canada, and Australia. Stratiform clouds over land responded to isolated pollution sources in  
much the same manner as marine stratiform clouds did. An expanded analysis, focusing on the Norilsk pollution hotspot in  
Russia but including some data from the United States, Europe, and eastern Asia in addition to that used in Toll et al. (2019),  
confirmed that competing LWP adjustments in varying conditions average out to a small offset of the Twomey effect (Trofimov  
et al., 2020).

### 220 2.3 Volcanoes

Large explosive volcanic eruptions have long been studied for their ability to affect the climate by injecting aerosols into  
the stratosphere, blocking sunlight and causing a temporary cooling (Hansen et al., 1992; Robock, 2000; Soden et al., 2002;  
McConnell et al., 2020). It has now been recognized that passive degassing and weakly explosive or effusive eruptions, in  
which volcanic emissions remain at relatively low altitudes, can also produce a cooling effect via their indirect effects on  
225 clouds (Graf et al., 1997; Gassó, 2008; Schmidt et al., 2012). Ship-track-like perturbations have been observed downwind of  
volcanoes at Hawai'i, South Sandwich Islands, Kuril Islands and Vanuatu Islands (Gassó, 2008; Yuan et al., 2011; Ebmeier  
et al., 2014; Toll et al., 2017; Gryspeerdt et al., 2019b; Toll et al., 2019) and also show increased  $N_d$ , decreased drop effective  
radius  $R_e$ , increased cloud brightness, and variable effects on LWP in larger-scale eruptions (Seifert et al., 2011; McCoy and  
Hartmann, 2015; McCoy et al., 2018).

230 Satellite measurements between 1978 and 2014 estimate an average SO<sub>2</sub> flux of  $23 \pm 2$  Tg into the troposphere from passive  
(non-eruptive) degassing (Andres and Kasgnoc, 1998; Carn et al., 2017). The average SO<sub>2</sub> emission rate from explosive  
and effusive eruptions is 3 Tg year<sup>-1</sup>, of which about 1 Tg year<sup>-1</sup> is injected into the upper troposphere and stratosphere





(Carn et al., 2016). Modeling studies indicate that passive degassing and weakly explosive or effusive eruptions elevate the tropospheric background level of sulfur and can induce a significant radiative forcing (Schmidt et al., 2012). The Kīlauea volcano on the island of Hawai'i is an effusive volcano that erupted continuously from 1983 to 2018, with large SO<sub>2</sub> emissions in 2008 and 2018. Kīlauea induces significant perturbations in  $R_e$  downwind of the island of Hawai'i (Yuan et al., 2011; Ebmeier et al., 2014). The eruptions resulted in a 3 standard deviation change in  $N_d$  in the downstream wake of the plume. Perhaps one of the most compelling pieces of evidence for cloud fraction increases due to indirect effects from opportunistic experiments are found in studies based on Kīlauea (Yuan et al., 2011). Mace and Abernathy (2016) also found higher cloud top heights in the Kīlauea plume relative to adjacent clouds unaffected by the plume. Finally, Kīlauea emits continuous SO<sub>2</sub> for long periods of time (months) and thus has the advantage of perturbing clouds over a larger timescale and region and may be more relevant (compared to ship tracks, which are shorter lived) to the climate-scale (Glassmeier et al., 2021).

The 2014-2015 Holuhraun eruption in Iceland lasted 6 months (31 August 2014 to 28 February 2015) and emitted a total of around 11 Tg of SO<sub>2</sub> into the lowermost troposphere (Gislason et al., 2015). Daily SO<sub>2</sub> emission rates averaged 60 kt/day (Gislason et al., 2015; Schmidt et al., 2015), which dwarfs other such eruptions in recent history. Space-based, multi-angle imaging of the eruption on September 11, 2014 shows sulfate particles growing in size downwind, and at about 350 km from the volcano, at an approximate plume age of 10–12 hours, the particles merge into clouds (Flower and Kahn, 2020). These observations may offer a constraint on the timescale of downwind particle aggregation, deposition, and/or new particle formation for different thermodynamic conditions (most notably the atmospheric static stability and wind shear at plume altitude).

An analysis of the 2014-2015 Holuhraun fissure eruption in Iceland revealed that global climate models can represent the decrease in  $R_e$  seen in satellite retrievals. Malavelle et al. (2017) show that the increases of LWP are far from uniform across models (e.g., HadGEM-UKCA shows almost zero LWP adjustment, while other models show a wide variation). Ship tracks and volcanic plumes that show variable cloud adjustments depending on meteorological conditions and precipitation state. Because LWP adjustments can influence the strength of the effective radiative forcing (Toll et al., 2017) due to aerosol-cloud-interactions (ERFaci) it is critical to establish the mechanistic pathways which give rise to this diversity amongst observational datasets and models.

## 2.4 Fires and Biomass burning

Agricultural burning as a promising natural laboratory for studying aerosol-cloud interactions was proposed as early as the 1960s, as there appeared to be a decrease in precipitation following an intensification of burning associated with sugar-cane production in northeastern Australia (Warner, 1968; Warner and Twomey, 1967). Biomass burning events in tropical forest and subtropical savanna regions have long been recognized as promising targets for studying aerosol-cloud interactions (Kaufman and Nakajima, 1993; Rosenfeld and Lensky, 1998; Haywood et al., 2003). Wang et al. (2018) revealed contrasting dependence of lightning on aerosol loading for smoke and dust aerosols in Africa. Under low loading conditions, lightning is enhanced by aerosol for both types, similar to the finding of Thornton et al. (2017) along one of the world's major shipping routes characterized by generally low aerosol loading. Although, low aerosol loading with more lightning is consistent with a signature



of rainfall scavenging and does not imply causality. Lightning exhibits little trend in response to biomass burning aerosol generated in central and southern Africa but decreases for dust aerosols due to both the much stronger aerosol radiative effect that suppresses convection and to differences in meteorology between the two regions (Wang et al., 2018).

270 The extensive seasonal biomass burning in sub-equatorial Africa has also received significant attention, especially in the last several years, when multiple aircraft campaigns took place across the region (Fishman et al., 1996; Garstang et al., 1996; Formenti et al., 2003; Swap et al., 2003; Haywood et al., 2003; Zuidema et al., 2016; Diamond et al., 2018; Zuidema et al., 2018; Formenti et al., 2019; Haywood et al., 2020; Redemann et al., 2020). Recent fire seasons in California in 2020 and in Australia in 2019/2020 generated many large-scale smoke plumes (example in Figure 5). These strong fire seasons have the  
275 potential to induce large-scale anomalies in cloud properties. Analysis of cloud anomalies compared to long-term climatology is challenging in the case of fires, as it is difficult to separate the aerosol effect from the influence of weather anomalies that favor the occurrence of the extreme fire season in the first place.

Some individual wildfire plumes were analyzed in the studies of Toll et al. (2019); Trofimov et al. (2020). Another opportunistic experiment is the smoke-cloud system that develops seasonally over the southeast Atlantic stratocumulus deck  
280 (Zuidema et al., 2016, 2018) where it is obvious that the smoke can be traced to the effects of agricultural burning over the continent rather than processes occurring over the ocean. The regional-scale perturbation lasts in some form for four or five months each year. The aerosol contribution from the smoke clearly overwhelms other aerosol sources in the free troposphere and on occasion dominates the marine boundary layer aerosol population. However, meteorological influences (e.g. the atmosphere stability profile) still play a major role in any observed cloud properties (Wilcox, 2010; Adebisi et al., 2015) and the  
285 large vertical and horizontal extents of the smoke plumes make disentangling strong and competing direct, semi-direct, and indirect effects over both the continent and ocean remain a challenge.

## 2.5 Hemispheric differences

The Southern Hemisphere (SH), in particular the remote Southern Ocean (SO), is our closest present-day (PD) analog to the pre-industrial (PI) aerosol state (Schwartz, 1988; Hamilton et al., 2014). Hemispheric differences in aerosols and clouds  
290 may thus provide a potential natural laboratory.  $R_e$  is smaller in the Northern Hemisphere (NH) (Han et al., 1994; Feng and Ramanathan, 2010) and  $N_d$  is larger (Feng and Ramanathan, 2010; McCoy et al., 2020) compared to the SH. However, high values of  $N_d$  can be found in pristine conditions over the ocean when clouds are coupled to a surface under conditions of high wind (McFarquhar et al., 2020). The hemispheric contrast between cloud properties in the pristine SH and the polluted NH is a unique form of natural laboratory for estimating the bulk effect of natural and anthropogenic aerosol emissions on our  
295 climate. Several studies have employed this method to understand the PI environment, estimate the change in climate due to industrialization, and improve the accuracy of our future climate predictions by constraining RFac. Boucher and Lohmann (1995) used the hemispheric difference in  $R_e$  to evaluate the robustness of RFac simulated in several global climate models (GCMs) after prescribing a relationship between sulfate mass and  $N_d$ . Feng and Ramanathan (2010) found that a chemical transport model driven by reanalysis meteorology was able to produce a difference in  $N_d$  between the NH and SH that is  
300 consistent with hemispheric contrasts in satellite retrievals of  $R_e$  and cloud optical depth. When comparing to satellite studies,



McCoy et al. (2020) found that the hemispheric  $N_d$  contrast is overestimated by a collection of CMIP5 (Ghan et al., 2016) and development GCM simulations (Mulcahy et al., 2018), as well as a perturbed parameter ensemble (PPE) exploring parametric uncertainty (Yoshioka et al., 2019). This bias was shown to be a result of models producing uniformly too little SH  $N_d$ , and thus too little inferred PI  $N_d$ , while also producing increasingly too much NH  $N_d$  with increasing RFaci. Application of the  $N_d$  contrast to the PPE was able to constrain RFaci by eliminating overly negative RFaci values (see example in Figure 6), producing an RFaci range consistent with independent analysis methods (e.g., Bellouin et al., 2020) and further substantiating the usefulness of the hemispheric contrast methodology.

## 2.6 Long Term Trends

Long-term trends in aerosol driven by economic growth and/or policy-driven reductions in pollution may also arguably serve as natural laboratories with the benefit that the long timescales minimize the effect of weather noise on results. For instance, the decrease in cloud reflectance between the 1980s and 1990s has been called the “Gorbachev” effect as it related to the economic restructuring of Eastern Europe following political changes (Krüger and Graßl, 2002). The co-incident upward trend in surface solar radiation (Wild et al., 2005) was found useful as an emergent constraint on simulated effective radiative forcing by aerosol-radiation interactions (ERFari) in the CMIP5 multi-model ensemble (Cherian et al., 2014). In other regions, there are large discrepancies between surface radiation trends and model results (Stjern et al., 2011; Moseid et al., 2020).

Figure 7 shows that, according to the CMIP6 emissions database, aerosol-generating  $\text{SO}_2$  emissions from the continental US increased steadily from 1850 to around 1910 where they stabilized and then later dropped fairly rapidly from just after 1960 until the end of the record in 2014. The latter decrease is associated with the various federal Clean Air and Air Pollution Acts, the first of which was introduced in 1955, and is also supported by OMI observations of atmospheric  $\text{SO}_2$  concentrations (McCoy et al., 2018) for the period after 2003. The  $\text{SO}_2$  emission changes are mirrored by  $N_d$  changes in the ensemble mean CMIP6 UK Earth System climate model (UKESM1; Sellar et al., 2019) for a region in the North Atlantic that is downwind of the US. The model  $N_d$  and trend match those from MODIS very well over the 2003-2014 period giving confidence in the CMIP6 emissions and the ability of this model to accurately translate emissions into changes in cloud properties, which involves several stages. However, Robson et al. (2020) and (Grosvenor and Carslaw, 2020) show that this model does exhibit biases in  $N_d$  and its trends in other regions.

It is tempting to relate these changes in  $N_d$  to observed and simulated trends in cloud fraction, LWP, and shortwave fluxes. For example, Robson et al. (2020) suggest that the negative upwelling shortwave top of atmosphere flux trend in UKESM1 for the wider North Atlantic region is too strong compared to CERES, with the model also displaying a positive bias in upwelling shortwave top of atmosphere fluxes coincident with a cloud fraction that is too high compared to CALIPSO (see also Grosvenor and Carslaw, 2020). The overly strong trend may be interpreted as an overly strong cloud response to aerosol. However, natural multi-decadal variations in the sea surface temperature in the North Atlantic (which are not necessarily captured by models) could also lead to cloud trends unrelated to aerosols (Vaideanu et al., 2018). Figure 7 provides a demonstration of this through the timeseries of the all-sky LWP (i.e., including the zero LWP values in the clear parts of gridboxes and hence showing the combined effect of both cloud thickness and cloud area fraction changes) from the CMIP6 UKESM1 model for the same region



335 downwind of the US where large negative  $N_d$  trends over the 1960-2014 period were described above. A negative 1971-2014  
LWP trend of  $-0.1 \pm 0.03 \text{ g m}^{-2} \text{ yr}^{-1}$  (significant to  $>99.9\%$ ) is apparent in the mean of the 16-member ensemble. However,  
the magnitude of the LWP change over this period is much smaller than the inter-ensemble spread in LWP for a given year  
(shading) and there are a large range of trends across the ensemble when computed using individual members ( $-0.21$  to  $-0.02 \text{ g}$   
 $\text{m}^{-2} \text{ yr}^{-1}$ ). This implies that, as far as we can trust the model, for the same forcing a large range of trends are equally plausible  
340 due to natural variability and that it would therefore be difficult to attribute an observed trend to a forcing (e.g., the aerosol  
forcing). This is supported by the observed LWP time series from the MAC (Multisensor Advanced Climatology) microwave  
satellite LWP dataset (Elsaesser et al., 2017), however the dataset is also very noisy and the 1988–2014 trend is not statistically  
significant.

Furthermore, climate models predict that greenhouse gas driven cloud changes (and by extension temperature driven changes  
345 i.e., cloud feedbacks) are very likely to have occurred over the historical period in addition to aerosol driven changes and natural  
variations (Norris et al., 2016; Cherian and Quaas, 2020; Schneider, 2020). This is true of the LWP trend from the UKESM1  
ensemble mean highlighted above, which can be shown to have been driven almost entirely by greenhouse gas forcing rather  
than by the aerosol changes. Thus, any observed cloud changes include natural variability, aerosol-cloud interactions, cloud  
feedbacks (due to surface temperature change) and cloud adjustments to the forcing ( $\text{CO}_2$ , aerosols, etc.) evolution. This makes  
350 it difficult to infer cloud-aerosol adjustments from long term trends since it requires knowledge of the non-aerosol driven  
changes. The agreement over the satellite era between the modelled CMIP5 cloud fraction trends and those from observations  
as demonstrated in Norris et al. (2016) gives some confidence in the ability of the models to represent changes in clouds in  
response to the different balance of forcings, but the uncertainty does not allow an easy quantification of the forcing. Further  
uncertainty comes from the possibility that spurious observed trends can be introduced due to several issues in satellite data  
355 such as instrument and platform changes, orbital drift, calibration issues and other unidentified stability problems, in addition  
to differences in retrieval algorithms (Evan et al., 2007; Levy et al., 2013; Norris and Evan, 2015; Norris et al., 2016).

Rapid changes in anthropogenic emissions have occurred over east and south Asia (especially China) over the last few  
decades. China's aerosol loading increased most strongly during the rapid industrial growth of the 1970s-1990s, followed by  
gentle increases from 2000-2010 and finally decreased thereafter as a result of increased political attention and action on air  
360 pollution (Jin et al., 2016; Zhang et al., 2019). Accompanying these trends were changes in surface radiation, temperature, and  
precipitation, some of which were attributed to the influences of ARI and ACI, at least to some extent (Li et al., 2016, 2019b;  
Shi and Brasseur, 2020). Yet, different types of aerosols were identified to play rather different roles, which helps explain the  
opposite decadal-trends in severe thunderstorms in central China (where absorbing aerosols dominate) and southeast China  
(where hygroscopic aerosols dominate; Yang et al., 2013; Yang and Li, 2014).

365 Increases in  $N_d$  over the East China Sea were observed from the 1980s to the 2000s (Bennartz et al., 2011). Co-incident  
with this is a decreasing trend in cloud fraction in the same region (Xia, 2010; Norris et al., 2016), which may be a hint at a  
reduction in cloudiness with increasing  $N_d$ , although the trend could also be due to other drivers. McCoy et al. (2018) observed  
a stabilization of  $N_d$  over China in the 2000s followed by a decreasing trend in the 2010s. In this more recent period (2006 -



2015), Benas et al. (2020) document an increase in LWP and cloud fraction that, if caused by the decrease in aerosol, would  
370 imply a reduction in both quantities with increasing aerosol.

More generally, Cherian and Quaas (2020) demonstrated that in the CMIP6 multi-model ensemble, aerosol optical depth  
(AOD) and  $N_d$  trends compared favorably to trends derived from MODIS over four different regions with different behaviors  
of anthropogenic aerosol sources. In contrast, CMIP5 model trends were erroneous, e.g. over north-western North America, but  
also over China. Both CMIP5 and CMIP6 models generally showed trends in LWP and cloud fraction that were inconsistent  
375 with the pattern derived from MODIS, although the observed trends were rarely statistically significant.

A MODIS analysis examining negative long-term AOD and aerosol index (a better measure of finer mode aerosol Nakajima  
et al., 2001), and hence CCN (Stier, 2016), trends off the eastern coasts of the United States and China, and off the western coast  
of Europe, found that  $N_d$  also decreased while LWP was relatively unaffected in 15 years of MODIS data (Bai et al., 2020).  
This is in line with the other forms of natural laboratory evidence that has also indicated small LWP adjustments. However, as  
380 discussed above, extreme caution is required when interpreting trends in cloud properties as being caused by aerosol forcing  
even when there are strong concurrent aerosol trends. Ways forward may involve using climate models or machine learning to  
identify situations when cloud trends are likely to be caused by aerosol rather than other factors and focusing on those for the  
quantification of cloud-aerosol adjustments.

## 2.7 Weekly cycle

385 A seven-day cycle is not a common naturally occurring phenomenon and the regional variation of weekdays with maxima and  
minima in anthropogenic reactive gases are clear evidence of an anthropogenic signal (Beirle et al., 2003). Weekend effects  
have been directly tied to the study of ACI in particular. Weekend declines and weekday peaks in pollution have also been  
observed in satellite  $N_d$  and reconstructed in climate models in Europe (Quaas et al., 2009). There is a clear weekly cycle in  
AOD with minima on Mondays, and a co-incident cycle in  $N_d$  (Fig. 8). However, trends in any other quantity (including LWP)  
390 are unclear or ambiguous. Higher weekday aerosol levels in the United States have been argued (controversially) to be linked  
to the invigoration of storms (Schultz et al., 2007; Bell et al., 2008, 2009; Rosenfeld and Bell, 2011). Similarly, lower weekend  
levels of absorbing aerosol have been hypothesized to suppress thunderstorm activity in central China whereas higher weekday  
levels of more hygroscopic aerosol in southeast China have been hypothesized to invigorate storms in that region (Yang et al.,  
2016). However, the occurrence of a single maximum and minimum each, among just seven instances, is rather likely, so that  
395 attribution using e.g. model evidence is required to corroborate conclusions (Barnet et al., 2009; Quaas et al., 2009; Stjern,  
2011; Daniel et al., 2012; Sanchez-Lorenzo et al., 2012).

## 2.8 Particular events

Effects on aerosols from short term events, at the regional or global scale may also provide a natural laboratory if the pertur-  
bations are large or abrupt enough. These events range in scale from a single holiday to sudden global economic changes (see  
400 below). Recurring holidays and days of rest have been investigated around the world (Forster and Solomon, 2003; Sanchez-  
Lorenzo et al., 2012; Earl et al., 2015; Pereira et al., 2015). Traffic and fireworks effects have sizable impacts on gaseous and



particulate pollutant concentrations during the extended Chinese Lunar New Year celebrations (Tan et al., 2009; Gong et al., 2014; Seidel and Birnbaum, 2015; Jiang et al., 2015; Pope et al., 2016; Lai and Brimblecombe, 2017).

### 2.8.1 Emission Events in China

405 There have been a number of special events held in China during which air quality experienced drastic changes over relatively short periods, such as the 2008 Olympics and Paralympics in Beijing (Cermak and Knutti, 2009; Witte et al., 2009; Wang et al., 2010; Guo et al., 2013), 2010 World Expo in Shanghai (Hao et al., 2011), 2014 Youth Olympic Games in Nanjing (Ding et al., 2015), the 2014 Asia-Pacific Economic Cooperation meeting (Sun et al., 2016), the 2015 China Victory Day parade (Wang et al., 2017; Zhao et al., 2017), and the 2016 G20 Summit (Li et al., 2019a). These have provided unique opportunities to  
410 investigate the impact of human activities on air quality, weather and climate. Perhaps the most famous example of an abrupt, ephemeral change in the environment clearly associated with human decisions is the massive effort to reduce air pollution surrounding the 2008 Beijing Olympic Games. Cermak and Knutti (2009) used a neural network to account for potential meteorological confounders of an aerosol effect from the Olympics-related cleanup. Although they were able to detect a decrease in satellite-retrieved aerosol loading around Beijing during the Summer Games, its magnitude was relatively small  
415 compared to meteorological variability. Cloud-seeding efforts using silver iodide were carried out ahead of the 2008 Olympics opening ceremony in an attempt to create a downpour but keep the stadium dry, although the efficacy of weather modification above natural variability remains difficult to verify (Flossmann et al., 2019). The annual Chinese New Year Spring Festival holiday is another major, yet more regular, occasion when the vast majority of the population stops working for 2 to 4 weeks, as hundreds of millions of migrant workers return to their hometowns in the countryside. Systematic changes in anthropogenic  
420 emissions and ensuing changes in gaseous pollutants and aerosol formation, especially on fine particulate matter (PM<sub>2.5</sub>), have been extensively studied (Tan et al., 2009; Wang et al., 2017). As shown recently by Wang et al. (2021), sharp reductions were observed during the 2019 festival in virtually all precursor gases (e.g. SO<sub>2</sub>, NO<sub>2</sub>), except ozone (O<sub>3</sub>), and aerosol particle (organic, sulfate, nitrate, BC, etc.) number and mass concentration at all sizes, while the meteorology remained relatively stable prior to and during the festival (Figure 9). Although even small changes in meteorology can have large implications for  
425 cloud radiative properties (Gryspeerd et al., 2016). There are relatively few studies concerning the impact of these events on meteorological variability (Li et al., 2019a), partially due to the short periods and thus limited data samples.

### 2.8.2 COVID Pandemic

The global COVID-19 pandemic that emerged and spread around the world in early 2020 created unprecedented socioeconomic changes. The resulting changes in economic activity have been linked with sharp and sudden declines in certain forms of air  
430 pollution such as nitrogen oxides in China, Europe, South Korea, and the United States (Bauwens et al., 2020; Liu et al., 2020). However, the effects of the shutdowns on other pollutants like ozone and aerosol particles have proven to be less straightforward (Chang et al., 2020; Diamond and Wood, 2020; Huang et al., 2020; Le et al., 2020; Shi and Brasseur, 2020; Wang et al., 2020). Carbon dioxide emissions declined modestly due to shutdown measures worldwide (IEA, 2020; Le Quéré et al., 2020). Strong declines in NO<sub>2</sub> have been observed in locations including eastern Asia, Europe, the Indian subcontinent, and North America



435 (Bauwens et al., 2020; Diamond and Wood, 2020; Liu et al., 2020). Estimates of changes in PM<sub>2.5</sub> from ground stations in China range from no or small changes to reductions of a third to a half (Shi and Brasseur, 2020).

Diamond and Wood (2020) found a substantial decline in NO<sub>2</sub> over China during the February 2020 shutdowns but no clear changes in AOD or  $R_e$  and thus suggested that the implications of the February 2020 shutdown on regional climate is negligible. In China, the reduction in emissions during the pandemic may have been offset by the shallowing of the planetary  
440 boundary layer (PBL). As a consequence, the occurrence of a very serious widespread pollution episode in the midst of the pandemic due largely to the accumulation of pollutants in the shallow PBL posed a special challenge to the evaluation of the influences of the pandemic-related reductions (Su et al., 2020). Loeb et al. (2021) show that there would have been a substantial reduction in AOD and aerosol direct radiative effect over China had February and March 2020 not been as humid as it was.

Ensembles of simulations with two different Earth System Models using emissions reductions from mobility data (Forster  
445 et al., 2020) to represent the COVID-19 response show a robust decrease in AOD and increase in  $R_e$  over China in February 2020 but at a level likely too small for observational methods to detect (Gettelman et al., 2021b). Nonetheless, the two models produce a sizable global mean forcing from reduced aerosol-radiation and aerosol-cloud interactions (up to +0.3 W/m<sup>-2</sup> in May 2020), although much of that effect is from later shutdown measures outside of China and would probably not be distinguishable from noise in actual observations. An assessment of the relative magnitude of the effects of pandemic-induced  
450 changes to greenhouse gases, air pollution and aerosols with a climate model emulator found that RF<sub>aci</sub> dominate the response over GHG and ozone changes. The net radiative effect is projected to be a negligible global warming for the next two years, followed by slight relative cooling from lowered CO<sub>2</sub> emissions (Forster et al., 2020; Gettelman et al., 2021b). Unless a prolonged global depression develops in response to the economic shock of COVID-19 and the curtailment of many normal business activities, it seems unlikely that large climate-relevant effects will be detectable in observations (Ming et al., 2021;  
455 Fyfe et al., 2021; Jones et al., 2021).

The aviation sector saw some of the most significant changes during the COVID-19 pandemic, with reductions in air traffic of up to 70% Gettelman et al. (2021a). Schumann et al. (2021), Gettelman et al. (2021a) and Quaas et al. (2021) have used these changes to try to quantify radiative forcing from contrail reductions. Schumann et al. (2021) found improved correspondence in radiative fields between observations and simulations when contrails were included, and Quaas et al. (2021) found corre-  
460 sponding changes in cirrus at a global scale in regions with large changes in air traffic, implying a global radiative forcing of 0.061 Wm<sup>-2</sup>. Gettelman et al. (2021a) found similar sign changes using a global model, which has an overall contrail radiative forcing from all aviation in 2020 of 0.050 Wm<sup>-2</sup>, helping to validate results of recent assessments of aviation radiative impacts (Lee et al., 2021).

### 3 Databases for Experiments of Opportunity

465 Over the decades, a growing number of databases have contributed to the increasing knowledge on this topic. Table S2 lists several cited databases that are either publicly available or downloadable through private means. Many of these databases are tagged to specific peer-review publications. Carn et al. (2017) catalogs the emission rates of SO<sub>2</sub> from several hundred



passive degassing volcanoes using a combination of satellite retrievals and ground-based measurements. In addition, natural experiments resulting from prominent industrial sites such as Norilsk (Fioletov et al., 2016), persistent and weakly-explosive volcanic eruptions, (e.g. South Sandwich Islands' volcanoes and Ambrym) and significant fire 'outbreak' seasons have been logged from satellite imagery in Toll et al. (2019) and Trofimov et al. (2020). Ship track databases identified from satellite imagery are available for the tracks: a) off the California coast (Coakley and Walsh, 2002; Segrin et al., 2007; Christensen et al., 2009), b) collocated to CloudSat and CALIPSO (Christensen and Stephens, 2011, 2012; Chen et al., 2012; Christensen et al., 2014), c) off the California coast for studying recent shipping emission regulations (Gryspeerd et al., 2019b) and d) globally through use of machine learning (Yuan et al., 2019).

These databases and emission estimates have already facilitated fruitful intercomparisons of observations and models (e.g. for GCMs see AeroCom ACI experiment, and for LES intercomparison see Glassmeier et al. (2021)), with the synthesized values used to construct the statistics in Figure 10 and Figure S4 (as described further in the results section). These figures were constructed from published estimates of  $N_d$ ,  $R_e$  and LWP for numerous opportunistic experiments derived from satellite and in situ observations, large eddy simulations, cloud resolving model simulations and global circulation models. Figure 10 contains satellite retrievals of volcano, industry and fire tracks (mostly from Toll et al. (2019)) and ship tracks. Shipping corridor perturbation results are from Diamond et al. (2020), effusive volcanic eruption is from Malavelle et al. (2017) and the global shipping model is from Lauer et al. (2007), two estimates from Peters et al. (2013). LES (Wang and Feingold, 2009; Berner et al., 2015) and cloud resolving model (Possner et al., 2015, 2018) simulation results for ship tracks are also included in Figure 10. An exact breakdown of each study used in the figure is provided in Table S1. This list is weighted more to observational studies partly due to their high occurrence in the literature. Thus, publications were sorted by they type of natural laboratory and data used in order to provide a comprehensive reference for the expected cloud responses. The expansion and synergistic use of these databases is key to providing constraints on aerosol radiative forcing and cloud perturbations in atmospheric modelling. Finally, while some sources like volcanoes or industrial sites are well documented from public sources, some key data like ship movements are proprietary and unavailable for most researchers.

## 4 Analysis and Methods

Below we briefly summarize the common usage of the wide range of field campaigns, models and observations used to study natural laboratories and experiments of opportunity.

### 4.1 Satellite Observations

One of the first applications of satellites was the use of imagery of cloud cover to supplement weather forecasting. Since Vanguard 2 and TIROS-1 in 1959, a multitude of platforms have provided almost continuous observations of the Earth. Satellite imagery provides a global perspective on aerosol and cloud processes unavailable from other vantages. Typically the pixel size is at most a few kilometres, though some sensors can sample down to tens of metres (e.g. Landsat, ASTER). Current





geostationary satellites provide imagery every 10-15 minutes over  $\sim 60\text{N} - 60\text{S}$ . The gigabytes of data produced every minute  
500 provide a vast trove of data with which to identify, and monitor, natural laboratories and experiments.

The retrieval of cloud properties is typically performed using a unique combination of visible, near-infrared and infrared  
channels, with many retrievals derived from the methods of Nakajima and King (1989). Very roughly, visible reflectance  
( $\lambda = 400 - 800 \text{ nm}$ ) and near-infrared radiance ( $\lambda = 1 - 4 \mu\text{m}$ ) provide information about cloud optical depth from scattering,  
and the size of cloud particles by their absorption, although these wavelengths do not strictly provide orthogonal information  
505 on the retrieved cloud properties. Infrared brightness temperatures ( $\lambda = 5 - 13 \mu\text{m}$ ) are sensitive to the cloud top height from  
their emission.

Coakley et al. (1987) provides an early demonstration of this principle by showing that, for populations with similar cloud  
top heights, ship tracks are brighter at  $3.7 \mu\text{m}$  than uncontaminated pixels while having similar reflectances at  $0.63 \mu\text{m}$ . They  
argue that when clouds are sufficiently dense, photons will interact with several droplets before being observed, and the  $3.7\text{-}\mu\text{m}$   
510 reflectance of a cloud is determined by the fraction of interactions that absorb rather than scatter light. As the cross-section for  
scattering is approximately proportional to droplet surface area while absorption cross-section scales with droplet volume, a  
cloud with smaller droplets appears brighter because due to decreased transmission through the cloud. Uncertainties that can  
influence the estimate of satellite retrieved  $R_{\text{Fac}}$  are the humidification of aerosols and enhanced reflectance due to scattering  
off the edges of clouds typically leads to larger estimates of the Twomey effect and adjustments in  $C_F$  (Gryspeerd et al., 2016;  
515 Christensen et al., 2017). Furthermore, invalid assumptions on adiabaticity for non plane-parallel clouds where 1D radiative  
transfer is used on 3D clouds can typically results in uncertainties in retrieved  $N_d$  typically larger than 70% (Grosvenor et al.,  
2018).

The spatial resolution of the passive satellite imagers such as AVHRR (Advanced Very High Resolution Radiometer) and  
MODIS are typically 1 km, making them very useful for detection and attribution. Geostationary satellites are an ideal tool  
520 for investigating time-dependent processes in response to aerosol (Goren and Rosenfeld, 2012, 2015; Christensen et al., 2020)  
because of their ability to take snapshots over time. With the new high-resolution Advanced Baseline Imager (ABI) on GOES  
and Himawari geostationary satellites, local-scale cloud retrievals can be performed within cloud fields perturbed by point-  
source emissions as the response evolves.

Instantaneous satellite observations from polar-orbiting satellites can be used to infer time-dependent processes. Gryspeerd  
525 et al. (2021) used MODIS imagery to study ship track evolution, assuming that the response of clouds to the ship emissions as  
a function of time is related to the distance from the head of the ship track. This novel methodology allows the use of higher  
resolution, with respect to most of the older generation geostationary satellites, to investigate aerosol-cloud interaction from  
satellites. Goren and Rosenfeld (2015) used geostationary satellite observations to relate long-lived extensive overcast stratocu-  
mulus deck-to-air pollution originating in Western Europe. Complementing their satellite analysis with an aerosol transport  
530 model and in-situ observations of CO concentration, they explicitly showed that a closed-cell cloud deck was associated with  
polluted continental outflow from Western Europe.



## 4.2 Field campaigns

A description of several prominent field campaigns targeting different laboratories are discussed below.

### 4.2.1 Field campaigns targeting shipping emissions

535 Airborne field campaigns have demonstrated success in examining boundary layer clouds affected by strong aerosol per-  
turbations. The most common case has been flights targeting ship plumes lofted into stratiform clouds off the U.S. West  
Coast, dating back to the Monterey Area Ship Track (MAST) experiment in 1994 (Durkee et al., 2000b). Several subsequent  
campaigns continued studying ship impacts on clouds, including the Marine Stratus/Stratocumulus Experiments (MASE) I  
and II (Lu et al., 2009), the Eastern Pacific Emitted Aerosol Experiment (E-PEACE) (Russell et al., 2013), and the Nucle-  
540 ation in California Experiment (NiCE) (Sorooshian et al., 2015). Flight planning was aided in large part by an online tool  
(<https://www.marinetraffic.com/en/>) reporting the physical characteristics of ships (e.g., length, beam, tonnage) and their lo-  
cation and speed. The majority of these campaigns were conducted using the Center for Interdisciplinary Remotely-Piloted  
Aircraft Studies (CIRPAS) Twin Otter aircraft, which would fly directly to ships and then conduct zigzag or racetrack patterns  
behind ships to characterize both the clean and perturbed boundary layer (Sorooshian et al., 2015, 2018). Relevant payload  
545 instruments included those measuring droplet size distributions, composition of both cloud water and droplet residual particles  
to chemically confirm evidence of ship influence, and aerosol size distributions and composition below cloud base. The data  
show clear evidence of clouds perturbed by ship plumes based on sharp enhancements in  $N_d$ .

A series of flights as part of the UK ACRUISE project using a wide range of instrumentation on the Facility for Airborne  
Atmospheric Measurements (FAAM) aircraft were conducted in summer 2019 through the English channel and off the west  
550 coasts of Portugal and the UK. The main goals of the flights, supported by large eddy simulations and satellite cloud detection,  
were to quantify ship emission rates and study cloud properties in ship tracks. Analysis to date that compares 2019 observations  
(Yu et al., 2020) outside and inside of the SECA indicate much lower emissions of sulfur dioxide gas, particulate sulfate, and  
aerosol particles large and/or hygroscopic enough to act as CCN within the SECA despite higher shipping traffic density (taken  
to be a proxy for the open ocean after 2020). Post-regulation flights in the same areas, scheduled for summer 2021, will be  
555 used to verify the anticipated changes in emissions and cloud sensitivities. Long-term ground observations of sulfate aerosol  
(and sulfur isotopes) at the Penlee Point Atmospheric Observatory in southwest UK and at the ARM-ENA site at the Azores  
is being examined within ACRUISE to quantify the impact of shipping regulation on the aerosol sulfur burden. Finally, both  
global modelling and satellite cloud detection (aided by machine learning) in conjunction with air mass trajectory analyses will  
be used to estimate the total radiative effect of ship emissions. In contrast to earlier studies, ACRUISE aims to quantify the  
560 impacts of ship emissions not only in the near field (e.g. ship tracks, which only occur for a very small fraction of the time),  
but also in the far field, where diffuse emissions are expected to affect the background aerosol concentrations.



#### 4.2.2 Field campaigns targeting continental outflow

Ship plumes are relatively narrow and often difficult to sample with airborne platforms, especially when winds are not favorable and if instruments have poor time resolution. Another avenue to examine strong perturbations superimposed on a natural marine background is offshore of major continents where pollution outflow impacts much broader spatial areas as compared to a single ship (Goren and Rosenfeld, 2015). Several airborne field campaigns have focused on the area off the U.S. East Coast including the North Atlantic Regional Experiment (NARE) and the International Consortium for Atmospheric Research on Transport and Transformation (ICARTT) (Sorooshian et al., 2020). However, the most recent campaign, the Aerosol Cloud meteorology Interactions over the western Atlantic Experiment (ACTIVATE), is making the most concerted effort of any past campaign to investigate aerosol-cloud interactions over the western North Atlantic Ocean where droplet concentrations exhibit sharp gradients offshore (Sorooshian et al., 2019). ACTIVATE is conducting detailed, simultaneous, and systematic measurements of aerosols and clouds from in situ and remote sensing instruments deployed on two coordinated aircraft. Aerosol Characterization Experiments (ACE-2) was a major campaign examining European continental outflow over the Canary Islands and NE Atlantic (Raes et al., 2000). In addition, VAMOS Ocean-Cloud-Atmosphere-Land Study focused considerable efforts on characterizing the outflow of sulfate aerosols from smelters in Chile (Wood et al., 2011). One of the key findings from these campaigns is that the transport of pollution into the remote marine PBL tends to occur in the free troposphere, and is then subsided and entrained into the PBL, rather than being transported entirely at low levels.

#### 4.2.3 Field campaigns targeting fires

While usually focused on ship track sampling, some of the more recent CIRPAS Twin Otter campaigns, beginning in 2013 with NiCE, experienced strong perturbations from an unexpected source, namely that of major biomass burning plumes from US West Coast wildfires. The NiCE campaign and subsequently the 2016 Fog and Stratocumulus Evolution Experiment (FASE) included numerous flights and quantified the impacts of biomass burning plumes on stratocumulus clouds including both when the plumes were above (Mardi et al., 2018) and in/below clouds (Brioude et al., 2009; Mardi et al., 2019).

Several campaigns have also targeted emissions from Africa into the S. E. Atlantic, where biomass burning plumes affect a shallow cloud layer. As mentioned above, multiple field deployments have focused on smoke from the southern African biomass burning season (roughly June-October), including the Transport and Atmospheric Chemistry near the Equator Atlantic (TRACE-A) campaign in 1992, the Southern African Regional Science Initiative (SAFARI) campaigns in 1992 and 2000 (Lindesay et al., 1996; Swap et al., 2003), and a number of recent campaigns that took place over the southeast Atlantic region since 2016 (Zuidema et al., 2016). The Observations of Aerosols above Clouds and their Interactions (ORACLES) campaign deployed a NASA P-3B Orion turboprop and ER-2 high-altitude aircraft from Walvis Bay, Namibia, in September 2016 and then only the P-3 from São Tomé, São Tomé e Príncipe, in August 2017 and October 2018 to study the interactions of smoke and clouds over the remote ocean (Redemann et al., 2020). The Clouds and Aerosol Radiative Impacts and Forcing: Year 2017 (CLARIFY) campaign deployed the FAAM aircraft from Ascension Island in August-September 2017 with similar objectives (Haywood et al., 2020). Both aircraft campaigns included payloads designed for intensive sampling of aerosol and



595 cloud properties and radiation both remotely and in situ. Around the same time, the Layered Atlantic Smoke Interactions with  
Clouds (LASIC) ground campaign deployed the Department of Energy Atmospheric Radiation Measurement Mobile Facility  
1 to Ascension Island from June 2016 to October 2017 (Zuidema et al., 2018). Focusing closer to the southwestern African  
coast, the Aerosols, Radiation and Clouds in southern Africa (AEROCLO-sA) campaign in August-September 2017 deployed  
the French Falcon 20 operated by the Service des Avions Français Instrumentés pour la Recherche en Environnement (SAFIRE)  
600 from Walvis Bay, Namibia, and a ground site at the SANUMARC Research Centre of the University of Namibia in Henties  
Bay (Formenti et al., 2019).

Results so far have shown that smoke from southern African biomass burning is often found within the remote southeast  
Atlantic boundary layer (Zuidema et al., 2018) and can have important radiative (Zhang and Zuidema, 2019) and microphysical  
(Gupta et al., 2021) effects. Important caveats have also been identified, including that methods that relate cloud properties  
605 to above-cloud rather than below-cloud aerosol concentrations likely misrepresent aerosol microphysical effects on clouds  
(Diamond et al., 2018); that at high smoke concentrations, clouds move from an aerosol-limited to an updraft-limited regime  
in which cloud sensitivity to further aerosol increases is limited (Kacarab et al., 2020); and that some of the lowest aerosol  
concentrations observed at Ascension Island occur during the biomass burning season, likely due to in-cloud scavenging  
(Pennypacker et al., 2020). Surprisingly, smoke from subequatorial Africa influences clouds north of the equator in southern  
610 West Africa as well, as documented by the Dynamics-aerosol-chemistry-cloud interactions in West Africa (DACCIWA) aircraft  
campaign that took place in June-July 2016 (Haslett et al., 2019).

### 4.3 Large Eddy & General Circulation Model Simulations

Numerical modelling is a useful tool to study ACI in opportunistic experiments. Models enable isolation of specific effects  
as well as conducting sensitivity tests, thus acting as a complementary analysis alongside observations. Numerical studies  
615 could either be designed to resolve cloud dynamics and processes on the relatively small scales in a large-eddy simulation  
(LES; usually grid spacing of  $< 100$  m and domain size of few to few tens of km e.g., Berner et al., 2015) and regional scale  
simulations (usually grid spacing of 1 km and domain size of 1000 km, e.g., Possner et al., 2015), or to focus on a global climate  
scale and atmospheric circulation with a general circulation model (GCM; usually grid spacing of 100 km, e.g., Gettelman et al.,  
2015). The latter can be run for many decades and capture the climate system responses and trends but cannot directly resolve  
620 cloud processes and hence rely on parameterizations of sub-grid scale processes. Climate scale models suffer from the coarse  
view of important sub-grid scale variations for clouds and aerosols (and their interactions) for numerical efficiency. On the  
other hand, cloud resolving modelling has proven to be a useful tool for improving process-level understanding but cannot  
capture the larger climate response, including interactions between cloud-scale processes and larger-scale circulation changes.  
The DYnamics of the Atmospheric general circulation Modeled On Non-hydrostatic Domains (DYAMOND; Stevens et al.,  
625 2019) initiative endeavors to represent the full three-dimensional fluid dynamics of the atmospheric circulation at 9-km spatial  
resolution over the globe which will be a useful tool for many natural laboratories discussed here.

These two approaches have been used to study opportunistic experiments and are complementary to each other. For example,  
Liu et al. (2000), performed numerical modeling experiments of ship emissions and found that boundary layer decoupling is



an important process that affects the vertical transport of ship emissions. Berner et al. (2015) used LES to simulate a particular  
630 observed ship-track case and demonstrated a good agreement with observations. LES sensitivity studies demonstrated the role  
of the alignment between the track and the winds in the boundary layer and of the ambient aerosol concentration in determining  
the magnitude of the response (Berner et al., 2015). LES were also demonstrated to be useful for studying the response of  
mixed-phase clouds to ship emissions (Possner et al., 2017). The commonalities to and differences between the response of  
mixed-phase and warm clouds were demonstrated. Wang and Feingold (2009) used LES to study how emitted aerosols are  
635 transported within the marine boundary layer and how they impact cloud microphysical processes, and development. They  
also demonstrated that the amount of cloud brightening strongly depends on meteorology, background aerosol conditions and  
effect of secondary circulations (discussed later). Goren et al. (2019) further used LES in a Lagrangian setup, in which clouds  
are simulated along a realistic observed trajectory and are driven by meteorological conditions taken from reanalysis. They  
showed that closed cells, which formed within a polluted air mass, would have broken up sooner in a cleaner atmosphere.  
640 While aerosol was the main factor determining the consistent delayed cloud breakup by suppressing precipitation onset, the  
breakup time was also significantly modulated by LWP changes driven by diurnal cycle and large scale meteorology.

Possner et al. (2015) demonstrated that a regional model running with a 2 km grid spacing was able to capture the structure  
of an observed ship-track. They demonstrated that the ship emissions generated a doubling of the cloud optical thickness, an  
increase in  $N_d$  by 300% and decrease in  $R_e$  by about 40%. In addition, Possner et al. (2016) studied the dependency of the  
645 clouds' response to ship emissions on the model resolution. They used a regional model at a range of resolutions, ranging  
from a GCM scale ( $D_x = 50$  km) to the convection-resolving scale ( $D_x = 1$  km), to assess the impact of emission dilution  
and mixing of aerosols in the atmosphere. They demonstrated that both processes contributed almost equally to the simulated  
increase in the shortwave cloud radiative effect at coarser (50km) horizontal resolution. The contrast in the aerosol radiative  
effect across model resolutions suggests more closure studies are needed to resolve this gap.

650 Cloud sensitivity to ship emissions on a larger, more climate relevant, scale is estimated using GCMs. For example, Lauer  
et al. (2007) used a GCM to study the impact of particulate matter from ship emissions on aerosols, clouds, and the radiation  
budget under different emission inventories. They demonstrated that emissions from ships increased the area mean  $N_d$  of low  
marine clouds by up to 30% depending on the geographic region, while the change in liquid water content was small. In  
addition, the  $R_e$  were shown to decrease, leading to an increase in cloud optical thickness of up to 5-10%, again, depending  
655 on the geographical region. Jin et al. (2018) used a GCM to show that the cloud response to ship emissions depended on the  
natural dimethyl sulfide (DMS) emissions, which determine the background aerosol concentration. In addition, they estimated  
the global net cloud radiative effect of ship emissions to be  $-0.153 \text{ W m}^{-2}$ . GCMs were also used to study the effect of the  
2014-2015 Holuhraun effusive eruption (referred to as the Nornahraun eruption in the paper, which was the unofficial name  
at the time) on the climate system by Gettelman et al. (2015). They estimated that emissions from the Holuhraun eruption in  
660 Iceland resulted in a regional radiative forcing of  $-0.21 \text{ W m}^{-2}$ , 80% of which was attributed to ACI. These GCM simulations  
demonstrated that had this level of emissions occurred in summer rather than in autumn, the radiative forcing would have been  
much larger ( $-0.61 \text{ W m}^{-2}$ , 94% of which attributable to ACI). During summer the radiative effects are larger due to a greater  
solar flux and a higher burden of sulfates from gas-phase oxidation.



## 5 Controlling Factors

665 This section lays out prominent “experimental conditions” that studies typically endeavor to hold fixed in a natural laboratory as  
 a means to compare different laboratories and systematic frameworks to one another. We have compiled a list of peer-reviewed  
 articles that quantify cloud properties and their responses in many opportunistic experiments. An opportunistic experiment  
 means an aerosol perturbation that affects the radiative properties of a cloud scene as a result of a chain of processes: After  
 emission there is nucleation, condensation and coagulation for the aerosol to reach CCN sizes. In addition, aerosol is diluted  
 670 while being transported to the cloud. Upon entering the cloud, aerosol particles act as CCN and increase  $N_d$ . This leads to a  
 distribution of available condensate to more, but smaller droplets, increases their overall surface area and thus cloud albedo.  
 In addition, the microphysical perturbation also affects processes that control the evolution of the macroscopic characteristics  
 of the cloud, in particular precipitation formation, entrainment, local circulations, LWP, cloud fraction and cloud depth. This  
 discussion can be formalized by the following relationship (Bellouin et al., 2020),

$$675 \quad \frac{\Delta\alpha}{\Delta\ln N_a} = \frac{\Delta\ln N_d}{\Delta\ln N_a} \left( \left. \frac{\Delta\alpha}{\Delta\ln N_d} \right|_{LWP, C_F} + \left. \frac{\Delta\alpha}{\Delta\ln LWP} \right|_{N_d, C_F} \frac{\Delta\ln LWP}{\Delta\ln N_d} + \left. \frac{\Delta\alpha}{\Delta\ln C_F} \right|_{N_d, LWP} \frac{\Delta\ln C_F}{\Delta\ln N_d} \right) \quad (1)$$

where  $N_a$  is the aerosol number concentration, and  $\Delta\alpha$  denotes the change in scene albedo in response to an aerosol pertur-  
 bation  $\Delta N_a$ . Here, single-directional difference quotients ( $(\Delta Y/\Delta X)|_Z \approx \partial Y/\partial X$ ) are represented as a linear relationship,  
 however, they depend upon meteorological conditions and the background aerosol conditions (Glassmeier et al., 2019). The  
 first term on the right hand side is the Twomey effect which represents the change in cloud albedo at constant LWP and  $C_F$   
 680 while the second and third terms on the right hand side are LWP and  $C_F$  adjustments. The sign of the LWP change can re-  
 verse too and therefore the joint PDF approach employed by Gryspeerdt et al. (2019a) is a useful methodology for quantifying  
 non-linear behavior. For warm cloud, the expression simplifies to

$$\frac{\Delta\alpha}{\Delta\ln N_d} = \phi_{atm} \frac{C_F \alpha_c (1 - \alpha_c)}{3} \left( 1 + \frac{5}{2} \frac{\Delta\ln LWP}{\Delta\ln N_d} + \frac{3(\alpha_c - \alpha_{clr})}{\alpha_c (1 - \alpha_c)} \frac{\Delta\ln C_F}{\Delta\ln N_d} \right) \quad (2)$$

685 where  $\phi_{atm}$  is the transfer function that relates a change in top of atmosphere albedo to a change in cloud albedo which  
 typically takes a value of 0.7 (Diamond et al., 2020),  $\alpha_c$  is the cloudy-sky albedo and  $\alpha_{clr}$  is the clear-sky albedo. The  
 complete derivation is described in the supplementary materials (Text S2). Table S1 shows the quantitative values of these cloud  
 properties across diverse laboratories and used to construct the statistics shown in Figure 10 and Figure S4 (but using fractional  
 changes instead).  $R_e$ , cloud optical thickness, LWP and  $N_d$  are included where provided in the peer-reviewed publications. The  
 extent to which each of these effects influences the overall cloud albedo is strongly dependent on the specific circumstances:  
 690 1) cloud susceptibility, 2) thermodynamic phase, 3) aerosol and precursor emission rate, 4) dilution, 5) methodology and  
 observing system, 6) meteorology and 7) buffering by local-scale dynamical circulations. Qualitatively, aerosols increase  $N_d$   
 and can increase or decrease LWP and  $C_F$ . Eventually cloud and scene averaged albedo impacts radiation as shown in Figure  
 10. Isolated volcanoes and ship tracks exhibit the largest fractional changes in  $N_d$  while the changes in clouds from shipping



695 corridors and global-scale average cloud perturbations exhibit weaker responses by comparison. Differences in the cloud responses are influenced by numerous controlling factors that gives rise to the diversity shown in Figure 10. Each factor is discussed below.

### 5.1 Cloud Susceptibility

The background cloud-state (namely,  $N_d$ ) to a large extent determines the specific sensitivities of scene albedo and cloud processes to aerosol perturbations. Twomey (1974) showed that cloud albedo sensitivity to a change in  $N_d$  is largest at low  $N_d$  and cloud albedo of 0.5 (Eq. 2), where the background  $N_d$  and  $\alpha$  sets the strength of the cloud albedo susceptibility as shown by the divisor by  $N_d$  and confirmed in many field campaigns (Ackerman et al., 2000; Durkee et al., 2000b; Ferek et al., 2000; Lu et al., 2009). While  $N_d$  changes at constant LWP can occur (i.e. the LWP in the polluted clouds is the same as the unpolluted clouds on either side of the track) in ship tracks, it is a relatively rare occurrence (roughly 10%) in satellite-derived ship track databases; (Segrin et al., 2007; Christensen and Stephens, 2012). In a majority of ship tracks the LWP actually decreases and in roughly 30% of tracks the decreases are so large that the cloud albedo becomes dimmer in the polluted clouds (Chen et al., 2012). Similar behavior has been observed in volcano, industry and fire tracks (Toll et al., 2019). Lower cloud albedo has also been identified in ship tracks from in situ measurements (Chen et al., 2012). This effect is generally attributed to the background meteorology (Sect. 5.6). Nevertheless, cloud susceptibility is a useful construct, and could be even more useful with an improved understanding of the relationship between meteorological controlling factors and the terms in Equation 2, as well as a better understanding of the timescales for LWP adjustments (Glassmeier et al., 2021).

### 5.2 Thermodynamic Phase

Decreases in cloud albedo are shown to occur more frequently in polluted clouds when they contain ice particles (Christensen et al., 2014). Cloud albedo in this context averages the cloud albedo retrievals from liquid and ice clouds in satellite imagery over the polluted section of an opportunistic experiment. Higher concentrations of ice in polluted ship track clouds have been identified from several hundred cases using the Cloud-Aerosol Lidar with Orthogonal Polarization (CALIOP). The higher occurrence of ice phase retrievals was hypothesized to be caused by an increase in contact or immersion freezing by the plumes of oceangoing vessels that have higher concentrations of solid species such as calcium, ash oxides of vanadium, nickel, sodium, iron oxides and other heavy metals (Agrawal et al., 2008) which may serve as an effective ice nucleating particles. The cloud albedo effect is weaker in mixed-phase clouds presumably due to enhanced precipitation occurring by greater amounts of ice particle production causing total water path to decrease via glaciation indirect effects (Lohmann, 2002). The cloud albedo effect may also be weaker because colder and deeper clouds with larger  $N_d$  are less susceptible than thinner shallower warm boundary layer clouds. As many of the cloud perturbations from volcanic aerosols occur at higher latitudes, careful screening of warm boundary layer clouds must be performed for comparison with other laboratories in warmer regions, and deeper investigation into glaciation indirect effects. As the distribution of super-cooled liquid clouds may increase with increasing global mean temperature (Mitchell et al., 1989) and more shipping activity is expected across the Arctic in the future as sea ice



extent declines further, the study of glaciation indirect effects will be pivotal for understanding the radiative effects of climate change.

### 5.3 Aerosol emission strength

730 Cloud perturbations are strongly influenced by the strength of the emissions of gases and particles into the atmosphere but emission rates are highly variable across laboratories. Passively degassing volcanoes typically emit several orders of magnitude more SO<sub>2</sub> than an oceangoing vessel. While estimates range from about 5,000 t/d at Kīlauea compared to 250 t/d at Mt. Michael in the South Sandwich Islands, both have been shown to produce bright volcano tracks (Gassó, 2008). Like industry, ship emissions also exhibit wide diversity in emission rates. Measurements from Hobbs et al. (2000) demonstrate that diesel powered ships burning low-grade marine fuel oil emitted 4–7 times more SO<sub>2</sub> than gas turbine engines. Brighter, more reflective  
735 ship tracks have also been shown to result from dirtier emissions (Gryspeerd et al., 2019b) or in locations where tracks intersect (Sechrist et al., 2012) but with non-linear diminishing returns related to weaker cloud susceptibility as  $N_d$  increases.

As mentioned before, a recent inadvertent climate experiment related to policy changes in 2020 required all oceangoing vessels to reduce their maximum SO<sub>2</sub> emissions from an effective fuel sulfur content (FSC) from 3.5 % pre-2020 to 0.5 % post-2020. This was largely accomplished by burning lower sulfur fuel oil (the strategy employed thus far by ca. 90% of the  
740 global fleet as of 2021) or installing scrubbers on ship exhaust (ca. 10% of ships). In 2015, similar policy changes were carried out but only surrounding the US and European nearshore coastal regions (i.e. in SECA zones). Interestingly, the occurrence of ship tracks within the Californian SECA were found to drop by 73% (Gryspeerd et al., 2019b) following this emission control area policy change. The extent to which the 2020 policy change has influenced the global occurrence of ship tracks or climate at large is a current research question under investigation in ACRUISE and, at least for 2020–2021, and may be obscured by  
745 COVID-19-related effects on both decreased shipping traffic (March et al., 2021) and enforcement efforts.

### 5.4 Dilution

Aerosols from ship stacks can overwhelm the ambient CCN by several orders of magnitude from local-scales (tens to hundreds of kilometers). Over time the emissions disperse and dilute over broader scales. Due to dilution, the aerosol concentration that reaches the cloud will generally be significantly smaller than at the source. For individual ships the typical area affected is  
750 approximately 2,500 km<sup>2</sup> from 250 kg of SO<sub>2</sub> emissions over a 7 hour period (Durkee et al., 2000a). Kabatas et al. (2013) examined dilution in ship tracks as a function of time and found that  $R_e$  increases at a rate of 0.5–1 μm per hour along the polluted portions of ship tracks. This translates to about a 2 μm increase over a distance of 100 km at typical container ship speeds of 24 knots (45 km h<sup>-1</sup>). Durkee et al. (2000a) and Gryspeerd et al. (2021) found that the change in the width of the ship track over time depends on the background concentration of  $N_d$ .

755 Dilution over larger scales may result in weaker cloud responses. The Holuhraun fissure eruption emitted about 120 kt of SO<sub>2</sub> per day (at its peak in 2014-2015), an equivalent of 4 times the 28 EU member states emission rates (Gislason et al., 2015; Schmidt et al., 2015). This event led to decreases in  $R_e$  across most of the Norwegian sea (Malavelle et al., 2017). Nevertheless, the volcanic emissions from Holuhraun have a much weaker effect when compared to isolated volcano track





760 studies (e.g., Gassó, 2008; Toll et al., 2017, 2019). The localized sampling of these highly polluted clouds within volcano or ship tracks and their surrounding cleaner clouds provide a significantly greater contrast in cloud properties compared to studies of aggregated emissions over larger areas (e.g. Holuhruan eruption or shipping corridors in the Peters et al. (2011) and Diamond et al. (2020) analyses). The smaller responses at these larger scale perturbations shown in Figure S4 may be the result of dilution. Interestingly, when fractional  $N_d$  increase (Diamond et al., 2020) is normalized by MERRA-2 sulfate perturbation, the ACI parameter is similar to other studies (McCoy et al. (2018), Gryspeerd et al. (2019b)).

765 Cloud perturbations near the emission sources are likely caused by primary aerosols (e.g. sulfate aerosols formed inside of the smoke stack, or black/organic carbon from combustion). Farther away from emission sources or on a larger scale, secondary aerosols (e.g. sulfate aerosols formed from atmospheric transformation of  $\text{SO}_2$ ) probably become more important (and contribute towards the ‘background’ aerosol state), while a larger fraction of larger-sized primary aerosols may be lost due to wet/dry deposition. Finally, weaker but more widespread effects due to greater dilution could also lead to greater overall  
770 reflection of sunlight since the Twomey effect is sublinear. Overall, the extent to which the magnitudes of cloud responses across these studies are influenced by dilution and whether the responses can be normalized by some other means for a comparative study remains an open research question.

## 5.5 Methodology and observing system

Methodology and observing systems (in situ, satellite and modeling) and spatiotemporal scale have been shown to influence  
775 ACI metrics (McComiskey and Feingold, 2012). The biases in coarse-scale models are likely related to parameterized physics and unresolved/missing processes (such as entrainment feedbacks). If there is a mismatch in the spatiotemporal scale of the perturbation in relation to the scale of the observing system then attributing aerosol-cloud interactions in a diluted manner (space or time) is also likely to induce biases (Kabatas et al., 2013; Possner et al., 2016; Gryspeerd et al., 2021; Glassmeier et al., 2021). The latter may be more of an issue for ship and industrial tracks than larger-scale volcanic eruptions. In the case  
780 of volcanoes, biases would be reduced to issues in representativeness of local measurements in an inhomogeneous field rather than scale mismatches (for a more complete discussion of representation error see Schutgens, 2020). Scale mismatches will also need to be considered if the scaling of results from plumes of differing degrees of dilution is to be attempted (see section 5.4 above).

## 5.6 Meteorology

785 The meteorological and aerosol background conditions determine the cloud regime and the processes that dominate cloud evolution. Figure 11 shows the dependence of cloud water response on the environmental conditions for the ocean-based and land-based polluted cloud tracks. The depth of the PBL and free tropospheric humidity have been identified as playing significant roles in the strength of the aerosol-cloud metrics shown in Figure S4. As the humidity in the free troposphere (above the cloud tops) becomes drier, polluted clouds with smaller droplets evaporate more efficiently (Ackerman et al., 2004; Dagan et al., 2017) causing liquid water paths and cloud albedo to decrease (Coakley and Walsh, 2002; Christensen and Stephens, 2011; Chen et al., 2012; Toll et al., 2019; Gryspeerd et al., 2021) (Figure 11). Also, the sign of LWP adjustments  $\frac{d \ln LWP}{d \ln N}$



is positive when cloud evolution is dominated by precipitation suppression and negative when dominated by evaporation-  
entrainment (Wang et al., 2003; Xue and Feingold, 2006; Small et al., 2009). Although, precipitation suppression also leads  
to greater turbulent kinetic energy and more entrainment, and the LWP increase by drizzle suppression (Albrecht, 1989) may  
795 only be active when precipitation reaches the surface (Wood, 2007). Figure 11 shows clear cloud water response dependence  
on baseline  $N_d$ : more pristine clouds are more likely to be precipitating and thus cloud water is more likely to increase.

## 5.7 Representativeness

Three other important challenges for applying lessons learned from natural laboratories and experiments to the study of aerosol-  
cloud interactions more broadly pertain to representativeness in terms of perturbation concentration, timescale and environ-  
800 ment.

### 5.7.1 Perturbation Concentration

Concentrated aerosol plumes surrounded by “clean” air behave fundamentally differently than the same amount of aerosol  
spread out more evenly. Models of isolated ship-track-like plumes show that such concentrated aerosol perturbations can create  
a secondary circulation transverse to the track. The circulation results in moisture convergence into the track and a positive  
805 LWP adjustment, and cloud-free downdrafts alongside the track (Wang and Feingold, 2009; Wang et al., 2011). The extent  
of cloud horizontal clearing along the edges of ship tracks has been shown to buffer the net cloud albedo effect in some ship  
tracks (Porch et al., 1990). These non-local effects may lead to the overall scene albedo change for an isolated perturbation to  
differ systematically from what would be obtained by a more uniform increase.

Although Toll et al. (2019) and Trofimov et al. (2020) have made great strides in extending the study of ship-track-like  
810 perturbations to deeper continental environments, it remains true that the special cases of shallow well-mixed marine boundary  
layer with low background aerosol concentrations are over-represented in the natural experiment literature due to the formation  
of clearly discernible tracks in such environments (Durkee et al., 2000b). However, real but less easily detectable effects may  
exist in other conditions (Possner et al., 2018), and different integrated aerosol-cloud responses are expected between shallow  
well-mixed marine boundary layers, deeper decoupled marine boundary layers, and continental boundary layers (Possner et al.,  
815 2020). The shipping corridor approach of Diamond et al. (2020) partially addressed this concern by capturing all shipping  
effects over a defined region from the “top down” rather than building up statistics of clearly detected cases from the “bottom  
up”. Improved approaches for the detection of pollution tracks via machine learning (Yuan et al., 2019) and trajectory analysis  
from known point sources (Gryspeerd et al., 2019a), taken by the ACRUISE project, also provide the opportunity to better  
sample a more diverse set of regimes via “natural experiment” methods.

### 820 5.7.2 Timescales

More recently, Glassmeier et al. (2021), hereafter G21, has argued that ship track studies underestimate climatological liquid  
water path decreases from aerosol injections into non-precipitating clouds because evaporation-entrainment adjustments take



place on timescales of  $\sim 20$  hours. G21 argue that clearly visible ship tracks only persist for  $\sim 6$ -7 hours and are on average sampled within 3 hours of forming and thus do not last long enough to develop substantially negative liquid water adjustments, whereas the results from Diamond et al. (2020) show a more negative liquid water path adjustment which G21 explain as resulting from a longer effective lifetime of ship tracks in the corridor methodology of  $\geq 9$  hours. Thus, the analysis of G21 suggests that short timescale adjustments observed in ship track studies may be unrepresentative of the climatological response to greater aerosol/cloud droplet number. Wood (2007) used mixed layer modeling to show that clouds can thin on short timescales (e.g., when the lifted condensation level rises more quickly than the inversion height) and thicken on longer ones. The adjustment timescale of G21 in fact falls in between these two timescales of an individual stratocumulus cloud system because when quantifying adjustments it compares perturbed and unperturbed systems, each of which have a different equilibration time. The added complexity here is that cloud adjustments seem to vary with timescale after emissions, and thus near source impacts are not sufficient for estimating global impacts. The lifetime of industry tracks has not been well quantified. It is unclear whether industry tracks live longer than ship tracks and whether these opportunistic experiments are more representative of the climatological cloud responses (Toll et al., 2019). All of these studies point to the need to account for, and quantify, the timescales of emissions and cloud adjustments for both local and climatically relevant conditions.

The timescale dependence of LWP adjustments demonstrated by G21 through a theoretical analysis of LES, is observationally confirmed (Gryspeerd et al., 2021), who study long-lived ship tracks and find, in accordance with G21, that the magnitude of the LWP adjustments increase over time. Although, not in all scenarios of G21 (e.g. clean background with a moist free troposphere) the LWP reductions can increase in magnitude with time. In addition to the effects of differing samplings of environments (Sect. 5.6), and boundary effects in spatially confined pollution (Sect. 5.7.1), one should keep in mind that satellite studies of LWP adjustment suffer from uncertainties that enter into satellite retrieved values of  $\frac{d \ln LWP}{d \ln N_d}$  via the retrieval uncertainties in  $N_d$  (Grosvenor et al., 2018). Further uncertainty then follows by different choices made during the quality checks applied to  $N_d$  retrievals. This is exemplified by inconsistent estimates of  $\frac{d \ln LWP}{d \ln N_d}$  in the subtropical stratocumulus regions (Michibata and Suzuki, 2020; Gryspeerd et al., 2019a; Possner et al., 2020). These estimates stem from the same retrievals. Yet, different choices made across the three studies in how to address the uncertainty in  $N_d$  lead to a considerable variability in both magnitude and sign of  $\frac{d \ln LWP}{d \ln N_d}$ . Such uncertainties in satellite retrievals and differing methods of filtering clouds are also a possible explanation for the observation that the LWP adjustments observed in Diamond et al. (2020) are comparable to those of the ship track work of Gryspeerd et al. (2019a) and Toll et al. (2019) for similar background values of  $R_e$  and  $N_d$ . Similarly, the diurnal cycle (Terra versus Aqua) of LWP adjustments observed in Diamond et al. (2020) cannot directly be explained by the framework of G21, which is based on interpolating simulations to equilibrium under the assumption of perpetually nocturnal radiation.

### 5.7.3 Environmental Representativeness

Altogether, the challenges raised above point to the necessity of coupling insights from both modeling and observations even for the seemingly straightforward case of natural experiments like clearly visible ship tracks, in order to extrapolate from the specific situations in which natural experiments can be studied to aerosol-cloud interactions more broadly, as has been



exemplified by G21. Observations of natural laboratories and experiments provide valuable opportunities for the evaluation of model processes at similar timescales and in similar environmental conditions. Theoretical insights from modeling studies like G21 provide a way forward to scaling results from different timescale and environmental conditions such that they can be compared and their consistency evaluated. Even if certain natural laboratory/experiment results cannot be scaled reliably, improvements in model physics that may emerge from tests in natural experiment settings will likely have implications for global aerosol-cloud responses (and potentially cloud feedbacks too depending on the cloud processes in question).

Although much effort has gone into constraining liquid water adjustments in natural laboratory and experiment settings (Diamond et al., 2020; Gryspeerd et al., 2019b; Toll et al., 2017, 2019), unambiguous cloud fraction adjustments have remained more elusive (except arguably in some of the volcano studies). Other lines of evidence suggest such adjustments could be important in both an Eulerian (Gryspeerd et al., 2016; Rosenfeld et al., 2019) and Lagrangian (Goren et al., 2019; Christensen et al., 2020) framework. To rectify this, additional observationally based constraints with greater confidence in causality (at least in the specific situation, even if not broadly generalized) would be helpful. A direct link with precipitation in climatological data-sets (such as in the southeast Atlantic shipping lane) would also be useful information.

## 870 6 Summary

Experiments of opportunity have been looked upon by some as a possible ‘Rosetta Stone’ connecting the effects of changing aerosol over the ocean and cloud albedo effects on climate (Porch et al., 1990). It could be argued that ship, volcano and industrial pollution tracks are the most striking examples of aerosol-cloud interactions in the climate system. A wealth of field campaigns, satellite observations and modeling studies related to these opportunistic experiments provide incontrovertible evidence that changes in aerosol concentration can lead to significant changes in the microphysics and macrophysics of clouds for the same meteorological conditions. Over the decades, several well known field campaigns have made a concerted effort to pin down controlling factors that lead to large uncertainty in cloud responses and aerosol indirect radiative forcing as a whole.

Natural laboratories are excellent for process-level understanding of aerosol-cloud interactions. One key result from the Monterey Area Ship Track (MAST) experiment revealed that the cloud condensation nuclei from individual ships are solely responsible for the reflectance perturbations in ship tracks as opposed to the hypotheses involving heat and moisture from the exhaust or sea salt produced in the wake of a ship (Durkee et al., 2000b). While this connection between the aerosol and cloud microphysics is understood, macrophysical responses (such as cloud liquid water path, geometrical thickness, precipitation, and fractional coverage) exhibit more diversity and are poorly understood. Several hypotheses have emerged to explain the bidirectional response in macrophysical responses and a greater understanding has emerged in recent decades. The dryness of free-tropospheric air can lead to greater evaporation in polluted clouds thereby decreasing liquid water path (Coakley and Walsh, 2002; Ackerman et al., 2004; Christensen et al., 2009; Chen et al., 2012; Toll et al., 2019; Gryspeerd et al., 2021). The evolution of the clouds and duration over which they have been influenced by aerosols can affect precipitation, circulation and liquid water path (Wang and Feingold, 2009; Gryspeerd et al., 2021).



It remains unclear how representative natural experiments and laboratories are for understanding of the global response  
890 of clouds to anthropogenic aerosols. Typically only shallow clouds are within reach of the emissions from underlying ships  
or industrial sources and the albedo cloud susceptibility typically becomes weaker as the PBL deepens (Chen et al., 2012).  
Furthermore, enhanced lightning in shipping may suggest deep convective clouds are also influenced by shipping aerosol  
(Thornton et al., 2017). Thus, it is unclear how reliable extrapolations of these opportunistic experiments are to the global  
scale. The timescale of cloud perturbations is one key aspect of these extrapolations for quantifying global aerosol radiative  
895 forcing (Glassmeier et al., 2021). Furthermore, satellite observations typically focus on the “hits” where tracks are observed  
instead of the “misses” where aerosols may influence clouds but not produce an evident track. The extent to which deeper  
clouds respond to dilute plumes and radiative forcing remains largely unanswered. It has been estimated that only 0.004%  
(Schreier et al., 2007; Possner et al., 2018) of ship emissions go into creating discernible “ship tracks”. Thus, a new framework  
may be needed to track individual plumes through to cloud responses when “tracks” are not directly observed in satellite data  
900 to accurately determine the global RF<sub>aci</sub>.

This review paper collates the results from experiments of opportunity in over 50 publications. The diversity in Figure 10  
and Figure S4 cloud droplet perturbations show strong agreement in drop number changes (Figure 10a) and droplet effective  
radius decreases as  $N_d$  increases (Figure 10b) but there is less agreement on the sign on the LWP response with uncertainties  
typically spanning a wide range of negative and positive values (Figure 10c). It is essential to pin down LWP and  $C_F$  adjustments  
905 for more accurate estimates of RF<sub>aci</sub>. The range of uncertainty in these ACI metrics denotes the important roles of several  
cloud controlling factors: spatial scale, emission strength, background cloud properties and meteorology. Two field campaigns,  
ACTIVATE and ACRUISE have recently shifted the focus from individual plume-scale cloud interactions to larger regional-  
and global-scale perturbations to better characterize dilution and non-linear cloud responses as they relate to emission strength.  
Furthermore, a better understanding of aerosol’s invigoration of convective and ice clouds alongside the temporal evolution  
910 as the clouds evolve and change in accordance with meteorology are essential to understand the albedo responses as they  
relate to macrophysical cloud property changes. Coordinated model experiments, such as AeroCom have been instrumental in  
pinpointing deficiencies in atmosphere models and their diversity of simulated effective aerosol radiative forcing (Malavelle  
et al., 2017).

More attention should be paid to potential changes in the width of the droplet size distribution (DSD) (Liu and Daum,  
915 2002), which cloud chamber experiments suggest could be quite important (Chandrakar et al., 2016, 2018). If both the width  
and center of the droplet size distribution are of first order importance, it may be more useful to think about primary indirect  
effects (traditional Twomey effect plus narrowing) and secondary indirect effects (adjustments to the DSD shift) rather than  
adjustments being due to the Twomey/first indirect effect of a larger number (zeroth moment of the DSD) and smaller effective  
radius (ratio of third and second moments) alone. Some evidence of a modification of the DSD width may be responsible for  
920 creating negative biases in the LWP retrievals within the first 100 km of ship tracks where LWP changes are expected to be zero  
as there would not have been enough time to modify the clouds (Gryspeerd et al., 2021). Feingold et al. (1997) showed the  
contrasting role of DSD width. When spectral broadening is associated with increasing  $N_d$  (because of competition for water  
vapor in the relatively polluted, condensation-dominated regime), albedo susceptibility is diminished, whereas when broaden-



ing is associated with a reduction in  $N_d$  (the cleaner, coalescence-dominated regime), susceptibility is enhanced. Polarimeter  
925 measurements can provide an estimate of the DSD width (e.g. POLDER, over a limited spatial scale) and would be useful  
additions (e.g. the upcoming NASA ATMOS mission or airborne polarimetry) to the observational toolbox.

Finally, opportunistic experiments can assist in understanding large scale sulfate injection or marine cloud brightening for  
geoengineering. They might be used to better understand potential geoengineering pathways in similar or analogous envi-  
ronments without worrying about additional environmental impacts (National Academies of Sciences, 2021). Many natural  
930 laboratories are low cloud perturbations that might be analogous for suggested climate intervention strategies, so understand-  
ing them is critical for future and past aerosol radiative forcing.

935

*Author contributions.* M.W.C. and A.G. are co-leads and wrote the manuscript with contributions in writing, figures and data from coauthors:  
J.C., G.D., M.S.D., A.D., G.F., F.G., T.G., D.P.G., E.G., R.K., Z.L., P.M., F.M., I.M., D.M., G.M., J.M., S.P., A.Possner, A.Povey, J.Q., D.R.,  
A.Schmidt, R.S., A.Sorooshian, P.S., V.T., D.W., R.W., M.Y., and T.Y.

940 *Competing interests.* No competing interests are present



*Acknowledgements.* This research was partly supported by European Research Council Project constRaining the EffeCts of Aerosols on Precipitation under the European Union's Horizon 2020 Research and Innovation Program Grant 724602. M.W.C., P.-L.M., and J.M. were supported by the "Enabling Aerosol-cloud interactions at GLobal convection-permitting scales (EAGLES)" project (74358), funded by the  
945 U.S. Department of Energy, Office of Science, Office of Biological and Environmental Research, Earth System Model Development program. The Pacific Northwest National Laboratory is operated for the U.S. Department of Energy by Battelle Memorial Institute under contract DE-AC05-76RL01830. M.Y., M.W.C, D.W.P, and P.S. were supported by the Natural Environment Research Council (UK) project ACRUISE (grant number: NE/S005390/1). V.T. acknowledges support from the Estonian Research Council grant PSG202. M.S.D. was supported in part  
950 by NASA headquarters under the NASA Earth and Space Science Fellowship Program, grant number NNX-80NSSC17K0404, and in part by the CIRES Visiting Fellows Program that is funded by the NOAA Cooperative Agreement with CIRES, grant number NA17OAR4320101. A.Sorooshian was supported by ONR grant N00014-21-1-2115 and NASA grant 80NSSC19K0442 in support of ACTIVATE, a NASA Earth Venture Suborbital-3 (EVS-3) investigation funded by NASA's Earth Science Division and managed through the Earth System Science Pathfinder Program Office. A. Schmidt acknowledges funding from NERC grants NE/S00436X/1 (V-PLUS), NE/T006897/1 (ADVANCE), and NE/P013406/1 (A-CURE). Z.L. is funded by the US National Science Foundation (AGS1837811) and NASA (80NSSC20K0131).  
955 A.Possner is funded by the Federal Ministry of Education and Research (BMBF) under the "Make our Planet Great Again - German Research Initiative", grant number 57429624, implemented by the German Academic Exchange Service (DAAD). E.G. was supported by a Royal Society University Research Fellowship (URF/R1/191602). F.G. acknowledges support from The Branco Weiss Fellowship - Society in Science, administered by the ETH Zürich, and from a Veni grant of the Dutch Research Council (NWO). J.Q. acknowledges support from the EU Horizon2020 projects ACACIA (GA 875036) and FORCES (GA 821205). P.S. acknowledges support by the European Research  
960 Council (ERC) project constRaining the EffeCts of Aerosols on Precipitation (RECAP) under the European Union's Horizon 2020 research and innovation program with grant agreement 724602 and from the FORCeS project under the European Union's Horizon 2020 research program with grant agreement 821205. R.W. acknowledges support from the US National Oceanographic and Atmospheric Administration (NOAA Award NA20OAR4320271). G.F. acknowledges funding from a NOAA Earth's Radiation Budget grant, NOAA CPO Climate & CI #03-01-07-001. The National Center for Atmospheric Research is funded by the U.S. National Science Foundation. A.Povey is funded as  
965 part of the Natural Environment Research Council's support of the National Centre for Earth Observation, contract number PR140015.



## References

- Ackerman, A. S., Toon, O. B., Taylor, J. P., Johnson, D. W., Hobbs, P. V., and Ferek, R. J.: Effects of Aerosols on Cloud Albedo: Evaluation of Twomey's Parameterization of Cloud Susceptibility Using Measurements of Ship Tracks, *Journal of the Atmospheric Sciences*, 57, 2684–2695, [https://doi.org/10.1175/1520-0469\(2000\)057<2684:EOAOCA>2.0.CO;2](https://doi.org/10.1175/1520-0469(2000)057<2684:EOAOCA>2.0.CO;2), 2000.
- 970 Ackerman, A. S., Kirkpatrick, M. P., Stevens, D. E., and Toon, O. B.: The Impact of Humidity above Stratiform Clouds on Indirect Aerosol Climate Forcing, *Nature*, 432, 1014–1017, <https://doi.org/10.1038/nature03174>, 2004.
- Adebiyi, A. A., Zuidema, P., and Abel, S. J.: The Convolution of Dynamics and Moisture with the Presence of Shortwave Absorbing Aerosols over the Southeast Atlantic, *Journal of Climate*, 28, 1997 – 2024, <https://doi.org/10.1175/JCLI-D-14-00352.1>, 2015.
- Agrawal, H., Malloy, Q. G., Welch, W. A., Wayne Miller, J., and Cocker, D. R.: In-use gaseous and particulate matter emissions from a modern ocean going container vessel, *Atmospheric Environment*, 42, 5504–5510, <https://doi.org/https://doi.org/10.1016/j.atmosenv.2008.02.053>, 2008.
- 975 Albrecht, B. A.: Aerosols, Cloud Microphysics, and Fractional Cloudiness, *Science*, 245, 1227–1230, <https://doi.org/10.1126/science.245.4923.1227>, 1989.
- Andres, R. J. and Kasgnoc, A. D.: A time-averaged inventory of subaerial volcanic sulfur emissions, *Journal of Geophysical Research: Atmospheres*, 103, 25 251–25 261, <https://doi.org/https://doi.org/10.1029/98JD02091>, 1998.
- 980 Bai, H., Wang, M., Zhang, Z., and Liu, Y.: Synergetic Satellite Trend Analysis of Aerosol and Warm Cloud Properties over Ocean and Its Implication for Aerosol-Cloud Interactions, *Journal of Geophysical Research: Atmospheres*, 125, e2019JD031598, <https://doi.org/10.1029/2019JD031598>, 2020.
- Barnet, P., Kuster, T., Muhlbauer, A., and Lohmann, U.: Weekly Cycle in Particulate Matter versus Weekly Cycle in Precipitation over Switzerland, *Journal of Geophysical Research: Atmospheres*, 114, <https://doi.org/10.1029/2008JD011192>, 2009.
- 985 Bauwens, M., Compennolle, S., Stavrakou, T., Müller, J. F., Gent, J., Eskes, H., Levelt, P. F., A. R., Veefkind, J. P., Vlietinck, J., Yu, H., and Zehner, C.: Impact of Coronavirus Outbreak on NO<sub>2</sub> Pollution Assessed Using TROPOMI and OMI Observations, *Geophysical Research Letters*, 47, e2020GL087978, <https://doi.org/10.1029/2020gl087978>, 2020.
- Beirle, S., Platt, U., Wenig, M., and Wagner, T.: Weekly Cycle of NO<sub>2</sub> by GOME Measurements: A Signature of Anthropogenic Sources, *Atmospheric Chemistry and Physics*, 3, 2225–2232, <https://doi.org/10.5194/acp-3-2225-2003>, 2003.
- 990 Bell, T. L., Rosenfeld, D., Kim, K.-M., Yoo, J.-M., Lee, M.-I., and Hahnenberger, M.: Midweek Increase in U.S. Summer Rain and Storm Heights Suggests Air Pollution Invigorates Rainstorms, *Journal of Geophysical Research*, 113, <https://doi.org/10.1029/2007jd008623>, 2008.
- Bell, T. L., Rosenfeld, D., and Kim, K.-M.: Weekly Cycle of Lightning: Evidence of Storm Invigoration by Pollution, *Geophysical Research Letters*, 36, <https://doi.org/10.1029/2009gl040915>, 2009.
- 995 Bellouin, N., Quaas, J., Gryspeerdt, E., Kinne, S., Stier, P., Watson-Parris, D., Boucher, O., Carslaw, K. S., Christensen, M., Daniou, A.-L., Dufresne, J.-L., Feingold, G., Fiedler, S., Forster, P., Gettelman, A., Haywood, J. M., Lohmann, U., Malavelle, F., Mauritsen, T., McCoy, D. T., Myhre, G., Mühlenthal, J., Neubauer, D., Possner, A., Rugenstein, M., Sato, Y., Schulz, M., Schwartz, S. E., Sourdeval, O., Storelvmo, T., Toll, V., Winker, D., and Stevens, B.: Bounding Global Aerosol Radiative Forcing of Climate Change, *Reviews of Geophysics*, 58, e2019RG000660, <https://doi.org/10.1029/2019RG000660>, 2020.
- 1000





- Benas, N., Meirink, J. F., Karlsson, K.-G., Stengel, M., and Stammes, P.: Satellite Observations of Aerosols and Clouds over Southern China from 2006 to 2015: Analysis of Changes and Possible Interaction Mechanisms, *Atmospheric Chemistry and Physics*, 20, 457–474, <https://doi.org/10.5194/acp-20-457-2020>, 2020.
- Bennartz, R., Fan, J., Rausch, J., Leung, L. R., and Heidinger, A. K.: Pollution from China Increases Cloud Droplet Number, Suppresses Rain over the East China Sea, *Geophysical Research Letters*, 38, L09 704, <https://doi.org/10.1029/2011gl047235>, 2011.
- Berner, A. H., Bretherton, C. S., and Wood, R.: Large Eddy Simulation of Ship Tracks in the Collapsed Marine Boundary Layer: A Case Study from the Monterey Area Ship Track Experiment, *Atmospheric Chemistry and Physics*, 15, 5851–5871, <https://doi.org/10.5194/acp-15-5851-2015>, 2015.
- Blossey, P. N., Bretherton, C. S., Thornton, J. A., and Virts, K. S.: Locally Enhanced Aerosols Over a Shipping Lane Produce Convective Invigoration but Weak Overall Indirect Effects in Cloud-Resolving Simulations, *Geophysical Research Letters*, 45, 9305–9313, <https://doi.org/10.1029/2018gl078682>, 2018.
- Boucher, O. and Lohmann, U.: The sulfate-CCN-cloud albedo effect, *Tellus B: Chemical and Physical Meteorology*, 47, 281–300, <https://doi.org/10.3402/tellusb.v47i3.16048>, 1995.
- Bowley, C. J.: Comments on Atmospheric Requirements for the Genesis of Anomalous Cloud Lines, *Journal of the Atmospheric Sciences*, 24, 596–597, [https://doi.org/10.1175/1520-0469\(1967\)024<0596:COARFT>2.0.CO;2](https://doi.org/10.1175/1520-0469(1967)024<0596:COARFT>2.0.CO;2), 1967.
- Bretherton, C. S., Blossey, P. N., and Uchida, J.: Cloud Droplet Sedimentation, Entrainment Efficiency, and Subtropical Stratocumulus Albedo, *Geophysical Research Letters*, 34, <https://doi.org/10.1029/2006gl027648>, 2007.
- Brioude, J., Cooper, O. R., Feingold, G., Trainer, M., Freitas, S. R., Kowal, D., Ayers, J. K., Prins, E., Minnis, P., McKeen, S. A., Frost, G. J., and Hsie, E.-Y.: Effect of biomass burning on marine stratocumulus clouds off the California coast, *Atmospheric Chemistry and Physics*, 9, 8841–8856, <https://doi.org/10.5194/acp-9-8841-2009>, 2009.
- Campmany, E., Grainger, R. G., Dean, S. M., and Sayer, A. M.: Automatic Detection of Ship Tracks in ATSR-2 Satellite Imagery, *Atmospheric Chemistry and Physics*, 9, 1899–1905, <https://doi.org/10.5194/acp-9-1899-2009>, 2009.
- Capaldo, K., Corbett, J. J., Kasibhatla, P., Fischbeck, P., and Pandis, S. N.: Effects of Ship Emissions on Sulphur Cycling and Radiative Climate Forcing over the Ocean, *Nature*, 400, 743–746, <https://doi.org/10.1038/23438>, 1999.
- Carn, S., Clarisse, L., and Prata, A.: Multi-decadal satellite measurements of global volcanic degassing, *Journal of Volcanology and Geothermal Research*, 311, 99–134, <https://doi.org/https://doi.org/10.1016/j.jvolgeores.2016.01.002>, 2016.
- Carn, S. A., Fioletov, V. E., McLinden, C. A., Li, C., and Krotkov, N. A.: A Decade of Global Volcanic SO<sub>2</sub> Emissions Measured from Space, *Scientific Reports*, 7, 44 095, <https://doi.org/10.1038/srep44095>, 2017.
- Cermak, J. and Knutti, R.: Beijing Olympics as an Aerosol Field Experiment, *Geophysical Research Letters*, 36, L10 806, <https://doi.org/10.1029/2009gl038572>, 2009.
- Chandrakar, K. K., Cantrell, W., Chang, K., Ciochetto, D., Niedermeier, D., Ovchinnikov, M., Shaw, R. A., and Yang, F.: Aerosol Indirect Effect from Turbulence-Induced Broadening of Cloud-Droplet Size Distributions, *Proc Natl Acad Sci U S A*, 113, 14 243–14 248, <https://doi.org/10.1073/pnas.1612686113>, 2016.
- Chandrakar, K. K., Cantrell, W., Kostinski, A. B., and Shaw, R. A.: Dispersion Aerosol Indirect Effect in Turbulent Clouds: Laboratory Measurements of Effective Radius, *Geophysical Research Letters*, 45, 10,738–10,745, <https://doi.org/10.1029/2018gl079194>, 2018.
- Chang, Y., Huang, R.-J., Ge, X., Huang, X., Hu, J., Duan, Y., Zou, Z., Liu, X., and Lehmann, M. F.: Puzzling Haze Events in China During the Coronavirus (COVID-19) Shutdown, *Geophysical Research Letters*, 47, e2020GL088 533, <https://doi.org/10.1029/2020gl088533>, 2020.



- Chen, Y. C., Christensen, M. W., Xue, L., Sorooshian, A., Stephens, G. L., Rasmussen, R. M., and Seinfeld, J. H.: Occurrence of Lower Cloud Albedo in Ship Tracks, *Atmospheric Chemistry and Physics*, 12, 8223–8235, <https://doi.org/10.5194/acp-12-8223-2012>, 2012.
- 1040 Cherian, R. and Quaas, J.: Trends in AOD, Clouds, and Cloud Radiative Effects in Satellite Data and CMIP5 and CMIP6 Model Simulations Over Aerosol Source Regions, *Geophysical Research Letters*, 47, e2020GL087132, <https://doi.org/10.1029/2020GL087132>, 2020.
- Cherian, R., Quaas, J., Salzmann, M., and Wild, M.: Pollution Trends over Europe Constrain Global Aerosol Forcing as Simulated by Climate Models, *Geophysical Research Letters*, 41, 2176–2181, <https://doi.org/10.1002/2013GL058715>, 2014.
- Christensen, M. W. and Stephens, G. L.: Microphysical and Macrophysical Responses of Marine Stratocumulus Polluted by Underlying Ships: Evidence of Cloud Deepening, *Journal of Geophysical Research: Atmospheres*, 116, <https://doi.org/10.1029/2010JD014638>, 2011.
- 1045 Christensen, M. W. and Stephens, G. L.: Microphysical and Macrophysical Responses of Marine Stratocumulus Polluted by Underlying Ships: 2. Impacts of Haze on Precipitating Clouds, *Journal of Geophysical Research: Atmospheres*, 117, <https://doi.org/10.1029/2011JD017125>, 2012.
- Christensen, M. W., Coakley, J. A., and Tahnk, W. R.: Morning-to-Afternoon Evolution of Marine Stratus Polluted by Underlying Ships: Implications for the Relative Lifetimes of Polluted and Unpolluted Clouds, *Journal of the Atmospheric Sciences*, 66, 2097–2106, <https://doi.org/10.1175/2009JAS2951.1>, 2009.
- 1050 Christensen, M. W., Suzuki, K., Zambri, B., and Stephens, G. L.: Ship Track Observations of a Reduced Shortwave Aerosol Indirect Effect in Mixed-Phase Clouds, *Geophysical Research Letters*, 41, 6970–6977, <https://doi.org/10.1002/2014GL061320>, 2014.
- Christensen, M. W., Neubauer, D., Poulsen, C. A., Thomas, G. E., McGarragh, G. R., Povey, A. C., Proud, S. R., and Grainger, R. G.: Unveiling Aerosol–Cloud Interactions – Part 1: Cloud Contamination in Satellite Products Enhances the Aerosol Indirect Forcing Estimate, *Atmos. Chem. Phys.*, 17, 13151–13164, <https://doi.org/10.5194/acp-17-13151-2017>, 2017.
- 1055 Christensen, M. W., Jones, W. K., and Stier, P.: Aerosols Enhance Cloud Lifetime and Brightness along the Stratus-to-Cumulus Transition, *Proc Natl Acad Sci U S A*, <https://doi.org/10.1073/pnas.1921231117>, 2020.
- Coakley, J. A. and Walsh, C. D.: Limits to the Aerosol Indirect Radiative Effect Derived from Observations of Ship Tracks, *Journal of the Atmospheric Sciences*, 59, 668–680, [https://doi.org/10.1175/1520-0469\(2002\)059<0668:LTTAIR>2.0.CO;2](https://doi.org/10.1175/1520-0469(2002)059<0668:LTTAIR>2.0.CO;2), 2002.
- 1060 Coakley, J. A., Bernstein, R. L., and Durkee, P. A.: Effect of Ship-Stack Effluents on Cloud Reflectivity, *Science*, 237, 1020–1022, 1987.
- Conover, J. H.: Anomalous Cloud Lines, *Journal of the Atmospheric Sciences*, 23, 778–785, [https://doi.org/10.1175/1520-0469\(1966\)023<0778:ACL>2.0.CO;2](https://doi.org/10.1175/1520-0469(1966)023<0778:ACL>2.0.CO;2), 1966.
- Crippa, M., Guizzardi, D., Muntean, M., Schaaf, E., Dentener, F., van Aardenne, J. A., Monni, S., Doering, U., Olivier, J. G. J., Pagliari, V., and Janssens-Maenhout, G.: Gridded Emissions of Air Pollutants for the Period 1970–2012 within EDGAR v4.3.2, *Earth System Science Data*, 10, 1987–2013, <https://doi.org/10.5194/essd-10-1987-2018>, 2018.
- 1065 Crippa, M., Solazzo, E., Huang, G., Guizzardi, D., Koffi, E., Muntean, M., Schieberle, C., Friedrich, R., and Janssens-Maenhout, G.: High Resolution Temporal Profiles in the Emissions Database for Global Atmospheric Research, *Scientific Data*, 7, 121–137, <https://doi.org/10.1038/s41597-020-0462-2>, 2020.
- 1070 Dagan, G., Koren, I., Altaratz, O., and Heiblum, R. H.: Time-dependent, non-monotonic response of warm convective cloud fields to changes in aerosol loading, *Atmospheric Chemistry and Physics*, 17, 7435–7444, <https://doi.org/10.5194/acp-17-7435-2017>, 2017.
- Daniel, J. S., Portmann, R. W., Solomon, S., and Murphy, D. M.: Identifying weekly cycles in meteorological variables: The importance of an appropriate statistical analysis, *Journal of Geophysical Research: Atmospheres*, 117, <https://doi.org/10.1029/2012JD017574>, 2012.



- 1075 Diamond, M. S. and Wood, R.: Limited Regional Aerosol and Cloud Microphysical Changes Despite Unprecedented Decline in Nitrogen Oxide Pollution During the February 2020 COVID-19 Shutdown in China, *Geophysical Research Letters*, 47, e2020GL088913, <https://doi.org/10.1029/2020GL088913>, 2020.
- Diamond, M. S., Dobracki, A., Freitag, S., Small Griswold, J. D., Heikkila, A., Howell, S. G., Kacarab, M. E., Podolske, J. R., Saide, P. E., and Wood, R.: Time-Dependent Entrainment of Smoke Presents an Observational Challenge for Assessing Aerosol–Cloud Interactions over the Southeast Atlantic Ocean, *Atmospheric Chemistry and Physics*, 18, 14 623–14 636, <https://doi.org/10.5194/acp-18-14623-2018>, 2018.
- 1080 Diamond, M. S., Director, H. M., Eastman, R., Possner, A., and Wood, R.: Substantial Cloud Brightening From Shipping in Subtropical Low Clouds, *AGU Advances*, 1, e2019AV000 111, <https://doi.org/10.1029/2019AV000111>, 2020.
- Ding, J., van der A, R. J., Mijling, B., Levelt, P. F., and Hao, N.: NO<sub>x</sub> Emission Estimates during the 2014 Youth Olympic Games in Nanjing, *Atmospheric Chemistry and Physics*, 15, 9399–9412, <https://doi.org/10.5194/acp-15-9399-2015>, 2015.
- 1085 Durkee, P. A., Chartier, R. E., Brown, A., Trehubenko, E. J., Rogerson, S. D., Skupniewicz, C., and Nielsen, K. E.: Composite Ship Track Characteristics, *Journal of the Atmospheric Sciences*, 57, 2542–2553, 2000a.
- Durkee, P. A., Noone, K. J., and Bluth, R. T.: The Monterey Area Ship Track Experiment, *Journal of the Atmospheric Sciences*, 57, 2523–2541, [https://doi.org/10.1175/1520-0469\(2000\)057<2523:TMASTE>2.0.CO;2](https://doi.org/10.1175/1520-0469(2000)057<2523:TMASTE>2.0.CO;2), 2000b.
- 1090 Earl, N., Simmonds, I., and Tapper, N.: Weekly Cycles of Global Fires—Associations with Religion, Wealth and Culture, and Insights into Anthropogenic Influences on Global Climate, *Geophysical Research Letters*, 42, 9579–9589, 2015.
- Ebmeier, S. K., Sayer, A. M., Grainger, R. G., Mather, T. A., and Carboni, E.: Systematic Satellite Observations of the Impact of Aerosols from Passive Volcanic Degassing on Local Cloud Properties, *Atmos. Chem. Phys.*, 14, 10 601–10 618, <https://doi.org/10.5194/acp-14-10601-2014>, 2014.
- 1095 Elsaesser, G. S., O’Dell, C. W., Lebsock, M. D., Bennartz, R., Greenwald, T. J., and Wentz, F. J.: The multisensor Advanced climatology of liquid water path (MAC-LWP), *J. Clim.*, 30, 10 193–10 210, <https://doi.org/10.1175/JCLI-D-16-0902.1>, 2017.
- Evan, A. T., Heidinger, A. K., and Vimont, D. J.: Arguments against a physical long-term trend in global ISCCP cloud amounts, *Geophys. Res. Lett.*, 34, L04 701, <https://doi.org/10.1029/2006GL028083>, 2007.
- Eyring, V., Isaksen, I. S. A., Berntsen, T., Collins, W. J., Corbett, J. J., Endresen, O., Grainger, R. G., Moldanova, J., Schlager, H., and Stevenson, D. S.: Transport Impacts on Atmosphere and Climate: Shipping, *Atmospheric Environment*, 44, 4735–4771, <https://doi.org/10.1016/j.atmosenv.2009.04.059>, 2010.
- 1100 Feingold, G., Boers, R., Stevens, B., and Cotton, W. R.: A modeling study of the effect of drizzle on cloud optical depth and susceptibility, *Journal of Geophysical Research: Atmospheres*, 102, 13 527–13 534, <https://doi.org/https://doi.org/10.1029/97JD00963>, 1997.
- Feingold, G., Koren, I., Yamaguchi, T., and Kazil, J.: On the Reversibility of Transitions between Closed and Open Cellular Convection, *Atmos. Chem. Phys.*, 15, 7351–7367, <https://doi.org/10.5194/acp-15-7351-2015>, 2015.
- 1105 Feng, Y. and Ramanathan, V.: Investigation of Aerosol–Cloud Interactions Using a Chemical Transport Model Constrained by Satellite Observations, *Tellus B: Chemical and Physical Meteorology*, 62, 69–86, <https://doi.org/10.1111/j.1600-0889.2009.00444.x>, 2010.
- Ferek, R. J., Garrett, T., Hobbs, P. V., Strader, S., Johnson, D., Taylor, J. P., Nielsen, K., Ackerman, A. S., Kogan, Y., Liu, Q., Albrecht, B. A., and Babb, D.: Drizzle Suppression in Ship Tracks, *Journal of the Atmospheric Sciences*, 57, 2707–2728, [https://doi.org/10.1175/1520-0469\(2000\)057<2707:DSIST>2.0.CO;2](https://doi.org/10.1175/1520-0469(2000)057<2707:DSIST>2.0.CO;2), 2000.
- 1110



- Fioletov, V. E., McLinden, C. A., Krotkov, N., Li, C., Joiner, J., Theys, N., Carn, S., and Moran, M. D.: A global catalogue of large SO<sub>2</sub> sources and emissions derived from the Ozone Monitoring Instrument, *Atmospheric Chemistry and Physics*, 16, 11 497–11 519, <https://doi.org/10.5194/acp-16-11497-2016>, 2016.
- 1115 Fishman, J., Hoell, J. M., Bendura, R. D., McNeal, R. J., and Kirchhoff, V. W. J. H.: NASA GTE TRACE A Experiment (September–October 1992): Overview, *Journal of Geophysical Research: Atmospheres*, 101, 23 865–23 879, <https://doi.org/10.1029/96jd00123>, 1996.
- Flossmann, A. I., Manton, M., Abshaev, A., Bruintjes, R., Murakami, M., Prabhakaran, T., and Yao, Z.: Review of Advances in Precipitation Enhancement Research, *Bulletin of the American Meteorological Society*, 100, 1465 – 1480, <https://doi.org/10.1175/BAMS-D-18-0160.1>, 2019.
- 1120 Flower, V. J. B. and Kahn, R. A.: The Evolution of Icelandic Volcano Emissions, as Observed From Space in the Era of NASA's Earth Observing System (EOS), *Journal of Geophysical Research: Atmospheres*, 125, e2019JD031 625, <https://doi.org/10.1029/2019JD031625>, 2020.
- Formenti, P., Elbert, W., Maenhaut, W., Haywood, J. M., Osborne, S. R., and Andreae, M. O.: Inorganic and Carbonaceous Aerosols during the Southern African Regional Science Initiative (SAFARI 2000) Experiment: Chemical Characteristics, Physical Properties, and Emission Data for Smoke from African Biomass Burning, *Journal of Geophysical Research*, 108, 8488, <https://doi.org/10.1029/2002JD002408>, 1125 2003.
- Formenti, P., D'Anna, B., Flamant, C., Mallet, M., Piketh, S. J., Schepanski, K., Waquet, F., Auriol, F., Brogniez, G., Burnet, F., Chaboureaud, J.-P., Chauvigné, A., Chazette, P., Denjean, C., Desboeufs, K., Doussin, J.-F., Elguindi, N., Feuerstein, S., Gaetani, M., Giorio, C., Klopfer, D., Mallet, M. D., Nabat, P., Monod, A., Solmon, F., Namwoonde, A., Chikwililwa, C., Mushi, R., Welton, E. J., and Holben, B.: The Aerosols, Radiation and Clouds in Southern Africa Field Campaign in Namibia: Overview, Illustrative Observations, and Way Forward, 1130 *Bulletin of the American Meteorological Society*, 100, 1277–1298, <https://doi.org/10.1175/bams-d-17-0278.1>, 2019.
- Forster, P. M. and Solomon, S.: Observations of a "Weekend Effect" in Diurnal Temperature Range, *Proc Natl Acad Sci U S A*, 100, 11 225–30, <https://doi.org/10.1073/pnas.2034034100>, 2003.
- Forster, P. M., Forster, H. I., Evans, M. J., Gidden, M. J., Jones, C. D., Keller, C. A., Lamboll, R. D., Quéré, C. L., Rogelj, J., Rosen, D., Schleussner, C.-F., Richardson, T. B., Smith, C. J., and Turnock, S. T.: Current and Future Global Climate Impacts Resulting from 1135 COVID-19, *Nature Climate Change*, pp. 1–7, <https://doi.org/10.1038/s41558-020-0883-0>, 2020.
- Fyfe, J. C., Kharin, V. V., Swart, N., Flato, G. M., Sigmond, M., and Gillett, N. P.: Quantifying the influence of short-term emission reductions on climate, *Science Advances*, 7, <https://doi.org/10.1126/sciadv.abf7133>, 2021.
- Garstang, M., Tyson, P. D., Swap, R., Edwards, M., Källberg, P., and Lindesay, J. A.: Horizontal and Vertical Transport of Air over Southern Africa, *Journal of Geophysical Research: Atmospheres*, 101, 23 721–23 736, <https://doi.org/10.1029/95jd00844>, 1996.
- 1140 Gassó, S.: Satellite Observations of the Impact of Weak Volcanic Activity on Marine Clouds, *Journal of Geophysical Research*, 113, <https://doi.org/10.1029/2007JD009106>, 2008.
- Gottelman, A., Schmidt, A., and Egill Kristjánsson, J.: Icelandic Volcanic Emissions and Climate, *Nature Geoscience*, 8, 243–243, <https://doi.org/10.1038/ngeo2376>, 2015.
- Gottelman, A., Chen, C.-C., and Bardeen, C. G.: The Climate Impact of COVID19 Induced Contrail Changes, *Atmospheric Chemistry and Physics Discussions*, pp. 1–17, <https://doi.org/10.5194/acp-2021-210>, 2021a.
- 1145 Gottelman, A., Lamboll, R., Bardeen, C. G., Forster, P. M., and Watson-Parris, D.: Climate Impacts of COVID-19 Induced Emission Changes, *Geophysical Research Letters*, n/a, e2020GL091 805, <https://doi.org/https://doi.org/10.1029/2020GL091805>, e2020GL091805, 2020GL091805, 2021b.



- 1150 Ghan, S., Wang, M., Zhang, S., Ferrachat, S., Gettelman, A., Griesfeller, J., Kipling, Z., Lohmann, U., Morrison, H., Neubauer, D., Partridge, D. G., Stier, P., Takemura, T., Wang, H., and Zhang, K.: Challenges in Constraining Anthropogenic Aerosol Effects on Cloud Radiative Forcing Using Present-Day Spatiotemporal Variability, *Proceedings of the National Academy of Sciences*, p. 201514036, <https://doi.org/10.1073/pnas.1514036113>, 2016.
- 1155 Gislason, S. R., Stefánsdóttir, G., Pfeffer, M. A., Barsotti, S., Th, J., Galeczka, I., Bali, E., Sigmarsson, O., Stefánsson, A., Keller, N. S., Sigurdsson, Á., Bergsson, B., Galle, B., Jacobo, V. C., Arellano, S., Aiuppa, A., Jónasdóttir, E. B., Eiríksdóttir, E. S., Jakobsson, S., Gudfinnsson, G. H., Halldórsson, S. A., Gunnarsson, H., Haddadi, B., Jónsdóttir, I., Thordarson, T., Riishuus, M., Högnadóttir, T., Dürig, T., Pedersen, G. B. M., Höskuldsson, Á., and Gudmundsson, M. T.: Environmental pressure from the 2014–15 eruption of Bárðarbunga volcano, Iceland, *Geochemical Perspectives Letters*, 1, 84–93, <https://doi.org/http://dx.doi.org/10.7185/geochemlet.1509>, 2015.
- 1160 Glassmeier, F., Hoffmann, F., Johnson, J. S., Yamaguchi, T., Carslaw, K. S., and Feingold, G.: An Emulator Approach to Stratocumulus Susceptibility, *Atmospheric Chemistry and Physics*, 19, 10 191–10 203, <https://doi.org/10.5194/acp-19-10191-2019>, 2019.
- 1160 Glassmeier, F., Hoffmann, F., Johnson, J. S., Yamaguchi, T., Carslaw, K. S., and Feingold, G.: Aerosol-cloud-climate cooling overestimated by ship-track data, *Science*, 371, 485–489, <https://doi.org/10.1126/science.abd3980>, 2021.
- Gong, D.-Y., Wang, W., Qian, Y., Bai, W., Guo, Y., and Mao, R.: Observed Holiday Aerosol Reduction and Temperature Cooling over East Asia, *Journal of Geophysical Research: Atmospheres*, 119, 6306–6324, <https://doi.org/10.1002/2014jd021464>, 2014.
- 1165 Goren, T. and Rosenfeld, D.: Satellite Observations of Ship Emission Induced Transitions from Broken to Closed Cell Marine Stratocumulus over Large Areas, *Journal of Geophysical Research: Atmospheres*, 117, n/a–n/a, <https://doi.org/10.1029/2012jd017981>, 2012.
- Goren, T. and Rosenfeld, D.: Extensive Closed Cell Marine Stratocumulus Downwind of Europe—A Large Aerosol Cloud Mediated Radiative Effect or Forcing?, *Journal of Geophysical Research: Atmospheres*, 120, 6098–6116, <https://doi.org/10.1002/2015JD023176>, 2015.
- Goren, T., Kazil, J., Hoffmann, F., Yamaguchi, T., and Feingold, G.: Anthropogenic Air Pollution Delays Marine Stratocumulus Break-up to Open-Cells, *Geophysical Research Letters*, 46, 14,135–14,144, <https://doi.org/10.1029/2019gl085412>, 2019.
- 1170 Grabowski, W. W. and Morrison, H.: Do Ultrafine Cloud Condensation Nuclei Invigorate Deep Convection?, *Journal of the Atmospheric Sciences*, 77, 2567–2583, <https://doi.org/10.1175/jas-d-20-0012.1>, 2020.
- Graf, H.-F., Feichter, J., and Langmann, B.: Volcanic sulfur emissions: Estimates of source strength and its contribution to the global sulfate distribution, *Journal of Geophysical Research: Atmospheres*, 102, 10 727–10 738, <https://doi.org/https://doi.org/10.1029/96JD03265>, 1997.
- 1175 Grosvenor, D. P. and Carslaw, K. S.: The decomposition of cloud-aerosol forcing in the UK Earth System Model (UKESM1), *Atmos. Chem. Phys.*, 20, 15 681–15 724, <https://doi.org/10.5194/acp-20-15681-2020>, 2020.
- Grosvenor, D. P. and Wood, R.: Daily MODIS (MODERate Imaging Spectroradiometer) derived cloud droplet number concentration global dataset for 2003–2015. Retrieved from:., <http://catalogue.ceda.ac.uk/uuid/cf97ccc802d348ec8a3b6f2995dfbbf>, 2018.
- 1180 Grosvenor, D. P., Sourdeval, O., Zuidema, P., Ackerman, A., Alexandrov, M. D., Bennartz, R., Boers, R., Cairns, B., Chiu, C., Christensen, M., Deneke, H., Diamond, M., Feingold, G., Fridlind, A., Hünerbein, A., Knist, C., Kollias, P., Marshak, A., McCoy, D., Merk, D., Painemal, D., Rausch, J., Rosenfeld, D., Russchenberg, H., Seifert, P., Sinclair, K., Stier, P., B. van D., Wendisch, M., Werner, F., Wood, R., Zhang, Z., and Quaas, J.: Remote sensing of cloud droplet number concentration in warm clouds: A review of the current state of knowledge and perspectives, *Rev. Geophys.*, 56, 409–453, <https://doi.org/10.1029/2017RG000593>, 2018.
- 1185 Gryspeerdt, E., Quaas, J., and Bellouin, N.: Constraining the aerosol influence on cloud fraction, *Journal of Geophysical Research: Atmospheres*, 121, 3566–3583, <https://doi.org/https://doi.org/10.1002/2015JD023744>, 2016.



- Gryspeerd, E., Goren, T., Sourdeval, O., Quaas, J., Mülmenstädt, J., Dipu, S., Unglaub, C., Gettelman, A., and Christensen, M.: Constraining the Aerosol Influence on Cloud Liquid Water Path, *Atmospheric Chemistry and Physics*, 19, 5331–5347, <https://doi.org/10.5194/acp-19-5331-2019>, 2019a.
- Gryspeerd, E., Smith, T. W. P., O’Keeffe, E., Christensen, M. W., and Goldsworth, F. W.: The Impact of Ship Emission Controls Recorded by Cloud Properties, *Geophysical Research Letters*, n/a, <https://doi.org/10.1029/2019GL084700>, 2019b.
- Gryspeerd, E., Goren, T., and Smith, T. W. P.: Observing the timescales of aerosol–cloud interactions in snapshot satellite images, *Atmos. Chem. Phys.*, 21, 6093–6109, <https://doi.org/10.5194/acp-21-6093-2021>, 2021.
- Guo, S., Hu, M., Guo, Q., Zhang, X., Schauer, J. J., and Zhang, R.: Quantitative Evaluation of Emission Controls on Primary and Secondary Organic Aerosol Sources during Beijing 2008 Olympics, *Atmospheric Chemistry and Physics*, 13, 8303–8314, <https://doi.org/10.5194/acp-13-8303-2013>, 2013.
- Gupta, S., McFarquhar, G. M., O’Brien, J. R., Delene, D. J., Poellot, M. R., Dobracki, A., Podolske, J. R., Redemann, J., LeBlanc, S. E., Segal-Rozenhaimer, M., and Pistone, K.: Impact of the variability in vertical separation between biomass burning aerosols and marine stratocumulus on cloud microphysical properties over the Southeast Atlantic, *Atmospheric Chemistry and Physics*, 21, 4615–4635, <https://doi.org/10.5194/acp-21-4615-2021>, 2021.
- Hamilton, D. S., Lee, L. A., Pringle, K. J., Reddington, C. L., Spracklen, D. V., and Carslaw, K. S.: Occurrence of Pristine Aerosol Environments on a Polluted Planet, *Proceedings of the National Academy of Sciences*, 111, 18466–18471, <https://doi.org/10.1073/pnas.1415440111>, 2014.
- Han, Q., Rossow, W. B., and Lacis, A. A.: Near-Global Survey of Effective Droplet Radii in Liquid Water Clouds Using ISCCP Data, *J. Climate*, 7, 465–497, 1994.
- Hansen, J., Lacis, A., Ruedy, R., and Sato, M.: Potential Climate Impact of Mount Pinatubo Eruption, *Geophysical Research Letters*, 19, 215–218, <https://doi.org/10.1029/91gl02788>, 1992.
- Hao, N., Valks, P., Loyola, D., Cheng, Y. F., and Zimmer, W.: Space-Based Measurements of Air Quality during the World Expo 2010 in Shanghai, *Environmental Research Letters*, 6, 044 004, <https://doi.org/10.1088/1748-9326/6/4/044004>, 2011.
- Haslett, S. L., Taylor, J. W., Evans, M., Morris, E., Vogel, B., Dajuma, A., Brito, J., Batenburg, A. M., Borrmann, S., Schneider, J., Schulz, C., Denjean, C., Bourriane, T., Knippertz, P., Dupuy, R., Schwarzenböck, A., Sauer, D., Flamant, C., Dorsey, J., Crawford, I., and Coe, H.: Remote biomass burning dominates southern West African air pollution during the monsoon, *Atmospheric Chemistry and Physics*, 19, 15 217–15 234, <https://doi.org/10.5194/acp-19-15217-2019>, 2019.
- Haywood, J. M., Osborne, S. R., Francis, P. N., Keil, A., Formenti, P., Andreae, M. O., and Kaye, P. H.: The Mean Physical and Optical Properties of Regional Haze Dominated by Biomass Burning Aerosol Measured from the C-130 Aircraft during SAFARI 2000, *Journal of Geophysical Research: Atmospheres*, 108, n/a–n/a, <https://doi.org/10.1029/2002jd002226>, 2003.
- Haywood, J. M., Abel, S. J., Barrett, P. A., Bellouin, N., Blyth, A., Bower, K. N., Brooks, M., Carslaw, K., Che, H., Coe, H., Cotterell, M. I., Crawford, I., Cui, Z., Davies, N., Dingley, B., Field, P., Formenti, P., Gordon, H., de Graaf, M., Herbert, R., Johnson, B., Jones, A. C., Langridge, J. M., Malavelle, F., Partridge, D. G., Peers, F., Redemann, J., Stier, P., Szpek, K., Taylor, J. W., Watson-Parris, D., Wood, R., Wu, H., and Zuidema, P.: Overview: The CLOUD-Aerosol-Radiation Interaction and Forcing: Year- 2017 (CLARIFY-2017) Measurement Campaign, *Atmospheric Chemistry and Physics Discussions*, <https://doi.org/10.5194/acp-2020-729>, 2020.
- Hobbs, P. V., Stith, J. L., and Radke, L. F.: Cloud-Active Nuclei from Coal-Fired Electric Power Plants and Their Interactions with Clouds, *Journal of Applied Meteorology*, 19, 439–451, [https://doi.org/10.1175/1520-0450\(1980\)019<0439:CANFCF>2.0.CO;2](https://doi.org/10.1175/1520-0450(1980)019<0439:CANFCF>2.0.CO;2), 1980.



- Hobbs, P. V., Garrett, T. J., Ferek, R. J., Strader, S. R., Hegg, D. A., Frick, G. M., Hoppel, W. A., Gasparovic, R. F., Russell, L. M., Johnson, D. W., O'Dowd, C., Durkee, P. A., Nielsen, K. E., and Innis, G.: Emissions from Ships with Respect to Their Effects on Clouds, *Journal of the Atmospheric Sciences*, 57, 2570–2590, [https://doi.org/10.1175/1520-0469\(2000\)057<2570:EFSWRT>2.0.CO;2](https://doi.org/10.1175/1520-0469(2000)057<2570:EFSWRT>2.0.CO;2), 2000.
- 1225 Hu, S., Zhu, Y., Rosenfeld, D., Mao, F., Lu, X., Pan, Z., Zang, L., and Gong, W.: The dependence of ship-polluted marine cloud properties and radiative forcing on background drop concentrations, *Journal of Geophysical Research: Atmospheres*, n/a, e2020JD033852, <https://doi.org/https://doi.org/10.1029/2020JD033852>, e2020JD033852 2020JD033852, 2021.
- Huang, X., Ding, A., Gao, J., Zheng, B., Zhou, D., Qi, X., Tang, R., Wang, J., Ren, C., Nie, W., Chi, X., Xu, Z., Chen, L., Li, Y., Che, F., Pang, N., Wang, H., Tong, D., Qin, W., Cheng, W., Liu, W., Fu, Q., Liu, B., Chai, F., Davis, S. J., Zhang, Q., and He, K.: Enhanced Secondary Pollution Offset Reduction of Primary Emissions during COVID-19 Lockdown in China, *National Science Review*, p. nwaal37, <https://doi.org/10.1093/nsr/nwaa137>, 2020.
- 1230 IEA: Global Energy Review 2020, 2020.
- IPCC: Summary for policymakers, in *Climate Change 2013: The Physical Science Basis, Contribution of Working Group I to the Fifth Assessment Report of the Intergovernmental Panel on Climate Change*, [T. F. Stocker, D. Qin, and G. Plattner (eds.)], Cambridge University Press, Cambridge, United Kingdom and New York, NY, USA., 2013.
- 1235 Jiang, Q., Sun, Y. L., Wang, Z., and Yin, Y.: Aerosol Composition and Sources during the Chinese Spring Festival: Fireworks, Secondary Aerosol, and Holiday Effects, *Atmospheric Chemistry and Physics*, 15, 6023–6034, <https://doi.org/10.5194/acp-15-6023-2015>, 2015.
- Jin, Q., Grandey, B. S., Rothenberg, D., Avramov, A., and Wang, C.: Impacts on Cloud Radiative Effects Induced by Coexisting Aerosols Converted from International Shipping and Maritime DMS Emissions, *Atmospheric Chemistry and Physics*, 18, 16 793–16 808, <https://doi.org/10.5194/acp-18-16793-2018>, 2018.
- 1240 Jin, Y., Andersson, H., and Zhang, S.: Air Pollution Control Policies in China: A Retrospective and Prospects, *International Journal of Environmental Research and Public Health*, 13, 1219–1240, <https://doi.org/10.3390/ijerph13121219>, 2016.
- Johnson, B. T., Shine, K. P., and Forster, P. M.: The semi-direct aerosol effect: Impact of absorbing aerosols on marine stratocumulus, *Quarterly Journal of the Royal Meteorological Society*, 130, 1407–1422, <https://doi.org/https://doi.org/10.1256/qj.03.61>, 2004.
- 1245 Jones, C. D., Hickman, J. E., Rumbold, S. T., Walton, J., Lamboll, R. D., Skeie, R. B., Fiedler, S., Forster, P. M., Rogelj, J., Abe, M., Botzet, M., Calvin, K., Cassou, C., Cole, J. N., Davini, P., Deushi, M., Dix, M., Fyfe, J. C., Gillett, N. P., Ilyina, T., Kawamiya, M., Kelley, M., Kharin, S., Koshiro, T., Li, H., Mackallah, C., MÅijller, W. A., Nabat, P., van Noije, T., Nolan, P., Ohgaito, R., OliviiÅl, D., Oshima, N., Parodi, J., Reerink, T. J., Ren, L., Romanou, A., Séférian, R., Tang, Y., Timmreck, C., Tjiputra, J., Tourigny, E., Tsigaridis, K., Wang, H., Wu, M., Wyser, K., Yang, S., Yang, Y., and Ziehn, T.: The Climate Response to Emissions Reductions due to COVID-19: Initial Results from CovidMIP, *Geophysical Research Letters*, n/a, e2020GL091 883, <https://doi.org/https://doi.org/10.1029/2020GL091883>, e2020GL091883 2020GL091883, 2021.
- 1250 Kabatas, B., Menzel, W. P., Bilgili, A., and Gumley, L. E.: Comparing Ship-Track Droplet Sizes Inferred from Terra and Aqua MODIS Data, *Journal of Applied Meteorology and Climatology*, 52, 230 – 241, <https://doi.org/10.1175/JAMC-D-11-0232.1>, 2013.
- 1255 Kacarab, M., Thornhill, K. L., Dobracki, A., Howell, S. G., O'Brien, J. R., Freitag, S., Poellot, M. R., Wood, R., Zuidema, P., Redemann, J., and Nenes, A.: Biomass burning aerosol as a modulator of the droplet number in the southeast Atlantic region, *Atmospheric Chemistry and Physics*, 20, 3029–3040, <https://doi.org/10.5194/acp-20-3029-2020>, 2020.
- Kaufman, Y. J. and Nakajima, T.: Effect of Amazon Smoke on Cloud Microphysics and Albedo-Analysis from Satellite Imagery, *Journal of Applied Meteorology*, 32, 729–744, [https://doi.org/10.1175/1520-0450\(1993\)032<0729:Eoasoc>2.0.Co;2](https://doi.org/10.1175/1520-0450(1993)032<0729:Eoasoc>2.0.Co;2), 1993.



- 1260 Krüger, O. and Graßl, H.: The Indirect Aerosol Effect over Europe, *Geophysical Research Letters*, 29, 31–1–31–4, <https://doi.org/10.1029/2001GL014081>, 2002.
- Lai, Y. and Brimblecombe, P.: Regulatory Effects on Particulate Pollution in the Early Hours of Chinese New Year, 2015, *Environ Monit Assess*, 189, 467, <https://doi.org/10.1007/s10661-017-6167-0>, 2017.
- Lauer, A., Eyring, V., Hendricks, J., Jöckel, P., and Lohmann, U.: Global Model Simulations of the Impact of Ocean-Going Ships on Aerosols, Clouds, and the Radiation Budget, *Atmospheric Chemistry and Physics*, 7, 5061–5079, <https://doi.org/10.5194/acp-7-5061-2007>, 2007.
- 1265 Le, T., Wang, Y., Liu, L., Yang, J., Yung, Y. L., Li, G., and Seinfeld, J. H.: Unexpected Air Pollution with Marked Emission Reductions during the COVID-19 Outbreak in China, *Science*, p. eabb7431, <https://doi.org/10.1126/science.abb7431>, 2020.
- Le Quéré, C., Jackson, R. B., Jones, M. W., Smith, A. J. P., Abernethy, S., Andrew, R. M., De-Gol, A. J., Willis, D. R., Shan, Y., Canadell, J. G., Friedlingstein, P., Creutzig, F., and Peters, G. P.: Temporary Reduction in Daily Global CO<sub>2</sub> Emissions during the COVID-19 Forced Confinement, *Nature Climate Change*, pp. 1–7, <https://doi.org/10.1038/s41558-020-0797-x>, 2020.
- 1270 Lee, D. S., Fahey, D. W., Skowron, A., Allen, M. R., Burkhardt, U., Chen, Q., Doherty, S. J., Freeman, S., Forster, P. M., Fuglestedt, J., Gettelman, A., De León, R. R., Lim, L. L., Lund, M. T., Millar, R. J., Owen, B., Penner, J. E., Pitari, G., Prather, M. J., Sausen, R., and Wilcox, L. J.: The Contribution of Global Aviation to Anthropogenic Climate Forcing for 2000 to 2018, *Atmospheric Environment*, 244, 117 834, <https://doi.org/10.1016/j.atmosenv.2020.117834>, 2021.
- 1275 Levy, R. C., Mattoo, S., Munchak, L. A., Remer, L. A., Sayer, A. M., Patadia, F., and Hsu, N. C.: The Collection 6 MODIS aerosol products over land and ocean, *J. Atmos. Meas. Tech*, 6, 2989–3032, <https://doi.org/10.5194/amt-6-2989-2013>, 2013.
- Li, K., Jacob, D. J., Liao, H., Shen, L., Zhang, Q., and Bates, K. H.: Anthropogenic Drivers of 2013–2017 Trends in Summer Surface Ozone in China, *Proceedings of the National Academy of Sciences*, 116, 422–427, <https://doi.org/10.1073/pnas.1812168116>, 2019a.
- Li, Z., Lau, W. K.-M., Ramanathan, V., Wu, G., Ding, Y., Manoj, M. G., Liu, J., Qian, Y., Li, J., Zhou, T., Fan, J., Rosenfeld, D., Ming, Y., Wang, Y., Huang, J., Wang, B., Xu, X., Lee, S.-S., Cribb, M., Zhang, F., Yang, X., Zhao, C., Takemura, T., Wang, K., Xia, X., Yin, Y., Zhang, H., Guo, J., Zhai, P. M., Sugimoto, N., Babu, S. S., and Brasseur, G. P.: Aerosol and Monsoon Climate Interactions over Asia, *Reviews of Geophysics*, 54, 866–929, <https://doi.org/10.1002/2015RG000500>, 2016.
- 1280 Li, Z., Wang, Y., Guo, J., Zhao, C., Cribb, M. C., Dong, X., Fan, J., Gong, D., Huang, J., Jiang, M., Jiang, Y., Lee, S.-S., Li, H., Li, J., Liu, J., Qian, Y., Rosenfeld, D., Shan, S., Sun, Y., Wang, H., Xin, J., Yan, X., Yang, X., Yang, X.-q., Zhang, F., and Zheng, Y.: East Asian Study of Tropospheric Aerosols and Their Impact on Regional Clouds, Precipitation, and Climate (EAST-AIRCPC), *Journal of Geophysical Research: Atmospheres*, 124, 13 026–13 054, <https://doi.org/10.1029/2019JD030758>, 2019b.
- 1285 Lindsay, J. A., Andreae, M. O., Goldammer, J. G., Harris, G., Annegarn, H. J., Garstang, M., Scholes, R. J., and van Wilgen, B. W.: International geosphere-biosphere programme/international global atmospheric chemistry SAFARI-92 field experiment: Background and overview, *Journal of Geophysical Research: Atmospheres*, 101, 23 521–23 530, <https://doi.org/https://doi.org/10.1029/96JD01512>, 1996.
- 1290 Liu, F., Page, A., Strode, S. A., Yoshida, Y., Choi, S., Zheng, B., Lamsal, L. N., Li, C., Krotkov, N. A., Eskes, H., van der A, R., Veefkind, P., Levelt, P. F., Hauser, O. P., and Joiner, J.: Abrupt Decline in Tropospheric Nitrogen Dioxide over China after the Outbreak of COVID-19, *Science Advances*, 6, eabc2992, <https://doi.org/10.1126/sciadv.abc2992>, 2020.
- Liu, Q., Kogan, Y. L., Lilly, D. K., Johnson, D. W., Innis, G. E., Durkee, P. A., and Nielsen, K. E.: Modeling of Ship Effluent Transport and Its Sensitivity to Boundary Layer Structure, *Journal of the Atmospheric Sciences*, 57, 2779 – 2791, [https://doi.org/10.1175/1520-0469\(2000\)057<2779:MOSETA>2.0.CO;2](https://doi.org/10.1175/1520-0469(2000)057<2779:MOSETA>2.0.CO;2), 2000.
- 1295 Liu, Y. G. and Daum, P. H.: Anthropogenic aerosols - Indirect warming effect from dispersion forcing, *Nature*, 419, 580–581, <https://doi.org/10.1038/419580a>, 2002.





- Loeb, N. G., Su, W., Bellouin, N., and Ming, Y.: Changes in Clear-Sky Shortwave Aerosol Direct Radiative Effects Since 2002, *Journal of Geophysical Research: Atmospheres*, 126, e2020JD034090, <https://doi.org/10.1029/2020JD034090>, e2020JD034090  
1300 2020JD034090, 2021.
- Lohmann, U.: A glaciation indirect aerosol effect caused by soot aerosols, *Geophysical Research Letters*, 29, 11–1–11–4, <https://doi.org/10.1029/2001GL014357>, 2002.
- Lu, M.-L., Sorooshian, A., Jonsson, H. H., Feingold, G., Flagan, R. C., and Seinfeld, J. H.: Marine Stratocumulus Aerosol-Cloud Relationships in the MASE-II Experiment: Precipitation Susceptibility in Eastern Pacific Marine Stratocumulus, *Journal of Geophysical Research: Atmospheres*, 114, <https://doi.org/10.1029/2009JD012774>, 2009.  
1305
- Mace, G. G. and Abernathy, A. C.: Observational Evidence for Aerosol Invigoration in Shallow Cumulus Downstream of Mount Kilauea, *Geophysical Research Letters*, p. 2016GL067830, <https://doi.org/10.1002/2016GL067830>, 2016.
- Malavelle, F. F., Haywood, J. M., Jones, A., Gettelman, A., Clarisse, L., Bauduin, S., Allan, R. P., Karset, I. H. H., Kristjánsson, J. E., Oreopoulos, L., Cho, N., Lee, D., Bellouin, N., Boucher, O., Grosvenor, D. P., Carslaw, K. S., Dhomse, S., Mann, G. W., Schmidt, A.,  
1310 Coe, H., Hartley, M. E., Dalvi, M., Hill, A. A., Johnson, B. T., Johnson, C. E., Knight, J. R., O'Connor, F. M., Partridge, D. G., Stier, P., Myhre, G., Platnick, S., Stephens, G. L., Takahashi, H., and Thordarson, T.: Strong Constraints on Aerosol–Cloud Interactions from Volcanic Eruptions, *Nature*, 546, 485–491, <https://doi.org/10.1038/nature22974>, 2017.
- March, D., Metcalfe, K., Tintor, J., and Godley, B. J.: Tracking the global reduction of marine traffic during the COVID-19 pandemic, *Nature Communications*, 12, 2415, <https://doi.org/10.1038/s41467-021-22423-6>, 2021.
- 1315 Mardi, A. H., Dadashazar, H., MacDonald, A. B., Braun, R. A., Crosbie, E., Xian, P., Thorsen, T. J., Coggon, M. M., Fenn, M. A., Ferrare, R. A., Hair, J. W., Woods, R. K., Jonsson, H. H., Flagan, R. C., Seinfeld, J. H., and Sorooshian, A.: Biomass Burning Plumes in the Vicinity of the California Coast: Airborne Characterization of Physicochemical Properties, Heating Rates, and Spatiotemporal Features, *Journal of Geophysical Research: Atmospheres*, 123, 13,560–13,582, <https://doi.org/10.1029/2018JD029134>, 2018.
- 1320 Mardi, A. H., Dadashazar, H., MacDonald, A. B., Crosbie, E., Coggon, M. M., Aghdam, M. A., Woods, R. K., Jonsson, H. H., Flagan, R. C., Seinfeld, J. H., and Sorooshian, A.: Effects of Biomass Burning on Stratocumulus Droplet Characteristics, Drizzle Rate, and Composition, *Journal of Geophysical Research: Atmospheres*, 124, 12 301–12 318, <https://doi.org/10.1029/2019JD031159>, 2019.
- McComiskey, A. and Feingold, G.: The scale problem in quantifying aerosol indirect effects, *Atmospheric Chemistry and Physics*, 12, 1031–1049, <https://doi.org/10.5194/acp-12-1031-2012>, 2012.
- 1325 McConnell, J. R., Sigl, M., Plunkett, G., Burke, A., Kim, W. M., Raible, C. C., Wilson, A. I., Manning, J. G., Ludlow, F., Chellman, N. J., Innes, H. M., Yang, Z., Larsen, J. F., Schaefer, J. R., Kipfstuhl, S., Mojtabavi, S., Wilhelms, F., Opel, T., Meyer, H., and Steffensen, J. P.: Extreme Climate after Massive Eruption of Alaska’s Okmok Volcano in 43 BCE and Effects on the Late Roman Republic and Ptolemaic Kingdom, *Proc Natl Acad Sci U S A*, 117, 15 443–15 449, <https://doi.org/10.1073/pnas.2002722117>, 2020.
- McCoy, D. T. and Hartmann, D. L.: Observations of a Substantial Cloud-Aerosol Indirect Effect during the 2014–2015 Bárðarbunga-Veiðivötn Fissure Eruption in Iceland, *Geophysical Research Letters*, 42, 10,409–10,414, <https://doi.org/10.1002/2015gl067070>, 2015.
- 1330 McCoy, D. T., Bender, F. A. M., Grosvenor, D. P., Mohrmann, J. K., Hartmann, D. L., Wood, R., and Field, P. R.: Predicting Decadal Trends in Cloud Droplet Number Concentration Using Reanalysis and Satellite Data, *Atmospheric Chemistry and Physics*, 18, 2035–2047, <https://doi.org/10.5194/acp-18-2035-2018>, 2018.
- 1335 McCoy, I. L., McCoy, D. T., Wood, R., Regayre, L., Watson-Parris, D., Grosvenor, D. P., Mulcahy, J. P., Hu, Y., Bender, F. A.-M., Field, P. R., Carslaw, K. S., and Gordon, H.: The Hemispheric Contrast in Cloud Microphysical Properties Constrains Aerosol Forcing, *Proceedings of the National Academy of Sciences*, 117, 18 998–19 006, <https://doi.org/10.1073/pnas.1922502117>, 2020.



- McFarquhar, G. M., Bretherton, C., Marchand, R., Protat, A., DeMott, P. J., Alexander, S. P., Roberts, G. C., Twohy, C. H., Toohey, D., Siems, S., Huang, Y., Wood, R., Rauber, R. M., Lasher-Trapp, S., Jensen, J., Stith, J., Mace, J., Um, J., Järvinen, E., Schnaiter, M., Gettelman, A., Sanchez, K. J., McCluskey, C. S., Russell, L. M., McCoy, I. L., Atlas, R., Bardeen, C. G., Moore, K. A., Hill, T. C. J., Humphries, R. S., Keywood, M. D., Ristovski, Z., Cravigan, L., Schofield, R., Fairall, C., Mallet, M. D., Kreidenweis, S. M., Rainwater, B., D'Álessandro, J., Wang, Y., Wu, W., Saliba, G., Levin, E. J. T., Ding, S., Lang, F., Truong, S. C., Wolff, C., Haggerty, J., Harvey, M. J., Klekociuk, A., and McDonald, A.: Observations of clouds, aerosols, precipitation, and surface radiation over the Southern Ocean: An overview of CAPRICORN, MARCUS, MICRE and SOCRATES, *Bulletin of the American Meteorological Society*, pp. 1 – 92, <https://doi.org/10.1175/BAMS-D-20-0132.1>, 2020.
- 1340 Michibata, T. and Suzuki, K.: Reconciling Compensating Errors Between Precipitation Constraints and the Energy Budget in a Climate Model, *Geophysical Research Letters*, 47, e2020GL088340, <https://doi.org/10.1029/2020GL088340>, 2020.
- 1345 Ming, Y., Loeb, N. G., Lin, P., Shen, Z., Naik, V., Singer, C. E., Ward, R. X., Paulot, F., Zhang, Z., Bellouin, N., Horowitz, L. W., Ginoux, P. A., and Ramaswamy, V.: Assessing the Influence of COVID-19 on the Shortwave Radiative Fluxes Over the East Asian Marginal Seas, *Geophysical Research Letters*, 48, e2020GL091699, <https://doi.org/https://doi.org/10.1029/2020GL091699>, e2020GL091699 2020GL091699, 2021.
- 1350 Mitchell, J. F. B., Senior, C. A., and Ingram, W. J.: CO<sub>2</sub> and climate: a missing feedback?, *Nature*, 341, 132–134, <https://doi.org/10.1038/341132a0>, 1989.
- Moseid, K. O., Schulz, M., Storelvmo, T., Julsrud, I. R., Olivié, D., Nabat, P., Wild, M., Cole, J. N. S., and Takemura, T.: Bias in CMIP6 Models Compared to Observed Regional Dimming and Brightening Trends (1961&ndash;2014), *Atmospheric Chemistry and Physics Discussions*, pp. 1–20, <https://doi.org/10.5194/acp-2019-1210>, 2020.
- 1355 Mulcahy, J. P., Jones, C., Sellar, A., Johnson, B., Boutle, I. A., Jones, A., Andrews, T., Rumbold, S. T., Mollard, J., Bellouin, N., Johnson, C. E., Williams, K. D., Grosvenor, D. P., and McCoy, D. T.: Improved Aerosol Processes and Effective Radiative Forcing in HadGEM3 and UKESM1, *Journal of Advances in Modeling Earth Systems*, 10, 2786–2805, <https://doi.org/10.1029/2018MS001464>, 2018.
- Nakajima, T. and King, M. D.: Determination of the Optical Thickness and Effective Particle Radius of Clouds from Reflected Solar Radiation Measurements. Part I: Theory, *Journal of the Atmospheric Sciences*, 47, 1878–1893, [https://doi.org/10.1175/1520-0469\(1990\)047<1878:DOTOTA>2.0.CO;2](https://doi.org/10.1175/1520-0469(1990)047<1878:DOTOTA>2.0.CO;2), 1989.
- 1360 Nakajima, T., Higurashi, A., Kawamoto, K., and Penner, J. E.: A Possible Correlation between Satellite-Derived Cloud and Aerosol Microphysical Parameters, *Geophysical Research Letters*, 28, 1171–1174, <https://doi.org/10.1029/2000gl012186>, 2001.
- National Academies of Sciences: Reflecting Sunlight: Recommendations for Solar Geoengineering Research and Research Governance., Tech. rep., National Academies Press, Washington, D. C., 2021.
- 1365 Norris, J. R. and Evan, A. T.: Empirical removal of artifacts from the ISCCP and PATMOS-x satellite cloud records, *J. Atmos. Ocean. Technol.*, 32, 691–702, <https://doi.org/10.1175/JTECH-D-14-00058.1>, 2015.
- Norris, J. R., Allen, R. J., Evan, A. T., Zelinka, M. D., O'Dell, C. W., and Klein, S. A.: Evidence for Climate Change in the Satellite Cloud Record, *Nature*, 536, 72–75, <https://doi.org/10.1038/nature18273>, 2016.
- Pennypacker, S., Diamond, M., and Wood, R.: Ultra-clean and smoky marine boundary layers frequently occur in the same season over the southeast Atlantic, *Atmospheric Chemistry and Physics*, 20, 2341–2351, <https://doi.org/10.5194/acp-20-2341-2020>, 2020.
- 1370 Pereira, J. M., Oom, D., Pereira, P., Turkman, A. A., and Turkman, K. F.: Religious Affiliation Modulates Weekly Cycles of Cropland Burning in Sub-Saharan Africa, *PLoS One*, 10, e0139189, <https://doi.org/10.1371/journal.pone.0139189>, 2015.



- Peters, K., Quaas, J., and Graßl, H.: A Search for Large-Scale Effects of Ship Emissions on Clouds and Radiation in Satellite Data, *Journal of Geophysical Research: Atmospheres*, 116, <https://doi.org/10.1029/2011JD016531>, 2011.
- 1375 Peters, K., Stier, P., Quaas, J., and Graßl, H.: Corrigendum to "Aerosol indirect effects from shipping emissions: sensitivity studies with the global aerosol-climate model ECHAM-HAM" published in *Atmos. Chem. Phys.*, 12, 5985–6007, 2012, *Atmospheric Chemistry and Physics*, 13, 6429–6430, <https://doi.org/10.5194/acp-13-6429-2013>, 2013.
- Peters, K., Quaas, J., Stier, P., and Graßl, H.: Processes Limiting the Emergence of Detectable Aerosol Indirect Effects on Tropical Warm Clouds in Global Aerosol-Climate Model and Satellite Data, *Tellus B: Chemical and Physical Meteorology*, 66, <https://doi.org/10.3402/tellusb.v66.24054>, 2014.
- 1380 Platnick, S., Meyer, K. G., King, M. D., Wind, G., Amarasinghe, N., Marchant, B., Arnold, G. T., Zhang, Z., Hubanks, P. A., Holz, R. E., Yang, P., Ridgway, W. L., and Riedi, J.: The MODIS Cloud Optical and Microphysical Products: Collection 6 Updates and Examples From Terra and Aqua, *IEEE Transact. Geosci. Remote Sens.*, 55, 502–525, <https://doi.org/10.1109/TGRS.2016.2610522>, 2017.
- Pope, R. J., Marshall, A. M., and O’Kane, B. O.: Observing UK Bonfire Night Pollution from Space: Analysis of Atmospheric Aerosol, *Weather*, 71, 288–291, <https://doi.org/10.1002/wea.2914>, 2016.
- 1385 Porch, W. M., Kao, C.-Y. J., and Kelley, R. G.: Ship trails and ship induced cloud dynamics, *Atmospheric Environment. Part A. General Topics*, 24, 1051 – 1059, [https://doi.org/https://doi.org/10.1016/0960-1686\(90\)90073-V](https://doi.org/https://doi.org/10.1016/0960-1686(90)90073-V), 1990.
- Possner, A., Zubler, E., Lohmann, U., and Schär, C.: Real-Case Simulations of Aerosol–Cloud Interactions in Ship Tracks over the Bay of Biscay, *Atmospheric Chemistry and Physics*, 15, 2185–2201, <https://doi.org/10.5194/acp-15-2185-2015>, 2015.
- 1390 Possner, A., Zubler, E., Lohmann, U., and Schär, C.: The Resolution Dependence of Cloud Effects and Ship-Induced Aerosol-Cloud Interactions in Marine Stratocumulus, *Journal of Geophysical Research: Atmospheres*, p. 2015JD024685, <https://doi.org/10.1002/2015JD024685>, 2016.
- Possner, A., Ekman, A. M. L., and Lohmann, U.: Cloud Response and Feedback Processes in Stratiform Mixed-Phase Clouds Perturbed by Ship Exhaust, *Geophysical Research Letters*, 44, 1964–1972, <https://doi.org/10.1002/2016GL071358>, 2017.
- 1395 Possner, A., Wang, H., Wood, R., Caldeira, K., and Ackerman, T.: The Efficacy of Aerosol-Cloud-Radiative Perturbations from near-Surface Emissions in Deep Open-Cell Stratocumuli, *Atmospheric Chemistry and Physics*, 18, 17 475–17 488, <https://doi.org/10.5194/acp-18-17475-2018>, 2018.
- Possner, A., Eastman, R., Bender, F., and Glassmeier, F.: Deconvolution of Boundary Layer Depth and Aerosol Constraints on Cloud Water Path in Subtropical Stratocumulus Decks, *Atmospheric Chemistry and Physics*, 20, 3609–3621, <https://doi.org/10.5194/acp-20-3609-2020>, 2020.
- 1400 Quaas, J.: Approaches to Observe Anthropogenic Aerosol-Cloud Interactions, *Current Climate Change Reports*, 1, 297–304, <https://doi.org/10.1007/s40641-015-0028-0>, 2015.
- Quaas, J., Boucher, O., Jones, A., Weedon, G. P., Kieser, J., and Joos, H.: Exploiting the Weekly Cycle as Observed over Europe to Analyse Aerosol Indirect Effects in Two Climate Models, *Atmos. Chem. Phys.*, 9, 8493–8501, <https://doi.org/10.5194/acp-9-8493-2009>, 2009.
- 1405 Quaas, J., Gryspeerdt, E., Vautard, R., and Boucher, O.: Climate impact of aircraft-induced cirrus assessed from satellite observations before and during COVID-19, *Environmental Research Letters*, 16, 064 051, <https://doi.org/10.1088/1748-9326/abf686>, 2021.
- Radke, L. F., Coakley, J. A., and King, M. D.: Direct and Remote Sensing Observations of the Effects of Ships on Clouds, *Science*, 246, 1146–1149, 1989.
- Raes, F., Bates, T., McGovern, F., and Liedekerke, M. V.: The 2nd Aerosol Characterization Experiment (ACE-2): general overview and main results, *Tellus B: Chemical and Physical Meteorology*, 52, 111–125, <https://doi.org/10.3402/tellusb.v52i2.16088>, 2000.
- 1410



- Randles, C. A., da Silva, A. M., Buchard, V., Colarco, P. R., Darmenov, A., Govindaraju, R., Smirnov, A., Holben, B., Ferrare, R., Hair, J., Shinozuka, Y., and Flynn, C. J.: The MERRA-2 Aerosol Reanalysis, 1980 Onward. Part I: System Description and Data Assimilation Evaluation, *Journal of Climate*, 30, 6823 – 6850, <https://doi.org/10.1175/JCLI-D-16-0609.1>, 2017.
- 1415 Redemann, J., Wood, R., Zuidema, P., Doherty, S. J., Luna, B., LeBlanc, S. E., Diamond, M. S., Shinozuka, Y., Chang, I. Y., Ueyama, R., Pfister, L., Ryoo, J.-m., Dobracki, A. N., da Silva, A. M., Longo, K. M., Kacenelenbogen, M. S., Flynn, C. J., Pistone, K., Knox, N. M., Piketh, S. J., Haywood, J. M., Formenti, P., Mallet, M., Stier, P., Ackerman, A. S., Bauer, S. E., Fridlind, A. M., Carmichael, G. R., Saide, P. E., Ferrada, G. A., Howell, S. G., Freitag, S., Cairns, B., Holben, B. N., Knobelspiesse, K. D., Tanelli, S., L'Ecuyer, T. S., Dzambo, A. M., Sy, O. O., McFarquhar, G. M., Poellot, M. R., Gupta, S., O'Brien, J. R., Nenes, A., Kacarab, M. E., Wong, J. P. S., Small-Griswold, J. D., Thornhill, K. L., Noone, D., Podolske, J. R., Schmidt, K. S., Pilewskie, P., Chen, H., Cochrane, S. P., Sedlacek, 1420 A. J., Lang, T. J., Stith, E., Segal-Rozenhaimer, M., Ferrare, R. A., Burton, S. P., Hostetler, C. A., Diner, D. J., Platnick, S. E., Myers, J. S., Meyer, K. G., Spangenberg, D. A., Maring, H., and Gao, L.: An Overview of the ORACLES (ObSERVations of Aerosols above CLouds and Their intERactionS) Project: Aerosol-Cloud-Radiation Interactions in the Southeast Atlantic Basin, *Atmospheric Chemistry and Physics Discussions*, <https://doi.org/10.5194/acp-2020-449>, 2020.
- Robock, A.: Volcanic eruptions and climate, *Reviews of Geophysics*, 38, 191–219, <https://doi.org/https://doi.org/10.1029/1998RG000054>, 1425 2000.
- Robson, J., Aksenov, Y., Bracegirdle, T. J., Dimdore-Miles, O., Griffiths, P. T., Grosvenor, D. P., Hodson, D. L., Keeble, J., MacIntosh, C., Megann, A., Osprey, S., Povey, A. C., Schröder, D., Yang, M., Archibald, A. T., Carslaw, K. S., Gray, L., Jones, C., Kerridge, B., Knappett, D., Kuhlbrodt, T., Russo, M., Sellar, A., Siddans, R., Sinha, B., Sutton, R., Walton, J., and Wilcox, L. J.: The Evaluation of the North Atlantic Climate System in UKESM1 Historical Simulations for CMIP6, *J. Adv. Model. Earth Syst.*, 12, 1430 <https://doi.org/10.1029/2020MS002126>, 2020.
- Rosenfeld, D.: TRMM Observed First Direct Evidence of Smoke from Forest Fires Inhibiting Rainfall, *Geophysical Research Letters*, 26, 3105–3108, <https://doi.org/10.1029/1999gl006066>, 1999.
- Rosenfeld, D. and Bell, T. L.: Why Do Tornadoes and Hailstorms Rest on Weekends?, *Journal of Geophysical Research*, 116, <https://doi.org/10.1029/2011jd016214>, 2011.
- 1435 Rosenfeld, D. and Lensky, I. M.: Satellite-Based Insights into Precipitation Formation Processes in Continental and Maritime Convective Clouds, *Bulletin of the American Meteorological Society*, 79, 2457–2476, [https://doi.org/10.1175/1520-0477\(1998\)079<2457:Sbiipf>2.0.Co;2](https://doi.org/10.1175/1520-0477(1998)079<2457:Sbiipf>2.0.Co;2), 1998.
- Rosenfeld, D., Zhu, Y., Wang, M., Zheng, Y., Goren, T., and Yu, S.: Aerosol-Driven Droplet Concentrations Dominate Coverage and Water of Oceanic Low Level Clouds, *Science*, 363, eaav0566, <https://doi.org/10.1126/science.aav0566>, 2019.
- 1440 Russell, L. M., Sorooshian, A., Seinfeld, J. H., Albrecht, B. A., Nenes, A., Ahlm, L., Chen, Y.-C., Coggon, M., Craven, J. S., Flagan, R. C., Frossard, A. A., Jonsson, H., Jung, E., Lin, J. J., Metcalf, A. R., Modini, R., Mülmenstädt, J., Roberts, G., Shingler, T., Song, S., Wang, Z., and Wonaschütz, A.: Eastern Pacific Emitted Aerosol Cloud Experiment, *Bulletin of the American Meteorological Society*, 94, 709–729, <https://doi.org/10.1175/BAMS-D-12-00015.1>, 2013.
- Sanchez-Lorenzo, A., Laux, P., Hendricks Franssen, H.-J., Calbó, J., Vogl, S., Georgoulias, A. K., and Quaas, J.: Assessing Large-Scale 1445 Weekly Cycles in Meteorological Variables: A Review, *Atmospheric Chemistry and Physics*, 12, 5755–5771, <https://doi.org/10.5194/acp-12-5755-2012>, 2012.



- Schmidt, A., Carslaw, K. S., Mann, G. W., Rap, A., Pringle, K. J., Spracklen, D. V., Wilson, M., and Forster, P. M.: Importance of Tropospheric Volcanic Aerosol for Indirect Radiative Forcing of Climate, *Atmospheric Chemistry and Physics*, 12, 7321–7339, <https://doi.org/10.5194/acp-12-7321-2012>, 2012.
- 1450 Schmidt, A., Leadbetter, S., Theys, N., Carboni, E., Witham, C. S., Stevenson, J. A., Birch, C. E., Thordarson, T., Turnock, S., Barsotti, S., Delaney, L., Feng, W., Grainger, R. G., Hort, M. C., Hlíðskuldsson, Á., Ialongo, I., Ilyinskaya, E., Jǫhannsson, T., Kenny, P., Mather, T. A., Richards, N. A. D., and Shepherd, J.: Satellite detection, long-range transport, and air quality impacts of volcanic sulfur dioxide from the 2014–2015 flood lava eruption at Bárðarbunga (Iceland), *Journal of Geophysical Research: Atmospheres*, 120, 9739–9757, <https://doi.org/https://doi.org/10.1002/2015JD023638>, 2015.
- 1455 Schneider, T.: *Climate 1970–2020. In Earth 2020: An Insider’s Guide to a Rapidly Changing Planet*, P. Tortell, Open Book Publishers, <https://www.openbookpublishers.com/product/1109>, 2020.
- Schreier, M., Mannstein, H., Eyring, V., and Bovensmann, H.: Global Ship Track Distribution and Radiative Forcing from 1 Year of AATSR Data, *Geophysical Research Letters*, 34, <https://doi.org/10.1029/2007GL030664>, 2007.
- Schultz, D. M., Mikkonen, S., Laaksonen, A., and Richman, M. B.: Weekly Precipitation Cycles? Lack of Evidence from United States Surface Stations, *Geophysical Research Letters*, 34, <https://doi.org/10.1029/2007gl031889>, 2007.
- Schumann, U., Bugliaro, L., Dörnbrack, A., Baumann, R., and Voigt, C.: Aviation Contrail Cirrus and Radiative Forcing Over Europe During 6 Months of COVID-19, *Geophysical Research Letters*, 48, e2021GL092771, <https://doi.org/10.1029/2021GL092771>, 2021.
- Schutgens, N. A. J.: Site representativity of AERONET and GAW remotely sensed aerosol optical thickness and absorbing aerosol optical thickness observations, *Atmospheric Chemistry and Physics*, 20, 7473–7488, <https://doi.org/10.5194/acp-20-7473-2020>, 2020.
- 1465 Schwartz, S.: Are cloud albedo and climate controlled by marine phytoplankton?, *Nature*, 336, 441–445, <https://doi.org/10.1038/336441a0>, 1988.
- Scorer, R.: Ship trails, *Atmospheric Environment* (1967), 21, 1417–1425, [https://doi.org/https://doi.org/10.1016/0004-6981\(67\)90089-3](https://doi.org/https://doi.org/10.1016/0004-6981(67)90089-3), 1987.
- Sechrist, B., Coakley, J. A., and Tahnk, W. R.: Effects of Additional Particles on Already Polluted Marine Stratus, *Journal of the Atmospheric Sciences*, 69, 1975 – 1993, <https://doi.org/10.1175/JAS-D-11-0291.1>, 2012.
- 1470 Segrin, M. S., Coakley, J. A., and Tahnk, W. R.: MODIS Observations of Ship Tracks in Summertime Stratus off the West Coast of the United States, *Journal of the Atmospheric Sciences*, 64, 4330–4345, <https://doi.org/10.1175/2007JAS2308.1>, 2007.
- Seidel, D. J. and Birnbaum, A. N.: Effects of Independence Day Fireworks on Atmospheric Concentrations of Fine Particulate Matter in the United States, *Atmospheric Environment*, 115, 192–198, <https://doi.org/10.1016/j.atmosenv.2015.05.065>, 2015.
- 1475 Seifert, P., Ansmann, A., Groß, S., Freudenthaler, V., Heinold, B., Hiebsch, A., Mattis, I., Schmidt, J., Schnell, F., Tesche, M., Wandinger, U., and Wiegner, M.: Ice formation in ash-influenced clouds after the eruption of the Eyjafjallajökull volcano in April 2010, *Journal of Geophysical Research: Atmospheres*, 116, <https://doi.org/https://doi.org/10.1029/2011JD015702>, 2011.
- Sellar, A. A., Jones, C. G., Mulcahy, J. P., Tang, Y., Yool, A., Wiltshire, A., O’Connor, F. M., Stringer, M., Hill, R., Palmieri, J., Woodward, S., de Mora, L., Kuhlbrodt, T., Rumbold, S. T., Kelley, D. I., Ellis, R., Johnson, C. E., Walton, J., Abraham, N. L., Andrews, M. B., 1480 Andrews, T., Archibald, A. T., Berthou, S., Burke, E., Blockley, E., Carslaw, K., Dalvi, M., Edwards, J., Folberth, G. A., Gedney, N., Griffiths, P. T., Harper, A. B., Hendry, M. A., Hewitt, A. J., Johnson, B., Jones, A., Jones, C. D., Keeble, J., Liddicoat, S., Morgenstern, O., Parker, R. J., Predoi, V., Robertson, E., Siahann, A., Smith, R. S., Swaminathan, R., Woodhouse, M. T., Zeng, G., and Zerroukat, M.: UKESM1: Description and Evaluation of the U.K. Earth System Model, *Journal of Advances in Modeling Earth Systems*, 11, 4513–4558, <https://doi.org/https://doi.org/10.1029/2019MS001739>, 2019.



- 1485 Shi, X. and Brasseur, G. P.: The Response in Air Quality to the Reduction of Chinese Economic Activities during the COVID-19 Outbreak, *Geophysical Research Letters*, 47, e2020GL088070, <https://doi.org/10.1029/2020GL088070>, 2020.
- Small, J. D., Chuang, P. Y., Feingold, G., and Jiang, H.: Can aerosol decrease cloud lifetime?, *Geophysical Research Letters*, 36, <https://doi.org/https://doi.org/10.1029/2009GL038888>, 2009.
- Soden, B. J., Wetherald, R. T., Stenchikov, G. L., and Robock, A.: Global Cooling After the Eruption of Mount Pinatubo: A Test of Climate  
1490 Feedback by Water Vapor, *Science*, 296, 727–730, <https://doi.org/10.1126/science.296.5568.727>, 2002.
- Sorooshian, A., Prabhakar, G., Jonsson, H., Woods, R. K., Flagan, R. C., and Seinfeld, J. H.: On the Presence of Giant Particles Downwind  
of Ships in the Marine Boundary Layer, *Geophysical Research Letters*, 42, 2024–2030, <https://doi.org/10.1002/2015GL063179>, 2015.
- Sorooshian, A., MacDonald, A. B., Dadashazar, H., Bates, K. H., Coggon, M. M., Craven, J. S., Crosbie, E., Hersey, S. P., Hodas, N.,  
1495 Lin, J. J., Negrón Marty, A., Maudlin, L. C., Metcalf, A. R., Murphy, S. M., Padró, L. T., Prabhakar, G., Rissman, T. A., Shingler,  
T., Varutbangkul, V., Wang, Z., Woods, R. K., Chuang, P. Y., Nenes, A., Jonsson, H. H., Flagan, R. C., and Seinfeld, J. H.: A Multi-  
Year Data Set on Aerosol-Cloud-Precipitation-Meteorology Interactions for Marine Stratocumulus Clouds, *Scientific Data*, 5, 180026,  
<https://doi.org/10.1038/sdata.2018.26>, 2018.
- Sorooshian, A., Anderson, B., Bauer, S. E., Braun, R. A., Cairns, B., Crosbie, E., Dadashazar, H., Diskin, G., Ferrare, R., Flagan, R. C., Hair,  
J., Hostetler, C., Jonsson, H. H., Kleb, M. M., Liu, H., MacDonald, A. B., McComiskey, A., Moore, R., Painemal, D., Russell, L. M.,  
1500 Seinfeld, J. H., Shook, M., Smith, W. L., Thornhill, K., Tselioudis, G., Wang, H., Zeng, X., Zhang, B., Ziemba, L., and Zuidema, P.:  
Aerosol-Cloud-Meteorology Interaction Airborne Field Investigations: Using Lessons Learned from the U.S. West Coast in the Design  
of ACTIVATE off the U.S. East Coast, *Bulletin of the American Meteorological Society*, 100, 1511–1528, <https://doi.org/10.1175/BAMS-D-18-0100.1>, 2019.
- Sorooshian, A., Corral, A. F., Braun, R. A., Cairns, B., Crosbie, E., Ferrare, R., Hair, J., Kleb, M. M., Mardi, A. H., Maring, H., McComiskey,  
1505 A., Moore, R., Painemal, D., Scarino, A. J., Schlosser, J., Shingler, T., Shook, M., Wang, H., Zeng, X., Ziemba, L., and Zuidema, P.:  
Atmospheric Research Over the Western North Atlantic Ocean Region and North American East Coast: A Review of Past Work and  
Challenges Ahead, *Journal of Geophysical Research: Atmospheres*, 125, e2019JD031626, <https://doi.org/10.1029/2019JD031626>, 2020.
- Stevens, B., Fiedler, S., Kinne, S., Peters, K., Rast, S., Müssé, J., Smith, S. J., and Mauritsen, T.: Simple Plumes: A parameterization of  
anthropogenic aerosol optical properties and an associated Twomey effect for climate studies, *Geosci. Model Dev. Discuss, Model Dev.*  
1510 *Discuss.*, doi: <http://dx.doi.org/10.5194/gmd-2016-189>, 2016.
- Stevens, B., Satoh, M., Auger, L., Biercamp, J., Bretherton, C. S., Chen, X., D'Áijben, P., Judt, F., Khairoutdinov, M., Klocke, D., Kodama,  
C., Kornbluh, L., Lin, S.-J., Neumann, P., Putman, W. M., RÄuber, N., Shibuya, R., Vanniere, B., Vidale, P. L., Wedi, N., and Zhou,  
L.: DYAMOND: the DYnamics of the Atmospheric general circulation Modeled On Non-hydrostatic Domains, *Progress in Earth and  
Planetary Science*, 6, 61, <https://doi.org/10.1186/s40645-019-0304-z>, 2019.
- 1515 Stier, P.: Limitations of Passive Remote Sensing to Constrain Global Cloud Condensation Nuclei, *Atmos. Chem. Phys.*, 16, 6595–6607,  
<https://doi.org/10.5194/acp-16-6595-2016>, 2016.
- Stjern, C. W.: Weekly cycles in precipitation and other meteorological variables in a polluted region of Europe, *Atmospheric Chemistry and  
Physics*, 11, 4095–4104, <https://doi.org/10.5194/acp-11-4095-2011>, 2011.
- Stjern, C. W., Stohl, A., and KristjÄnsson, J. E.: Have aerosols affected trends in visibility and precipitation in Europe?, *Journal of Geo-  
1520 physical Research: Atmospheres*, 116, <https://doi.org/https://doi.org/10.1029/2010JD014603>, 2011.



- Su, T., Li, Z., Zheng, Y., Luan, Q., and Guo, J.: Abnormally Shallow Boundary Layer Associated With Severe Air Pollution During the COVID-19 Lockdown in China, *Geophysical Research Letters*, 47, e2020GL090041, <https://doi.org/https://doi.org/10.1029/2020GL090041>, e2020GL090041 2020GL090041, 2020.
- 1525 Sun, Y., Wang, Z., Wild, O., Xu, W., Chen, C., Fu, P., Du, W., Zhou, L., Zhang, Q., Han, T., Wang, Q., Pan, X., Zheng, H., Li, J., Guo, X., Liu, J., and Worsnop, D. R.: “APEC Blue”: Secondary Aerosol Reductions from Emission Controls in Beijing, *Scientific Reports*, 6, 20 668, <https://doi.org/10.1038/srep20668>, 2016.
- Swap, R. J., Annegarn, H. J., Suttles, J. T., King, M. D., Platnick, S., Privette, J. L., and Scholes, R. J.: Africa Burning: A Thematic Analysis of the Southern African Regional Science Initiative (SAFARI 2000), *Journal of Geophysical Research: Atmospheres*, 108, n/a–n/a, <https://doi.org/10.1029/2003jd003747>, 2003.
- 1530 Tan, P.-H., Chou, C., Liang, J.-Y., Chou, C. C. K., and Shiu, C.-J.: Air Pollution “Holiday Effect” Resulting from the Chinese New Year, *Atmospheric Environment*, 43, 2114–2124, <https://doi.org/10.1016/j.atmosenv.2009.01.037>, 2009.
- Taylor, J. P. and Ackerman, A. S.: A Case-Study of Pronounced Perturbations to Cloud Properties and Boundary-Layer Dynamics Due to Aerosol Emissions, *Quarterly Journal of the Royal Meteorological Society*, 125, 2643–2661, <https://doi.org/10.1002/qj.49712555915>, 1999.
- 1535 Thornton, J. A., Virts, K. S., Holzworth, R. H., and Mitchell, T. P.: Lightning Enhancement over Major Oceanic Shipping Lanes, *Geophysical Research Letters*, 44, 9102–9111, <https://doi.org/10.1002/2017GL074982>, 2017.
- Toll, V., Christensen, M., Gassó, S., and Bellouin, N.: Volcano and Ship Tracks Indicate Excessive Aerosol-Induced Cloud Water Increases in a Climate Model, *Geophysical Research Letters*, <https://doi.org/10.1002/2017gl075280>, 2017.
- Toll, V., Christensen, M., Quaas, J., and Bellouin, N.: Weak Average Liquid-Cloud-Water Response to Anthropogenic Aerosols, *Nature*, 572, 1540 51–55, <https://doi.org/10.1038/s41586-019-1423-9>, 2019.
- Trofimov, H., Bellouin, N., and Toll, V.: Large-Scale Industrial Cloud Perturbations Confirm Bidirectional Cloud Water Responses to Anthropogenic Aerosols, *Journal of Geophysical Research: Atmospheres*, 125, e2020JD032 575, <https://doi.org/10.1029/2020JD032575>, 2020.
- Twomey, S.: Pollution and the Planetary Albedo, *Atmospheric Environment*, 8, 1251–1256, 1974.
- Twomey, S., Howell, H. B., and Wojciechowski, T. A.: Comments on “Anomalous Cloud Lines”, *Journal of the Atmospheric Sciences*, 25, 1545 333–334, [https://doi.org/10.1175/1520-0469\(1968\)025<0333:COCL>2.0.CO;2](https://doi.org/10.1175/1520-0469(1968)025<0333:COCL>2.0.CO;2), 1968.
- Vaideanu, P., Dima, M., and Voiculescu, M.: Atlantic Multidecadal Oscillation footprint on global high cloud cover, *Theoretical and Applied Climatology*, 134, 1245–1256, <https://doi.org/10.1007/s00704-017-2330-3>, 2018.
- Wang, H. and Feingold, G.: Modeling Mesoscale Cellular Structures and Drizzle in Marine Stratocumulus. Part II: The Microphysics and Dynamics of the Boundary Region between Open and Closed Cells, *Journal of the Atmospheric Sciences*, 66, 3257–3275, 1550 <https://doi.org/10.1175/2009jas3120.1>, 2009.
- Wang, H., Rasch, P. J., and Feingold, G.: Manipulating Marine Stratocumulus Cloud Amount and Albedo: A Process-Modelling Study of Aerosol-Cloud-Precipitation Interactions in Response to Injection of Cloud Condensation Nuclei, *Atmospheric Chemistry and Physics*, 11, 4237–4249, <https://doi.org/10.5194/acp-11-4237-2011>, 2011.
- Wang, P., Chen, K., Zhu, S., Wang, P., and Zhang, H.: Severe Air Pollution Events Not Avoided by Reduced Anthropogenic Activities during COVID-19 Outbreak, *Resources, Conservation, & Recycling*, 158, 104 814, <https://doi.org/10.1016/j.resconrec.2020.104814>, 2020.
- 1555 Wang, Q., Li, Z., Guo, J., Zhao, C., and Cribb, M.: The climate impact of aerosols on the lightning flash rate: is it detectable from long-term measurements?, *Atmospheric Chemistry and Physics*, 18, 12 797–12 816, <https://doi.org/10.5194/acp-18-12797-2018>, 2018.



- 1560 Wang, S., Wang, Q., and Feingold, G.: Turbulence, Condensation, and Liquid Water Transport in Numerically Simulated Nonprecipitating Stratocumulus Clouds, *Journal of the Atmospheric Sciences*, 60, 262–278, [https://doi.org/10.1175/1520-0469\(2003\)060<0262:TCALWT>2.0.CO;2](https://doi.org/10.1175/1520-0469(2003)060<0262:TCALWT>2.0.CO;2), 2003.
- Wang, T., Nie, W., Gao, J., Xue, L. K., Gao, X. M., Wang, X. F., Qiu, J., Poon, C. N., Meinardi, S., Blake, D., Wang, S. L., Ding, A. J., Chai, F. H., Zhang, Q. Z., and Wang, W. X.: Air Quality during the 2008 Beijing Olympics: Secondary Pollutants and Regional Impact, *Atmospheric Chemistry and Physics*, 10, 7603–7615, <https://doi.org/10.5194/acp-10-7603-2010>, 2010.
- 1565 Wang, Y., Zhang, F., Li, Z., Tan, H., Xu, H., Ren, J., Zhao, J., Du, W., and Sun, Y.: Enhanced Hydrophobicity and Volatility of Submicron Aerosols under Severe Emission Control Conditions in Beijing, *Atmospheric Chemistry and Physics*, 17, 5239–5251, <https://doi.org/10.5194/acp-17-5239-2017>, 2017.
- Wang, Y., Li, Z., Wang, Q., Jin, X., Yan, P., Cribb, M., Li, Y., Yuan, C., Wu, H., Wu, T., Ren, R., and Cai, Z.: Enhancement of Secondary Aerosol Formation by Reduced Anthropogenic Emissions during Spring Festival 2019 and Enlightenment for Regional PM<sub>2.5</sub> Control in Beijing, *Atmospheric Chemistry and Physics*, 21, 915–926, <https://doi.org/10.5194/acp-21-915-2021>, 2021.
- 1570 Warner, J.: A Reduction in Rainfall Associated with Smoke from Sugar-Cane Fires—An Inadvertent Weather Modification?, *Journal of Applied Meteorology*, 7, 247–251, [https://doi.org/10.1175/1520-0450\(1968\)007<0247:Ariraw>2.0.Co;2](https://doi.org/10.1175/1520-0450(1968)007<0247:Ariraw>2.0.Co;2), 1968.
- Warner, J. and Twomey, S.: The Production of Cloud Nuclei by Cane Fires and the Effect on Cloud Droplet Concentration, *Journal of the Atmospheric Sciences*, 24, 704–706, [https://doi.org/10.1175/1520-0469\(1967\)024<0704:Tpcnbn>2.0.Co;2](https://doi.org/10.1175/1520-0469(1967)024<0704:Tpcnbn>2.0.Co;2), 1967.
- Wilcox, E. M.: Stratocumulus cloud thickening beneath layers of absorbing smoke aerosol, *Atmospheric Chemistry and Physics*, 10, 11 769–11 777, <https://doi.org/10.5194/acp-10-11769-2010>, 2010.
- 1575 Wild, M., Gilgen, H., Roesch, A., Ohmura, A., Long, C. N., Dutton, E. G., Forgan, B., Kallis, A., Russak, V., and Tsvetkov, A.: From Dimming to Brightening: Decadal Changes in Solar Radiation at Earth’s Surface, *Science*, 308, 847–850, <https://doi.org/10.1126/science.1103215>, 2005.
- Witte, J. C., Schoeberl, M. R., Douglass, A. R., Gleason, J. F., Krotkov, N. A., Gille, J. C., Pickering, K. E., and Livesey, N.: Satellite Observations of Changes in Air Quality during the 2008 Beijing Olympics and Paralympics, *Geophysical Research Letters*, 36, L17 803, <https://doi.org/10.1029/2009gl039236>, 2009.
- 1580 Wood, R.: Cancellation of Aerosol Indirect Effects in Marine Stratocumulus through Cloud Thinning, *Journal of the Atmospheric Sciences*, 64, 2657–2669, <https://doi.org/10.1175/jas3942.1>, 2007.
- Wood, R., Mechoso, C. R., Bretherton, C. S., Weller, R. A., Huebert, B., Straneo, F., Albrecht, B. A., Coe, H., Allen, G., Vaughan, G., Daum, P., Fairall, C., Chand, D., Gallardo Klenner, L., Garreaud, R., Grados, C., Covert, D. S., Bates, T. S., Krejci, R., Russell, L. M., de Szoeko, S., Brewer, A., Yuter, S. E., Springston, S. R., Chaigneau, A., Toniazzo, T., Minnis, P., Palikonda, R., Abel, S. J., Brown, W. O. J., Williams, S., Fochesatto, J., Brioude, J., and Bower, K. N.: The VAMOS Ocean-Cloud-Atmosphere-Land Study Regional Experiment (VOCALS-REx): goals, platforms, and field operations, *Atmospheric Chemistry and Physics*, 11, 627–654, <https://doi.org/10.5194/acp-11-627-2011>, 2011.
- 1585 Xia, X.: A Closer Looking at Dimming and Brightening in China during 1961–2005, *Annales Geophysicae*, 28, 1121–1132, <https://doi.org/10.5194/angeo-28-1121-2010>, 2010.
- Xue, H. and Feingold, G.: Large-Eddy Simulations of Trade Wind Cumuli: Investigation of Aerosol Indirect Effects, *Journal of the Atmospheric Sciences*, 63, 1605 – 1622, <https://doi.org/10.1175/JAS3706.1>, 2006.
- 1590 Yang, X. and Li, Z.: Increases in Thunderstorm Activity and Relationships with Air Pollution in Southeast China, *Journal of Geophysical Research: Atmospheres*, 119, 1835–1844, <https://doi.org/10.1002/2013JD021224>, 2014.





- Yang, X., Yao, Z., Li, Z., and Fan, T.: Heavy Air Pollution Suppresses Summer Thunderstorms in Central China, *Journal of Atmospheric and Solar-Terrestrial Physics*, 95-96, 28–40, <https://doi.org/10.1016/j.jastp.2012.12.023>, 2013.
- Yang, X., Li, Z., Liu, L., Zhou, L., Cribb, M., and Zhang, F.: Distinct Weekly Cycles of Thunderstorms and a Potential Connection with Aerosol Type in China, *Geophysical Research Letters*, 43, 8760–8768, <https://doi.org/10.1002/2016GL070375>, 2016.
- 1600 Yoshioka, M., Regayre, L. A., Pringle, K. J., Johnson, J. S., Mann, G. W., Partridge, D. G., Sexton, D. M. H., Lister, G. M. S., Schutgens, N., Stier, P., Kipling, Z., Bellouin, N., Browse, J., Booth, B. B. B., Johnson, C. E., Johnson, B., Mollard, J. D. P., Lee, L., and Carslaw, K. S.: Ensembles of Global Climate Model Variants Designed for the Quantification and Constraint of Uncertainty in Aerosols and Their Radiative Forcing, *Journal of Advances in Modeling Earth Systems*, 11, 3728–3754, <https://doi.org/10.1029/2019MS001628>, 2019.
- 1605 Yu, C., Pasternak, D., Lee, J., Yang, M., Bell, T., Bower, K., Wu, H., Liu, D., Reed, C., Bauguitte, S., Cliff, S., Trembath, J., Coe, H., and Allan, J. D.: Characterizing the Particle Composition and Cloud Condensation Nuclei from Shipping Emission in Western Europe, *Environmental Science & Technology*, 54, 15 604–15 612, <https://doi.org/10.1021/acs.est.0c04039>, PMID: 33206512, 2020.
- Yuan, T., Remer, L. A., and Yu, H.: Microphysical, Macrophysical and Radiative Signatures of Volcanic Aerosols in Trade Wind Cumulus Observed by the A-Train, *Atmospheric Chemistry and Physics*, 11, 7119–7132, <https://doi.org/10.5194/acp-11-7119-2011>, 2011.
- 1610 Yuan, T., Wang, C., Song, H., Platnick, S., Meyer, K., and Oreopoulos, L.: Automatically Finding Ship Tracks to Enable Large-Scale Analysis of Aerosol-Cloud Interactions, *Geophysical Research Letters*, 46, 7726–7733, <https://doi.org/10.1029/2019gl083441>, 2019.
- Zhang, J. and Zuidema, P.: The diurnal cycle of the smoky marine boundary layer observed during August in the remote southeast Atlantic, *Atmospheric Chemistry and Physics*, 19, 14 493–14 516, <https://doi.org/10.5194/acp-19-14493-2019>, 2019.
- Zhang, Q., Zheng, Y., Tong, D., Shao, M., Wang, S., Zhang, Y., Xu, X., Wang, J., He, H., Liu, W., Ding, Y., Lei, Y., Li, J., Wang, Z., Zhang, X., Wang, Y., Cheng, J., Liu, Y., Shi, Q., Yan, L., Geng, G., Hong, C., Li, M., Liu, F., Zheng, B., Cao, J., Ding, A., Gao, J., Fu, Q., Huo, J., Liu, B., Liu, Z., Yang, F., He, K., and Hao, J.: Drivers of Improved PM<sub>2.5</sub> Air Quality in China from 2013 to 2017, *Proceedings of the National Academy of Sciences*, 116, 24 463–24 469, <https://doi.org/10.1073/pnas.1907956116>, 2019.
- 1615 Zhao, J., Du, W., Zhang, Y., Wang, Q., Chen, C., Xu, W., Han, T., Wang, Y., Fu, P., Wang, Z., Li, Z., and Sun, Y.: Insights into Aerosol Chemistry during the 2015 China Victory Day Parade: Results from Simultaneous Measurements at Ground Level and 260 m in Beijing, *Atmospheric Chemistry and Physics*, 17, 3215–3232, <https://doi.org/10.5194/acp-17-3215-2017>, 2017.
- 1620 Zuidema, P., Redemann, J., Haywood, J., Wood, R., Piketh, S., Hipondoka, M., and Formenti, P.: Smoke and Clouds above the Southeast Atlantic: Upcoming Field Campaigns Probe Absorbing Aerosol’s Impact on Climate, *Bulletin of the American Meteorological Society*, 97, 1131–1135, <https://doi.org/10.1175/bams-d-15-00082.1>, 2016.
- 1625 Zuidema, P., Sedlacek III, A. J., Flynn, C., Springston, S., Delgado, R., Zhang, J., Aiken, A. C., Koontz, A., and Muradyan, P.: The Ascension Island Boundary Layer in the Remote Southeast Atlantic Is Often Smoky, *Geophysical Research Letters*, 45, 4456–4465, <https://doi.org/10.1002/2017gl076926>, 2018.

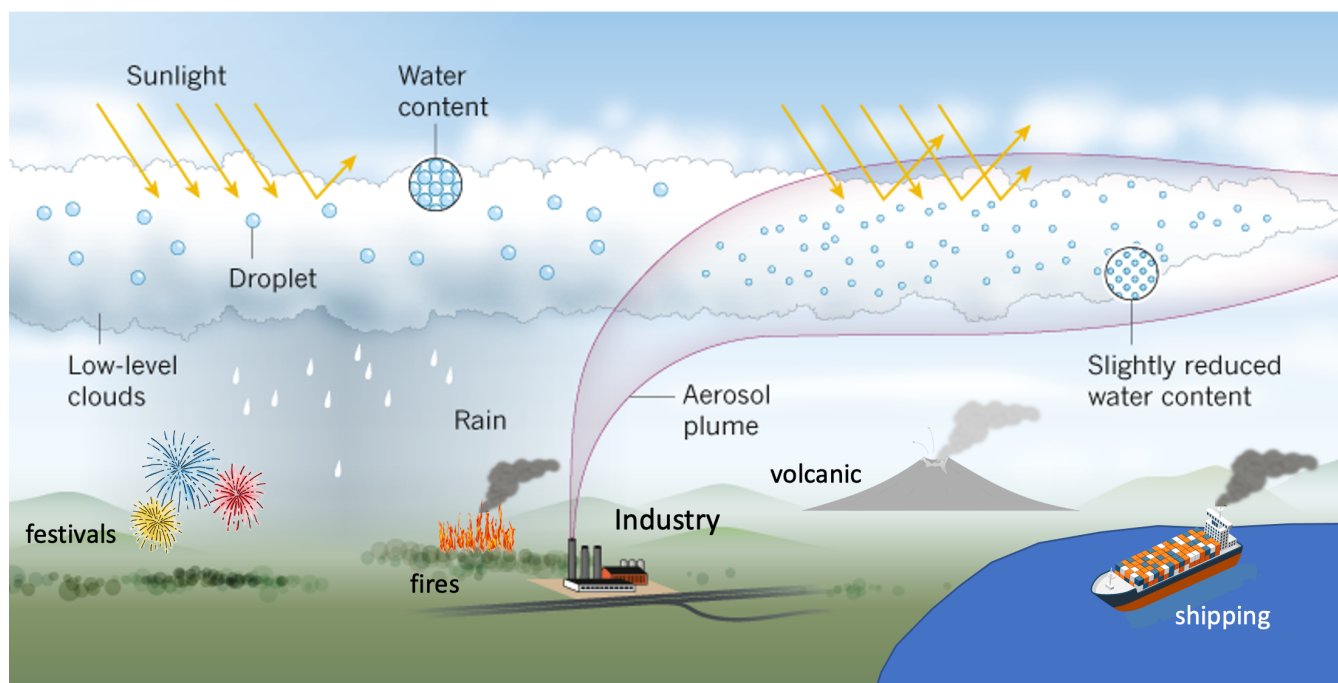


**Figure 1.** Schematic showing examples of the aerosol effect on boundary layer liquid clouds from some prominent natural laboratories found over the globe. Adapted from Possner et al., 2019.

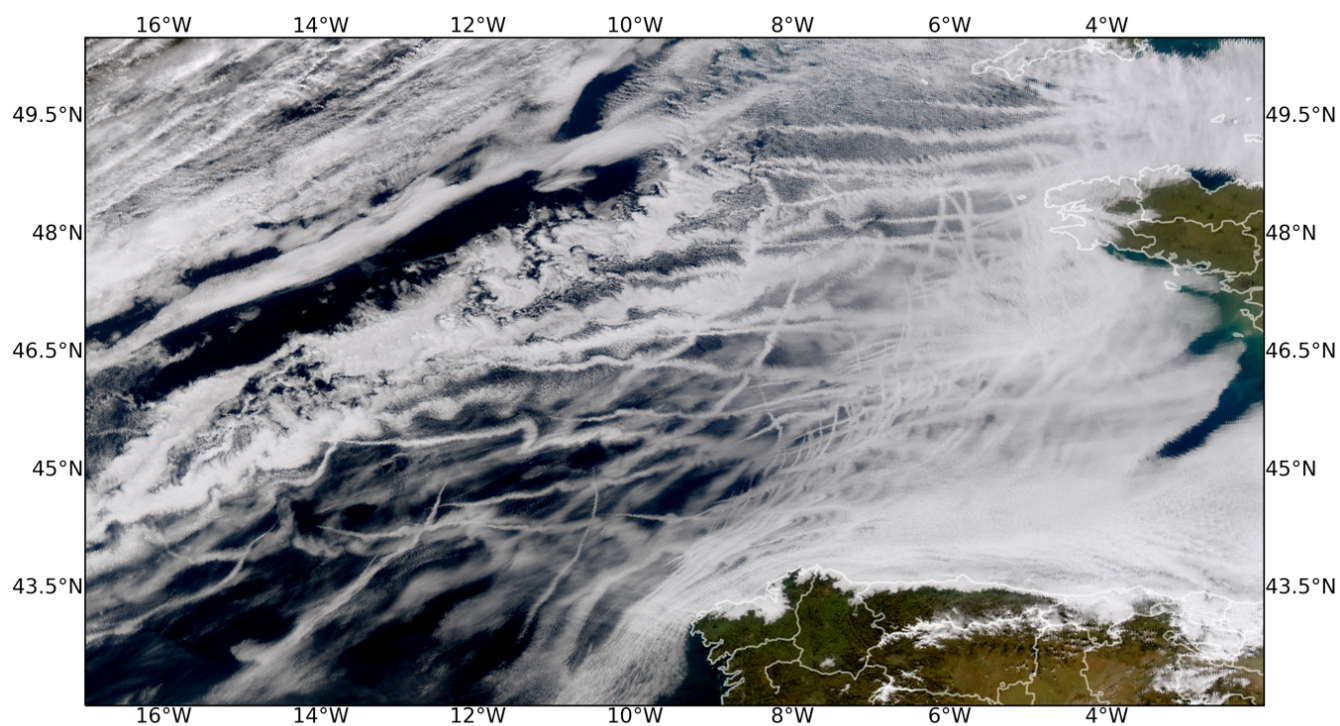


**Figure 2.** Ship tracks across the Bay of Biscay are shown in true color imagery from MODIS on the Aqua satellite on 01/27/2003 at 13:40 UTC.

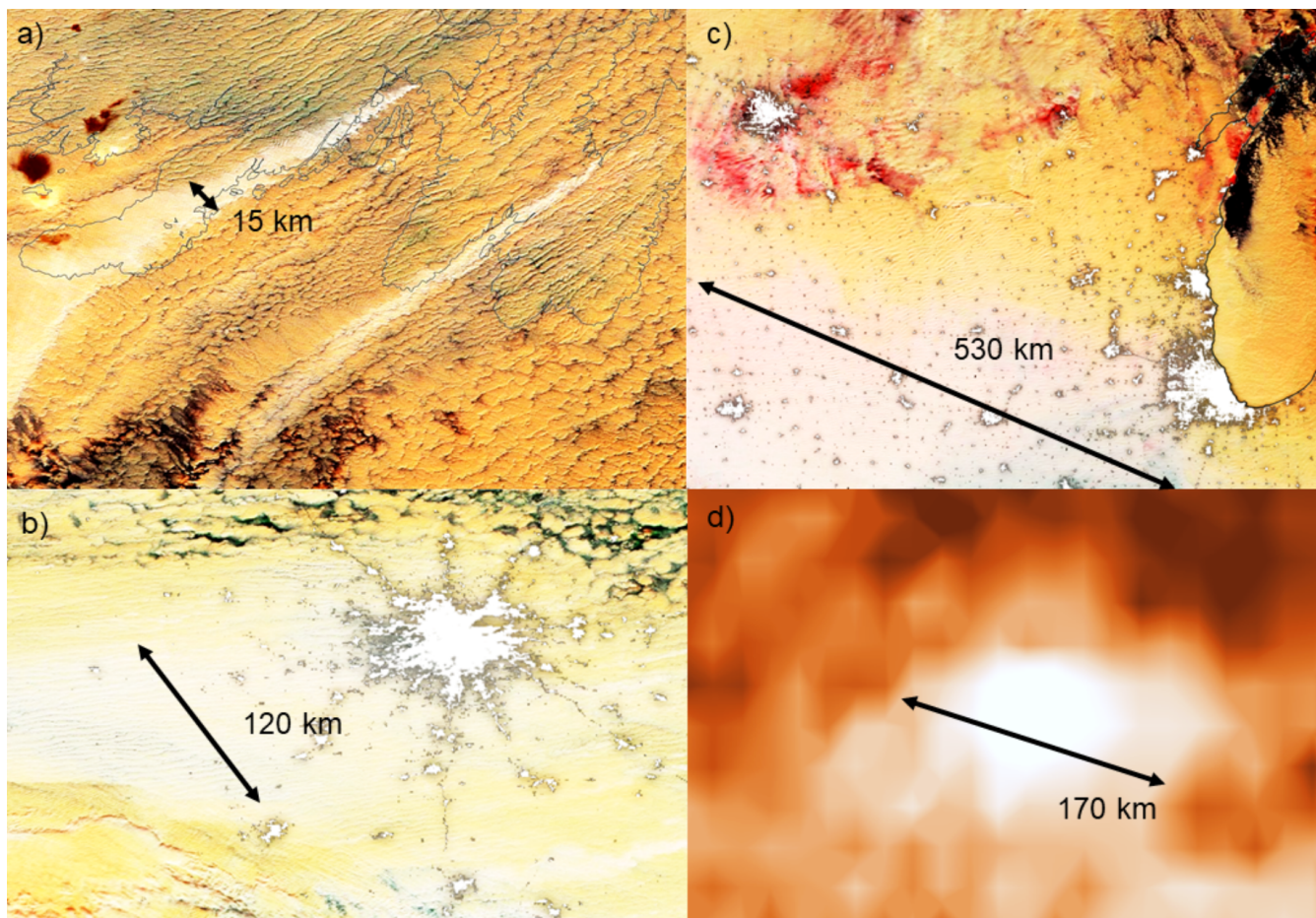


**Figure 3.** Polluted cloud tracks across spatial and temporal scales. Snapshot MODIS daytime near-infrared composite satellite images are shown in panels a, b and c: the polluted clouds are shown in bright greyish colours and unpolluted clouds in yellowish-brownish colours. Night lights are overlaid in white. a) Two localized aerosol sources induce ship-track-like polluted cloud lines in Newfoundland, Canada, on the 17th of December 2014. Near the surface wind is blowing from the North based on MERRA reanalysis. b) Emissions from Moscow, Russia, induce a more than 100 km wide polluted cloud area on the 11th of October 2016. Near the surface wind is blowing from the East based on MERRA reanalysis. c) Many aerosol sources in the Great Lakes Region, USA, induce a more than 500 km wide polluted cloud area on the 3rd of January 2016. Near the surface wind is blowing from the North-West based on MERRA reanalysis. In panel d) AVHRR cloud droplet effective radius data averaged over the years 1982 to 2015 is shown for the larger Moscow region. In the long-term average data, the cloud droplet effective radius decreases by 1 to 1.5  $\mu\text{m}$  in the Moscow region compared to the nearby less polluted clouds. In panel d) brownish colours represent larger droplets, and whiteish colours represent smaller droplets.

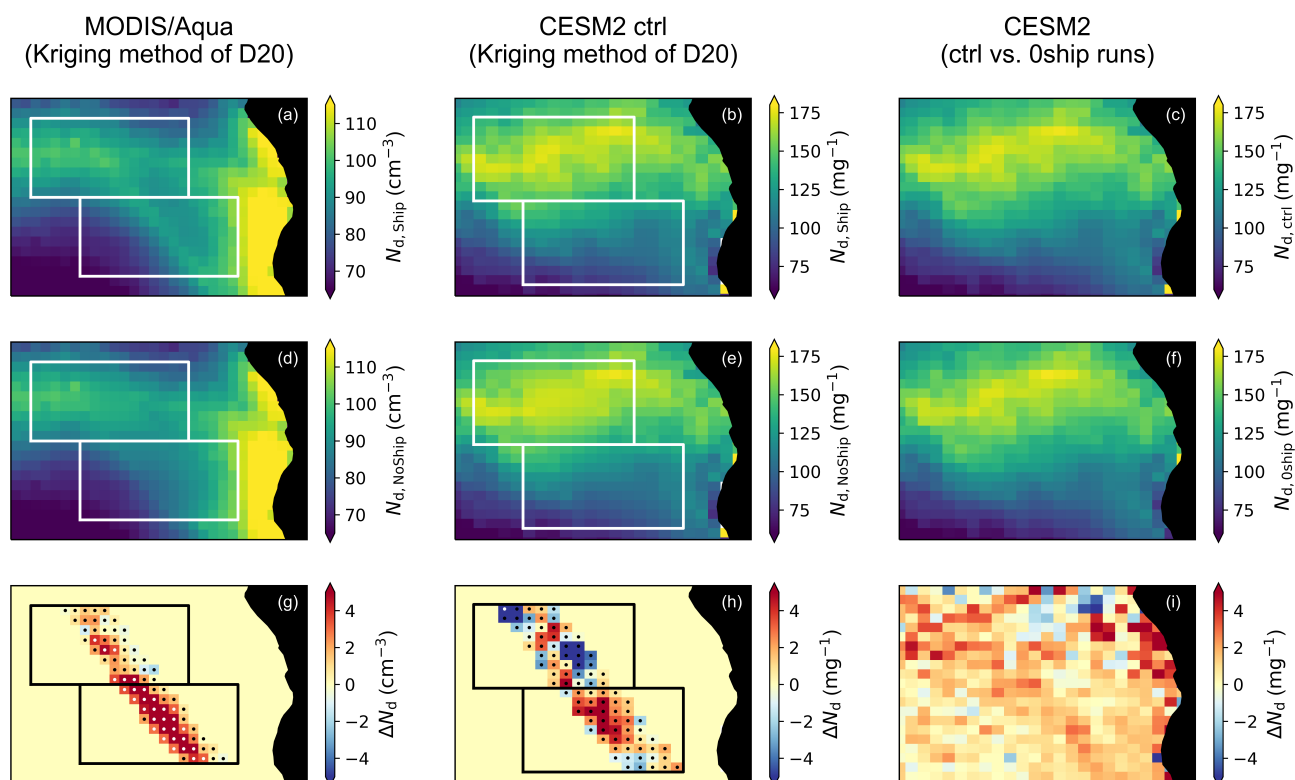


**Figure 4.** Comparison of Diamond et al. (2020) shipping corridor results for cloud droplet number concentration with CESM2 output. Factual (“Ship”) fields for a) MODIS/Aqua and b-c) CESM2 control (“ctrl”); counterfactual (“NoShip”) fields obtained by kriging for d) MODIS/Aqua and e) CESM2 ctrl and f) results from CESM2 with zero shipping emissions (“0ship”); and the g-h) factual-counterfactual or i) ctrl-0ship differences. For panels g-h), white dots indicate significance at 95% confidence whereas black dots indicate values that are not statistically significant.

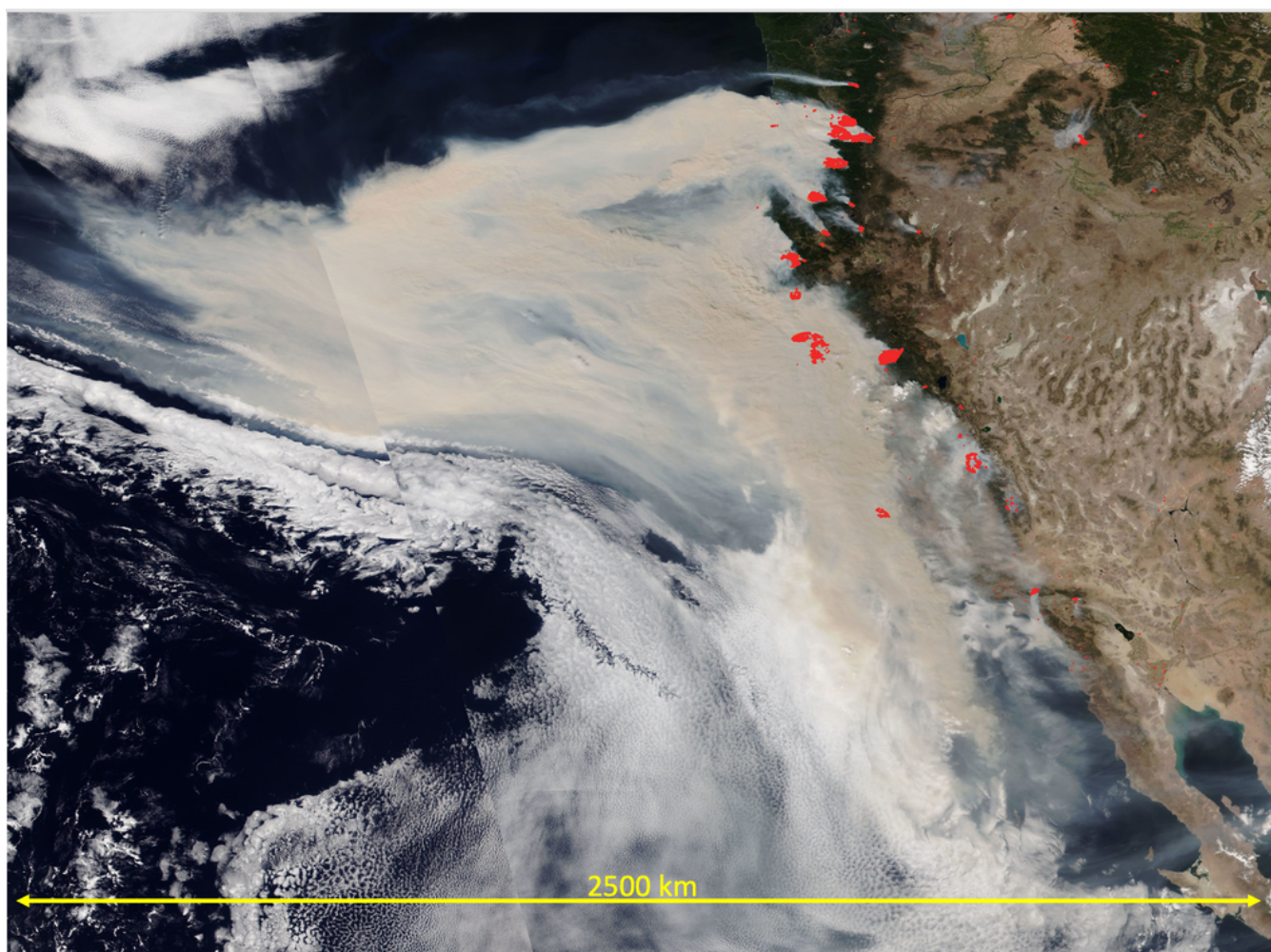


**Figure 5.** Smoke plume and clouds at US west coast on the 9th of September 2020 as seen by NOAA-20 VIIRS.

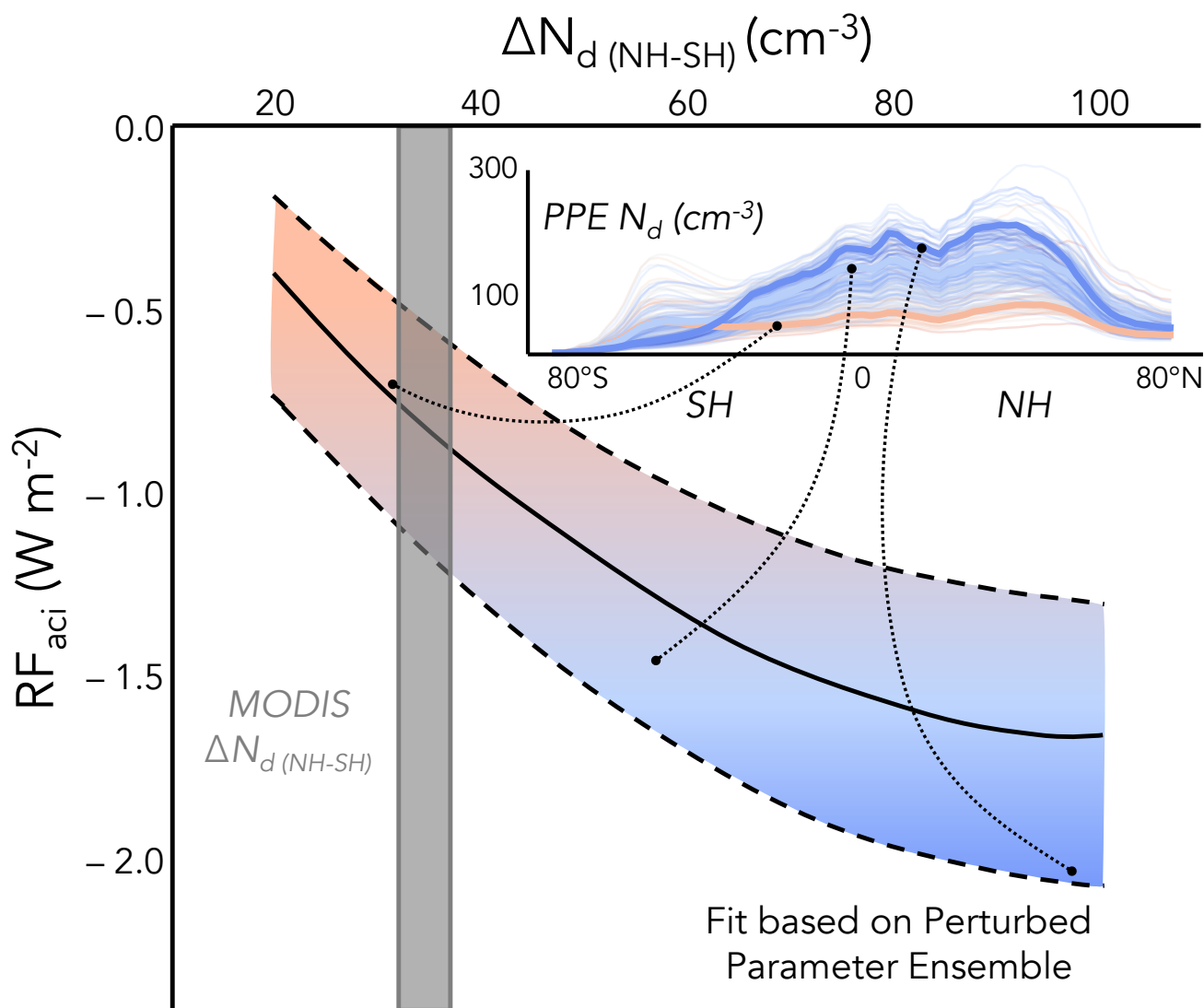


**Figure 6.** Example of using the hemispheric contrast in  $N_d$  ( $\Delta N_{d(NH-SH)}$ ) to constrain radiative forcing associated with aerosol-cloud interactions (RFaci). A smaller hemispheric  $N_d$  contrast has a smaller RFaci magnitude and thus less cooling. Curves (solid line is linear fit, dashed lines are 95% prediction bands) based on Perturbed Parameter Ensemble (PPE) results described in McCoy et al. (2020) and approximately shaded by RFaci (blue for more aerosol cooling, orange for less). Inset shows zonal  $N_d$  of individual PPE members colored by RFaci approximately corresponding to shading along the best fit line (dotted lines). Gray bar shows 95% confidence on the inter-annual range of  $\Delta N_{d(NH-SH)}$  from MODIS satellite estimates between 2003-2015 (Grosvenor and Wood, 2018), yielding an observational constraint on RFaci between  $-1.2$  to  $-0.6 \text{ W m}^{-2}$  (McCoy et al., 2020).

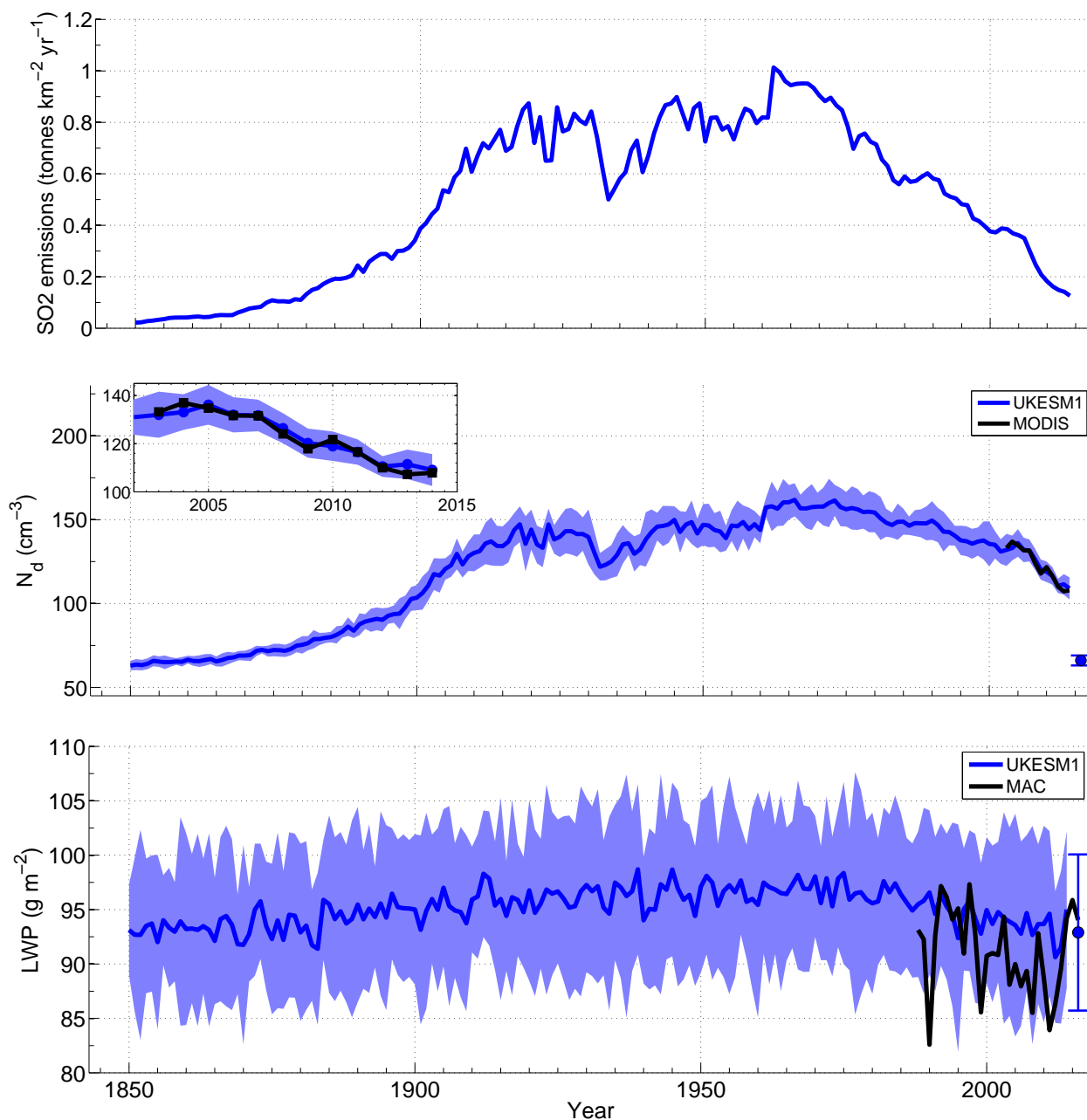


**Figure 7.** Timeseries of the annual mean CMIP6 emission rate for anthropogenic  $\text{SO}_2$  (top) for the continental US region ( $26\text{--}50^\circ \text{N}$ ,  $70\text{--}100^\circ \text{W}$ ; land-only gridpoints), the cloud droplet number concentration ( $N_d$ , middle) and the all-sky (i.e., including both cloudy and clear parts of gridboxes) liquid water path (LWP, bottom) for a region in the Atlantic ocean downwind of the US ( $26\text{--}42^\circ \text{N}$ ,  $56\text{--}80^\circ \text{W}$ ; ocean-only gridpoints). Lines are shown for the UKESM1 model ensemble mean, the MODIS satellite instrument using the collection 5.1 product and the MAC microwave satellite LWP dataset. The blue shading denotes  $\pm 2$  times the intermodel standard deviation across the ensemble. The error bar plotted at year 2016 for the  $N_d$  and LWP plots show the  $\pm 2\sigma$  range of of the annual average values from the pre-industrial control run along with the time mean (blue dot). The inset figure in the  $N_d$  plot shows a closeup of the time period for which observations are available using the same axes.



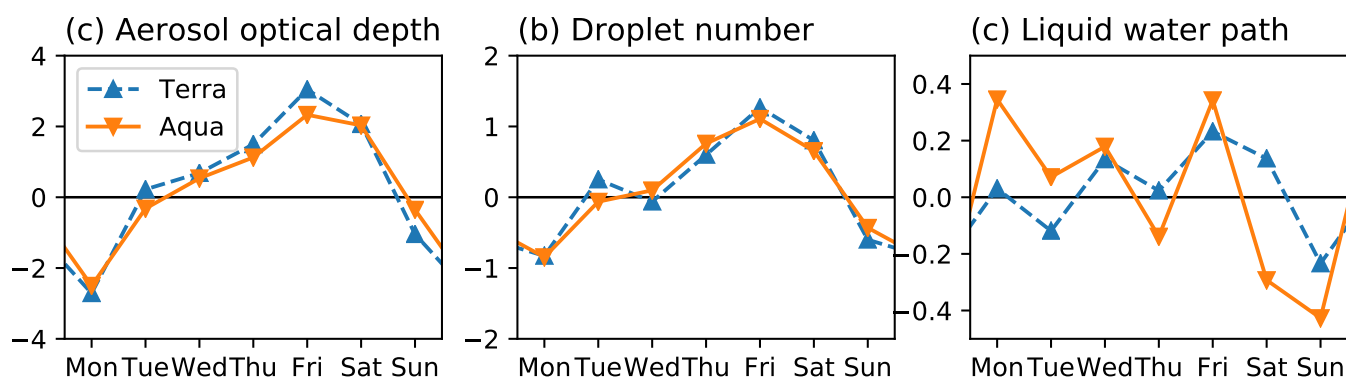


**Figure 8.** Weekly cycle of (a)  $AOD$ , (b)  $N_d$ , and (c)  $LWP$ , in percent deviation from the temporal average, as an average over continental Europe ( $35^\circ\text{N}$  to  $70^\circ\text{N}$ ,  $10^\circ\text{W}$  to  $30^\circ\text{E}$ , land only) from MODIS Collection 6 retrievals (Levy et al., 2013; Platnick et al., 2017) where  $N_d$  and  $LWP$  are computed assuming adiabatic clouds (Grosvenor et al., 2018). In an update to Quaas et al. (2009), the period 2003 to 2020 is used for Terra (10.30 h local overpass time, blue triangles up, dashed line) and Aqua (13.30 h local overpass time, orange triangles down, plain line).

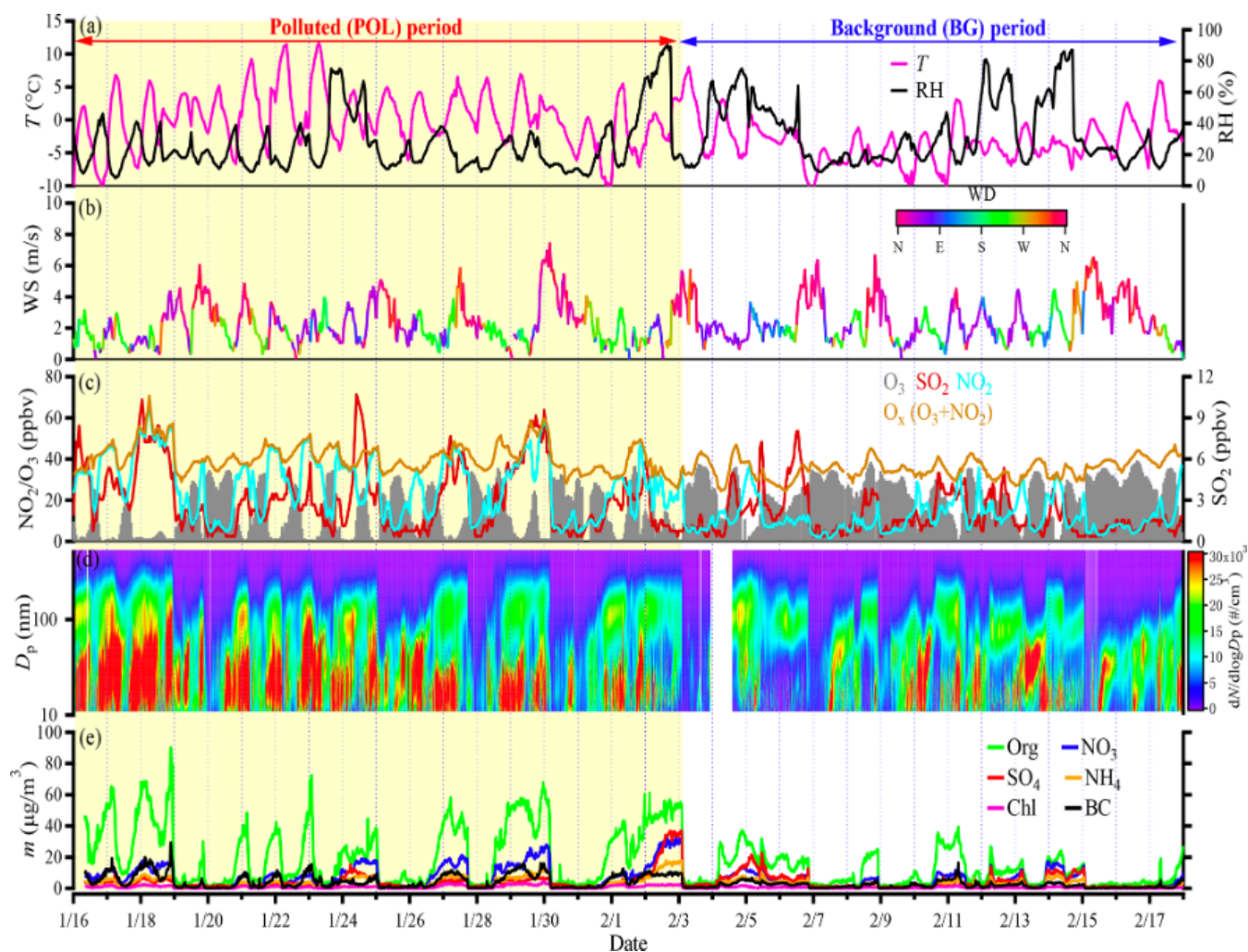


**Figure 9.** Time series of meteorology and aerosol precursor gases and species before (polluted) and during (background) the 2019 Chinese Spring Festival (16 January to 17 February 2019) in Beijing, China. (a) ambient temperature ( $T$ ) and relative humidity ( $RH$ ), (b) wind direction ( $WD$ ) and speed ( $WS$ ), (c) volume mixing ratios of trace gases [ $O_3$ ,  $SO_2$ ,  $NO_2$ , and  $O_x$  ( $O_3 + NO_2$ )], (d) the aerosol particle number size distribution measured by the SMPS, and (e) mass concentrations of aerosol chemical species in  $PM_{2.5}$  measured by the ACSM and the AE-33. (adopted from Wang et al., 2021).

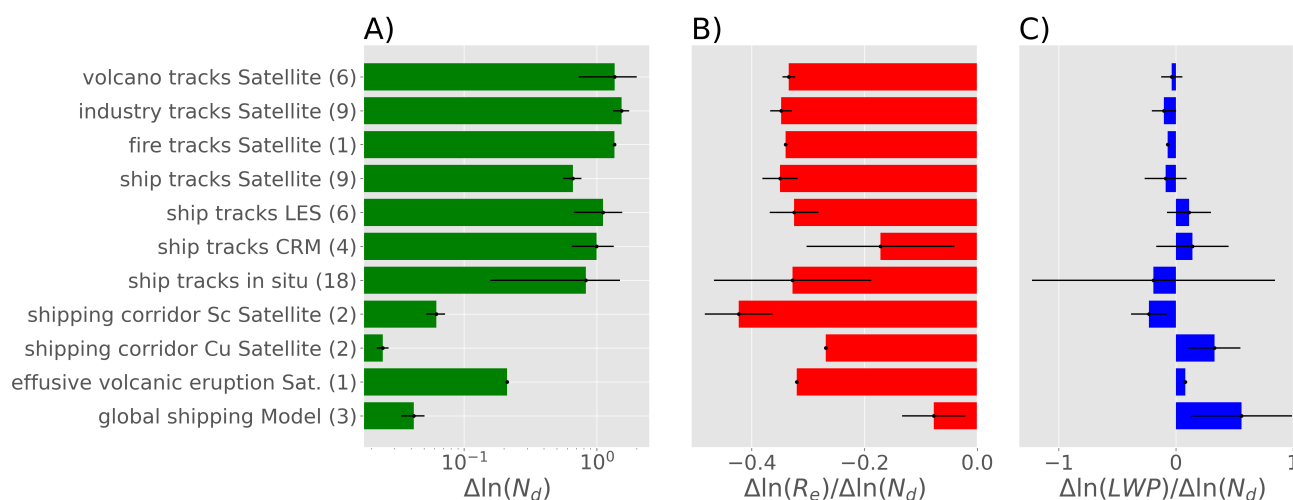


**Figure 10.** Change in a) cloud droplet concentration  $\Delta N_d$ , b) sensitivity of cloud droplet effective radius change to  $N_d$  and c) sensitivity of liquid water path change (LWP) to  $N_d$  averaged over numerous studies (shown in parenthesis on y-axis) involving experiments of opportunity listed in Table S1. Volcano, industry, fire and ship tracks are localized perturbations. Shipping corridor perturbation results are from Diamond et al. (2020), effusive volcanic eruption is from Malavelle et al. (2017) and the global shipping Model is from Lauer et al. (2007), and two estimates from Peters et al. (2013). Error bars represent one standard deviation of reported values for each category representing diversity of the mean amongst studies.

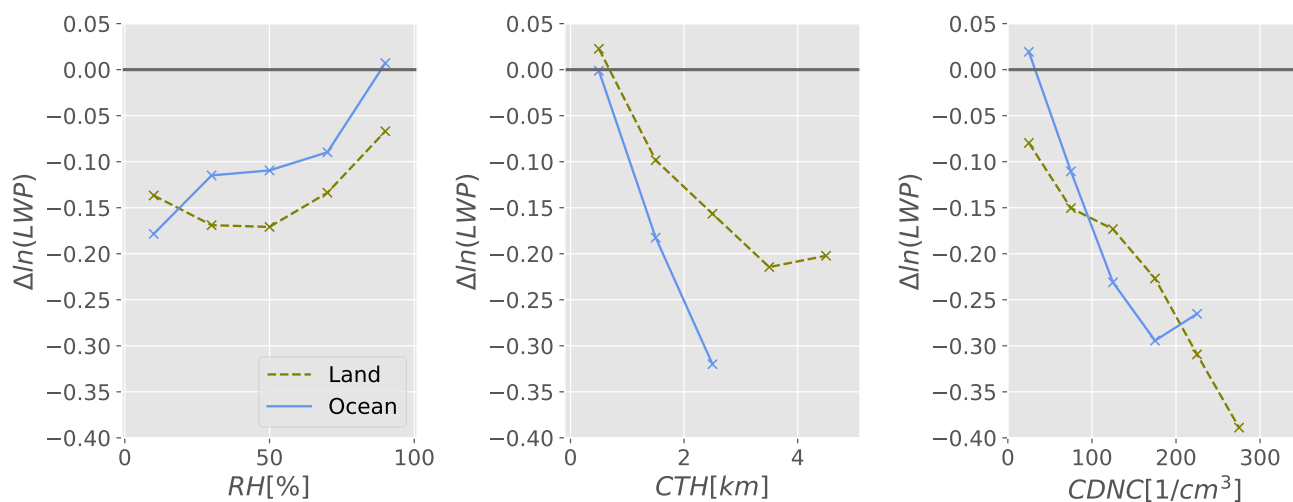


**Figure 11.** Cloud water response depends on the meteorological conditions. Dependence on above cloud relative humidity (RH, left), cloud top height (CTH, center) and background cloud droplet number concentration ( $N_d$ , right) is shown independently for ocean-based ship (Christensen and Stephens, 2012) and volcano tracks (Toll et al., 2017) and land-based industry and fire tracks (Toll et al., 2019).